

**ELUCIDATING MECHANISMS OF
BENZO[A]PYRENE MEDIATED APOPTOTIC
AND AUTOPHAGIC CELL DEATH
AND ITS PREVENTION WITH PHYTOTHERAPEUTICS**

Durgesh Nandini Das

**Elucidating mechanisms of benzo[a]pyrene mediated apoptotic and autophagic
cell death and its prevention with phytotherapeutics**

*Thesis submitted to
National Institute Of Technology
For the partial fulfillment of the degree*

Of

Doctor of Philosophy

By

Durgesh Nandini Das

(510LS304)

under the supervision of

Dr. Sujit Kumar Bhutia

Head of the Department



**DEPARTMENT OF LIFE SCIENCE
NATIONAL INSTITUTE OF TECHNOLOGY**

2015



**Department of Life Science
National Institute of Technology Rourkela**

Certificate of Examination

Roll Number: **510LS304**

Name: **Durgesh Nandini Das**

Title of Dissertation: **Elucidating mechanisms of benzo[a]pyrene mediated apoptotic and autophagic cell death and its prevention with phytotherapeutics**

We the below signed, after checking the dissertation mentioned above and the official record book (s) of the student, hereby state our approval of the dissertation submitted in partial fulfillment of the requirements of the degree of Doctor of Philosophy in Department of Life Science at National Institute of Technology Rourkela. We are satisfied with the volume, quality, correctness, and originality of the work.

Principal Supervisor

Member (DSC)

Member (DSC)

Member (DSC)

Examiner

Chairman (DSC)



**Department of Life Science
National Institute of Technology Rourkela**

Dr. Sujit Kumar Bhutia
Assistant Professor
Department of Life Science

December 7, 2015

Supervisor's Certificate

This is to certify that the work presented in this dissertation entitled "**Elucidating mechanisms of benzo[a]pyrene mediated apoptotic and autophagic cell death and its prevention with phytotherapeutics**" by **Durgesh Nandini Das**, Roll Number **510LS304**, is a record of original research carried out by her under my supervision and guidance in partial fulfillment of the requirements of the degree of *Doctor of Philosophy* in Department of Life Science. Neither this dissertation nor any part of it has been submitted for any degree or diploma to any institute or university in India or abroad.

Date:

(Sujit Kumar Bhutia)

Declaration of Originality

I, **Durgesh Nandini Das**, Roll Number **510LS304** hereby declare that this dissertation entitled **"Elucidating mechanisms of benzo[a]pyrene mediated apoptotic and autophagic cell death and its prevention with phytotherapeutics"** represents my original work carried out as a doctoral student of NIT Rourkela and, to the best of my knowledge, it contains no material previously published or written by another person, nor any material presented for the award of any other degree or diploma of NIT Rourkela or any other institution. Any contribution made to this research by others, with whom I have worked at NIT Rourkela or elsewhere, is explicitly acknowledged in the dissertation. Works of other authors cited in this dissertation have been duly acknowledged under the section "Bibliography". I have also submitted my original research records to the scrutiny committee for evaluation of my dissertation. I am fully aware that in case of any non-compliance detected in future, the Senate of NIT Rourkela may withdraw the degree awarded to me on the basis of the present dissertation.

Date:

Durgesh Nandini Das

NIT Rourkela

**DEDICATED TO MY
BELOVED PARENTS AND
THE ALMIGHTY**

Acknowledgements

It is pleasure for me to thank everyone for their unconditional help, valuable suggestions, timely guidance, love and affection for the completion of this thesis in due course of time. I am really grateful to all of them from the core of my heart without them I could not have made it a persuasive journey in my Ph.D. career.

I would like to take this opportunity to express my deep sense of gratitude to my supervisor Dr. Sujit Kumar Bhutia (Assistant Professor, Head of the Department, Department of Life Science, NIT Rourkela) for his patient counsel, constant encouragement, invaluable suggestions, thoughtful and constructive criticisms during the course of investigation and preparation of this manuscript.

I wish to thank all members of my Doctoral Scrutiny Committee Dr. Samir Kumar Patra, Dr. Surajit Das, Dr. Braja Gopal Mishra and Dr. Harmohan Jena, their counsel and guidance has been beneficial in all aspects of my Ph.D. work. I am extremely indebted to all faculty members of Department of Life Science for their advice and cooperation during the course of this study. I wish to thank all the staff members of Department of Life Science for helping in my research work and official assistance. I thank to Dr. Bibekanand Mallick, Department of Life Science for his help and invaluable suggestion for my *in silico* study. I am very grateful to Dr. Sanjay Kumar Mallick for helping me in immunophenotyping analysis. I thank to Dr. Kakoli Karar for PM particle collection study. I would also like to acknowledge CSIR, New Delhi, India for funding research fellowship during my PhD tenure.

I would specially like to express my gratitude to my lab mates Prashanta, Subhadip, Niharika, Prajna and Prakash for their constant support and help on and off the working bench and also supporting me and making my life so enjoyable in NIT which help me to go deep inside research. I express my heartfelt gratitude to all the scholars of Department of Life Science for their invaluable helps and suggestions. Special appreciation to Moonmoon, Neelam, Pradipta, Hirak and all others for their support during my Ph.D.

Last but not the least I am express my deepest gratitude to my beloved parents and lovable brother, for being so supportive and patient during this time of my life. At last it is Almighty to reach this stage.

NIT, Rourkela

November2015

Durgesh Nandini Das

Abstract

Polycyclic aromatic hydrocarbons form an active source of air pollution that affects our health and environment. In this study, we deciphered the role of benzo[a]pyrene (B[a]P) on cellular mechanism associated cell death. The particulate matter collected from an industrial area of Rourkela city found to have B[a]P and other unidentified environmental pollutants that had mutagenic and proapoptotic activity. The apoptotic potential of B[a]P was supported by ligand-protein and protein-protein interaction *in silico* which was validated on human keratinocyte (HaCaT) cell line. Our prediction showed that B[a]P was activated by cytochrome P450 (CYP1B1) to induce multiple cellular effects related to activation of the aryl hydrocarbon receptor (AhR) due to formation of toxic metabolites and this in turn activated caspases. Further, we showed that B[a]P induced mitochondrial mediated autophagy dependent cell death through the canonical pathway in HaCaT cells. The autophagic cell death induced by B[a]P was found to be mediated through AMPK/mTOR pathway. We showed that B[a]P abrogated ATP generation and activated reactive oxygen production to induce toxic mitophagy in HaCaT cells. In addition, we identified *Bacopa monneiri* (BM) plant extract as an inducer of protective autophagy, which may directly contribute to the antioxidant promoting potential of BM on B[a]P induced cell death through Beclin-1 dependent autophagy activation. The present study provided deep insight into the mechanism of B[a]P-mediated cellular toxicity and elucidated the further scope for the development of phytotherapeutics against environmental air pollutants.

Keywords: Benzo[a]pyrene, cytochrome p450, aryl hydrocarbon receptor, apoptosis, autophagy, *Bacopa monneiri*

Contents

Table of Contents	Page No
Abstract	
Chapter 1 Introduction	1-8
1.1 Introduction	2
1.2 Source of PAHs production	2
1.3 PAH mediated health effects	3
1.3.1 PAH exposure to skin	3
1.3.2 PAH and skin cancer	4
1.3.3 Environmental pollution and cell death	5
Chapter 2 Review of Literature and objectives	9-24
2.1 Introduction	10
2.2 Cytochrome P450 induction is mediated by aryl hydrocarbon receptor	10
2.3 Mechanisms by which polycyclic aromatic hydrocarbons affect cellular Processes	12
2.3.1 Free radicals, oxidative stress, and genotoxicity with PAHs	12
2.3.2 PAHs forms adducts with DNA, lipids, and protein	13
2.4 Mechanism of PAH-mediated carcinogenesis	16
2.4.1 PAHs and multistage characterization of carcinogenesis	16
2.4.2 DNA damage and genetic mutations associated with PAHs	17
2.5 PAHs act as modulators of cell death (apoptosis and autophagy)	19
2.6 Activation and suppression of immune cells with PAHs	21
2.7 Modulation of cytochrome P450: Novel options for cancer therapeutics	22
2.8 Scope of present investigation and objective	23
Chapter 3 <i>In vitro</i> mutagenic and genotoxic effects of native airborne particulate matter and its clinical significance	25-45
Abstract	26
3.1 Introduction	27
3.2 Materials and methods	28
3.2.1 Chemicals and reagents	28
3.2.2 Study areas	28
3.2.3 Sampling and analysis of particulate matter from Rourkela	29
3.2.4 Fluorescence spectroscopy	29
3.2.5 NMR analysis	29
3.2.6 Ames test	29
3.2.7 Cell culture	30
3.2.8 Cell viability by the MTT assay	30
3.2.9 Annexin V staining	30
3.2.10 Caspase assays	30
3.2.11 CYP1B1 knockdown using siRNA	30
3.2.12 7-Ethoxyresorufin-O-deethylase (EROD) assay	30

3.2.13	ROS generation	31
3.2.14	Nitric oxide (NO) determination	31
3.2.15	Single cell gel electrophoresis	31
3.2.16	Immunophenotyping by flow cytometry	32
3.2.17	Statistical analysis	32
3.3	Results	32
3.3.1	Characterization and mutagenic potential of PM from Rourkela	32
3.3.2	PM-induced apoptosis in HaCaT cells	36
3.3.3	Generation of ROS and NO by PM	37
3.3.4	PM-induced DNA damage analyzed by the comet assay	37
3.3.5	Activation of CYP1B1 by PM and inhibition of PM-induced apoptosis by siCYP1B1 and CTZ	39
3.3.6	Blood analysis for people living in Rourkela, by immunophenotyping and the comet assay	40
3.4	Discussions	43
Chapter 4 Prediction and validation of apoptosis through cytochrome P450 activation by benzo[a]pyrene		46-64
	Abstract	47
4.1	Introduction	48
4.2	Materials and methods	49
4.2.1	Chemicals and reagents	49
4.2.2	Cell culture	49
4.2.3	Cell viability by MTT assay	50
4.2.4	Annexin V and propidium iodide staining	50
4.2.5	Caspase assays	50
4.2.6	CYP1B1 knockdown using small interfering RNA	50
4.2.7	RNA extraction and semiquantitative RT-PCR	50
4.2.8	In silico study	51
4.2.9	Statistical analysis	51
4.3.	Results	51
4.3.1	Benzo[a]pyrene activated by cytochrome P450: in silico approach	51
4.3.2.	Benzo[a]pyrene induced apoptosis in human skin keratinocytes	54
4.3.3	Benzo[a]pyrene induced activation of intrinsic and extrinsic caspase Activation	56
4.3.4	Caspase inhibitors suppressed the B[a]P mediated apoptotic death	56
4.3.5	CYP1B1 deficiency decreased B[a]P induced apoptosis	58
4.3.6	Clotrimazole potent inhibitor of cytochrome P450 playing crucial role in inhibit activity of benzo[a]pyrene	62
4.4	Discussions	62
Chapter 5 Benzo[a]pyrene mediated mitochondrial stress induces autophagy dependent cell death		65-83
	Abstract	66
5.1	Introduction	67

5.2	Materials and methods	68
5.2.1	Chemicals and reagents	68
5.2.2	Cell culture	68
5.2.3	Cell viability by MTT assay	69
5.2.4	Caspase assays	69
5.2.5	Measurement of autophagy	69
5.2.6	Measurement of Mitochondrial ROS	69
5.2.7	Measurement of cellular ATP level	69
5.2.8	Western blotting analysis	70
5.2.9	Beclin-1 knockdown using small interfering RNA	70
5.2.10	Visualization of mitophagy	70
5.2.11	Measurement of mitochondrial respiration rate and glycolysis study	70
5.2.12	Statistical Analysis	71
5.3	Results	71
5.3.1	Autophagic cell death with benzo[a]pyrene in HaCaT cells	71
5.3.2	Activated benzo[a]pyrene induced autophagic cell death	74
5.3.3	Relation between benzo[a]pyrene mediated apoptosis and autophagic cell death	74
5.3.4	Benzo[a]pyrene induced mitophagy	77
5.3.5	Benzo[a]pyrene induced cellular energy deficiency leading to AMPK/mTor Pathway- dependent Autophagy	77
5.3.6	Measurement of mitochondrial respiration rate and glycolysis study	80
5.4	Discussions	80

Chapter 6 Cytoprotective activity of *Bacopamonneri* against benzo[a]pyrene induced apoptosis through modulation of autophagy 84-98

	Abstract	85
6.1	Introduction	86
6.2	Materials and methods	87
6.2.1	Chemicals and reagents	87
6.2.2	Cell culture	87
6.2.3	Cell viability by MTT assay	87
6.2.4	Beclin-1 knockdown using small interfering RNA	88
6.2.5	Annexin V/ Propidium iodine staining	88
6.2.6	Caspase assays	88
6.2.7	Western blotting analysis	88
6.2.8	Measurement of Mitochondrial ROS	88
6.2.9	Mitochondrial membrane potential measurement	88
6.2.10	Measurement of autophagy	89
6.2.11	Visualization of mitochondria and lysosome	89
6.2.12	Statistical Analysis	89
6.3	Results	89
6.3.1	BM found to protect B[a]P induced cytotoxicity	89
6.3.2	BM diminished B[a]P-induced mitochondrial dysfunction	91
6.3.3	Autophagy induction by BM in HaCaT cells	92

List of Figure

Figure No	Figure legend	Page No
Fig.1.1	Benzo[a]pyrene activated pathway	3
Fig.1.2	Apoptosis and Autophagy pathways	6
Fig.1.3	Connection between autophagy and apoptosis	7
Fig.1.4	Connection between autophagy and extrinsic and intrinsic apoptosis pathways	7-8
Fig. 2.1.	Schematic diagram of basic model of the molecular events associated with polycyclic aromatic hydrocarbons (PAHs) at cellular level	14
Fig. 2.2.	Role of activated PAHs on genotoxic and non-genotoxic effects.	15
Fig.2.3.	Chemical carcinogenesis is a multistep process.	19
Fig.3.1.	The PM was collected from different sites of Rourkela city, Odisha and the mutagenicity of PM	33
Fig.3.2.	The presence of PAHs, including B[a]P and dioxin, in PM from the industrial zone was demonstrated by fluorescence spectroscopy and ¹ H NMR	35
Fig.3.3.	Effect of PM on apoptosis	36
Fig.3.4	Generation of ROS and NO by PM in HaCaT cells	38
Fig.3.5.	PM-induced DNA damage analyzed by the comet assay	39
Fig.3.6.	Role of cytochrome P450 in PM mediated apoptosis	41
Fig.3.7.	Analysis of immune cells from people of Rourkela city by box plot	42
Fig.3.8.	DNA damage analysis in blood of people of Rourkela city	43
Fig.4.1.	Benzo[a]pyrene activated by cytochrome P450 in silico approach	53
Fig.4.2.	Benzo[a]pyrene induced apoptosis	55
Fig.4.3.	Benzo[a]pyrene induced activation of intrinsic and extrinsic caspase activation	57
Fig.4.4.	Inhibition of B[a]P induced apoptosis by caspase inhibitor	59
Fig4.5.	CYP1B1 knockdown affects B[a]P induced apoptosis	60
Fig.4.6.	Clotrimazole potent inhibitor of cytochrome P450 playing crucial role in inhibit activity of B[a]P	61

Fig.5.1.	Benzo[a]pyrene induced autophagic cell death in HaCaT cells	72
Fig.5.2.	Benzo[a]pyrene induced autophagic cell death through canonical pathway.	73
Fig.5.3.	Benzo[a]pyrene activated by CYP1B1 and AhR induced autophagic cell death.	74
Fig.5.4.	Benzo[a]pyrene mediated apoptosis and autophagic cell death occurred simultaneously	75
Fig.5.5.	Benzo[a]pyrene induced mitophagic cell death.	76
Fig.5.6.	Benzo[a]pyrene activates AMPK/mTOR-axis leading to autophagy dependent cell death in response to cellular energy deficiency in HaCaT cells	78
Fig.5.7.	Activation of mitochondrial oxidative stress associated with B[a]P mediated autophagy	79
Fig.6.1.	<i>Bacopa monneiri</i> (BM) found to protect benzo[a]pyrene (B[a]P) induced cytotoxicity in HaCaT cells.	90
Fig.6.2.	BM diminished B[a]P-induced mitochondrial dysfunction.	91
Fig.6.3.	Autophagy induction by BM in HaCaT cells.	93
Fig.6.4.	Suppression of autophagy block the cytoprotection of BM	95
Fig.6.5.	Role of BM in mitochondrial ROS generation by B[a]P in beclin-1 deficient HaCaT cells	96
Fig.6.6.	B[a]P-induced reactive mitochondria were cleared by BM-promoted autophagy	96
Fig.7.1	Proposed model of molecular mechanism of B[a]P mediated cell death and its prevention by phytochemicals BM.	102

List of Tables

Table 1	Table legend	Page No
4.1	Binding energy value for ligand–protein interaction	52
4.2	Binding energy value for protein–protein interaction	54

List of symbols

PAHs	Polycyclic aromatic hydrocarbons
B[a]P	Benzo[a]pyrene
IARC	International Agency for Research on Cancer
°C	Centigrade
°F	Fahrenheit
CYP450	CytochromeP450
Anti-B[a]PDE	(+)-anti-7,8- dihydroxy-9,10-epoxy-7,8,9,10-tetrahydrobenzo[a]pyrene
AKR	Aldo-keto reductases
ROS	Reactive oxygen species
RT-PCR	Real time-Polymerase chain reaction
FADD	Fas-associated death domain
DISC	Death-inducing signaling complex
FasL/FasR and TNF- /TNFR1	Fas associated Ligand/Receptor and Tumor necrosis factor/Receptor1
Smac/DIABLO	Second mitochondrial activator of caspase/direct IAP binding protein with low PI
Apaf-1	Apoptotic protease activating factor
dATP	2'-deoxyadenosine 5'-triphosphate
PUMA	p53 upregulated modulator of apoptosis
MOMP	Mitochondrial outer membrane permeabilization
Atg	Autophagy-related genes
AhR	Aryl hydrocarbon receptor
BPDE	BP-7,8-dihydrodiol-9,10-epoxide
2,3,7,8-TCDD	2,3,7,8-tetrachlorodibenzo- <i>para</i> -dioxin
PCDDs	Polychlorinated dibenzo- <i>p</i> -dioxins
HSP-90	Heat shock protein 90
XAP2	X-associated protein 2
ARNT	Aryl hydrocarbon receptor nuclear translocator
XRE	Xenobiotic responsive element
MAPK	Mitogen activated protein kinases
NF- κ B	Nuclear factor kappa light chain enhancer of the activated B cell
CYP1B1	Cytochrome P450 1B1
IZ	Industrial zone
NIZ	Non-industrial zone
TG	Triglycerides
DNA	Deoxyribonucleic acid
Hb	Haemoglobin
BPTs	Benzo[<i>a</i>]pyrene tetrols
3-MA	3-methyladenine
2,4,3',5'-TMS	2,4,3',5'-tetramethoxystilbene
EROD	7-ethoxyresorufin- <i>O</i> -deethylase

3-MC	3-methylcholanthrene
DMBA	7,12-dimethylbenz(a)anthracene
PM	Particulate matter
μM	Micromolar
μl	Microlitre
μg	Microgram
$\Delta\psi$	Membrane potential
Rpm	Rotation per minute
NMR	Nuclear magnetic resonance
RNS	Reactive nitrogen species
MTT	3-[4,5-dimethylthiazol-2-yl]-2,5-Diphenyltetrazolium bromide
CTZ	Clotrimazole
CD	Cluster of differentiation
DMSO	Dimethyl sulfoxide
TLC	Thin layer chromatography
H_2CCl_2	Chloroform
MR	Mutagenic ratio
DMEM	Dulbecco's Modified Eagle's Medium
FBS	Fetal bovine serum
PBS	Phosphate buffer saline
DHR 123	Dihydrorhodamine 123
Rh 123	Rhodamine 123
NO	Nitric oxide
PI	Propidium iodide
WHO	World Health Organization
PDB	Protein data bank
GAPDH	Glyceraldehyde-3-phosphate dehydrogenase
chEBI	Chemical Entities of Biological Interest
ANF	α -naphthoflavone
FFT	Fast Fourier transform
PBST	Phosphate buffered saline with Tween-20
MMP	Mitochondrial membrane potential
H_2O_2	Hydrogen peroxide
h(s)	Hour(s)
FACS	Fluorescence cell sorter
FCAP	Flow Cytometric Analysis Program
FITC	Fluorescein isothiocyanate
%	Percentage
CQ	Chloroquine
mtDNA	Mitochondrial DNA
mTOR	Mammalian target of rapamycin
GFP-LC3	Green fluorescent protein-Light Chain 3

AO	Acridine Orange
Caspase	Cysteine-aspartic proteases or cysteine-dependent aspartate-directed proteases
CYP1B1	Cytochrome P450 1B1
AVO	Acidic vesicular organelles
DHE	Dihydroethidium
PVDF	Polyvinylidene difluoride
SDS-PAGE	Sodium dodecyl sulfate-Polyacrylamide gel electrophoresis
AMPK	Adenosine monophosphate-activated protein kinase
mm	Millimetre
nM	Nanomolar
mg	Milligram
ml	Millilitre
ATP	Adenosine triphosphate
AMP	Adenosine monophosphate
MP	methylpyruvate
TSC2	Tuberous Sclerosis 2
LPO	Lipid peroxidation
PtdIns(3)P	phosphatidylinositol3-phosphate
BM	<i>Bacopa monnieri</i>

Chapter 1

Introduction



1.1. Introduction

Polycyclic aromatic hydrocarbons (PAHs) are organic compounds made of two or more fused benzene rings in a linear or cluster arrangement (Annweiler et al., 2000; Peng et al., 2008). PAHs are extremely stable organic pollutants that occur ubiquitously in the environment as complex mixtures and are of serious concern due to their toxic, mutagenic and/or carcinogenic effects (IARC, 1983, 1984). They generally exist as colorless, white or pale yellow-green solid particulate matter with varied structures and toxicity (Atlanta, GA, 1990). In general, it is accepted that a greater number of benzene rings in the PAH molecule lead to increased hydrophobicity and toxicity of the specific PAH molecule (Bamforth and Singleton, 2005).

Most of them are formed by a process of thermal decomposition (pyrolysis) and subsequent recombination (pyrosynthesis) of organic molecules. PAHs include benzo[a]pyrene, anthracene, 1,2-Benzpyrene, dioxin, fluoranthene, benz[a]anthracene, dibenzofuran, and amongst them benzo[a]pyrene (B[a]P) is the most potent as assessed by the Environmental Protection Agency (EPA). The compound benzo[a]pyrene, is formed by the fusion of tetracyclic pyrene to the alpha position of monocyclic benzene ring, and is the product of incomplete combustion at temperatures between 300 °C and 600 °C. B[a]P is often used as a marker for total exposure to carcinogenic PAHs, as the contribution of B[a]P to the total carcinogenic potential is high (51–64%) (Ohura T, et al., 2004).

1.2. Source of PAHs production

The main industrial sources of PAHs include aluminum production (Armstrong et al., 1994), iron steel foundries and coke production units (Boffetta et al., 1997). PAHs are predominantly emitted from the exhaust fumes of vehicles and are ubiquitously associated with diesel fuel, oils, gasoline, coal and lubricant oil. PAH exposure through dermal contact, inhalation, and ingestion in both occupational and non-occupational settings occurs on a consistent basis for most people. Some exposures may involve more than one route simultaneously, affecting the total absorbed dose (such as dermal and inhalation exposures from the contaminated air). All non-workplace sources of exposure are diet, smoking and burning coal and wood. B[a]P is one of the 105 reagents that were classified by the International Agency for Research on Cancer (IARC) to be carcinogenic to humans (group 2A, IARC 1983). The ability of B[a]P to induce



tumors upon local administration is well documented (Wang et al., 2015; Sánchez-Martín et al., 2015).

1.3. PAH mediated health effects

Cytochrome P450 (CYP450)-mediated oxidative metabolism often serves a beneficial role in the clearance of foreign compounds. However, the reaction catalyzed by CYP450 inadvertently activates pro-carcinogens to carcinogens (Rodríguez-Antona and Ingelman-Sundberg, 2006). In this regard, a noteworthy case is the carcinogenic effect of the diol-epoxide pathway. B[a]P is first activated by CYP450 monooxygenase to B[a]P-7,8-oxide, which serves as a substrate for hydration by the epoxide hydrolase to trans-B[a]P-7,8-dihydrodiol (B[a]P-7,8-diol). This is then transformed into the ultimate carcinogen r-7,t-8-dihydrodiol-t-9,10-oxy-7,8,9,10-tetrahydrobenzo[a]pyrene (anti-BPDE) and the less carcinogenic isomer r-7,t-8-dihydrodiol-c-9,10-oxy-7,8,9,10-tetrahydrobenzo[a]pyrene (syn-BPDE), which has been used as a signature metabolite for this pathway (Fig.1.1.) (Jiang et al., 2005). BPDE can enter the nucleus to form deoxyguanoside–DNA adducts or adducts with proteins (Poirier et al., 2000; Gao et al., 2011). Much of the current information pertaining to health effects following B[a]P exposure come from adult occupational exposure studies and experimental animal studies, although there are reports on human developmental studies as well (Poirier et al., 1992; Swenberg et al., 2008).

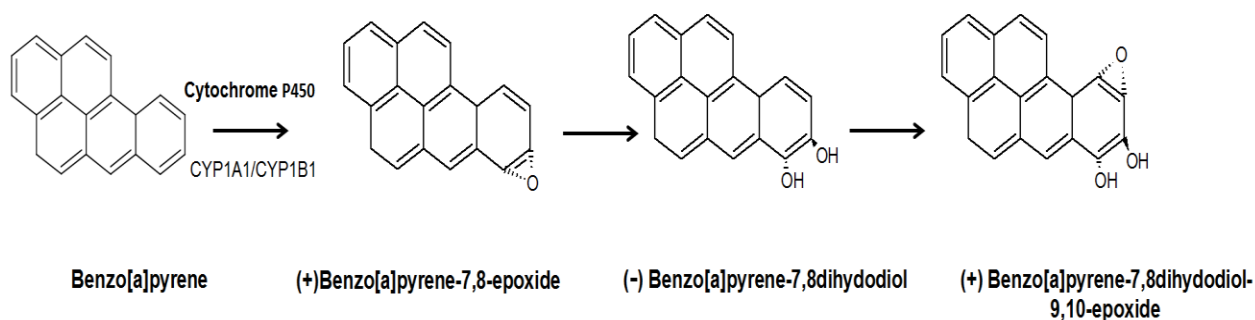


Fig.1.1. Benzo[a]pyrene activation pathway

1.3.1. PAH exposure to skin

Dermal exposure to PAHs can occur in two ways: first being the direct contact with contaminated surfaces or equipment, and second from the airborne particulate matter. The deposition of vapors and the splashing of oils are common occurrences at workplaces. Mc Clean et al. showed that higher molecular weight PAHs are prone to dermal exposure whereas the lighter ones are more likely to be inhaled (Mc Clean et al., 2004; Fusinoni et al., 2010). The

reason for this could be that lower molecular weight compounds are more volatile and are, therefore, more likely to become airborne. Larger molecules, such as B[a]P are more likely to settle on the skin easily.

Our skin is a multifaceted and multifunctional organ that provides protection and acts as the first barrier against environmental intimidations. Xenobiotic exposure to B[a]P aggravates the chances of skin cancer caused by a series of genetic alterations that mainly affects cell growth, survival, and differentiation processes. Mutations leading to activated (proto) oncogenes or inactivated tumor suppressor genes play a key role in the commencement of cancer. Since the last decade, the incidence of skin cancer has been dramatically increased as a major public health burden.

1.3.2. PAH and skin cancer

Malignancies in the skin can be divided into cutaneous malignant melanoma, basal cell carcinoma, and squamous cell carcinoma (Kim et al., 2010; Peña-Vilabelda et al., 2014). Cutaneous malignant melanoma is the most severe skin cancer type because of its aggressive nature and its tendency to metastasize; for most cancers, the causative agent is unknown. The key event in the discovery of PAHs that cause tumors in humans was an observation by the British surgeon Sir Percival Pott in 1775. He proposed that scrotal cancer in chimney sweepworkers originated from occupational exposure to soot. In 1875 Von Volkman reported that elevated incidences of skin cancer in workers in the coal tar industry. Workers employed in the destructive distillation of coal were among the first occupational groups included in studies which reported an increase in scrotal and other skin cancers linked to exposure to tar or pitch. The occupational exposure of workers to PAHs has been associated with an increased risk of developing cancer of the lung, stomach, bladder, skin (including non-melanoma skin cancer) and blood. Many PAHs are considered to be complete carcinogens, i.e. the compounds are tumor initiators and promoters.

B[a]P forms intermediary metabolites (epoxide-benzo[a]pyrene and dihydrodiol-epoxide-benzo[a]pyrene) that can covalently bind to nucleophilic sites in DNA to form B[a]P-DNA-adducts (Perera et al., 2015). These intermediate metabolites are thought to be the carcinogenic form of B[a]P that interfere with DNA replication, transcription and protein synthesis. B[a]P-DNA-adducts are intimately associated with their mutagenic and carcinogenic potency on chronic occupational dermal exposure. It was found that approximately 24% of



applied B[a]P penetrated the skin to enter the systemic circulation. Moreover, it reported that workers handling PAH-containing materials had a significant risk of developing skin cancer. PAHs can be activated by light irradiation without requiring metabolizing enzymes. The assessment of dermal exposure, on the other hand, is much more difficult as there is no general agreement on the wide range of available procedures or their underlying assumptions. PAHs can easily penetrate the lipoprotein layers of the skin, because of the complexity of its structure.

Humans living near industrial areas experience high level of exposure to air pollutants; evoking oxidative stress as they interact with DNA, lipids, proteins leading to DNA mutation, lipid peroxidation and protein damage respectively. The common cellular mechanism that most industrial pollutants exert their adverse effects is their potential to act directly as pro-oxidants of lipids and proteins or as free radicals generators, promoting oxidative stress and the induction of inflammatory responses. This oxidative state has been implicated in a wide variety of degenerative diseases such as heart attack, chronic inflammatory diseases (rheumatoid arthritis), cardiovascular diseases, chest tightness, cough, loss of memory, tension, occupational fatigue and stress, central nervous system disorders, age related disorders and finally cancer (Dalle-Donne et al., 2006; Uttara et al., 2009). At high levels of oxidative stress, disruption of the mitochondrial permeability transition pore and the electron transfer chain cause apoptotic, autophagic and necrotic cell death.

1.3.3. Environmental pollution and cell death

Toxic air pollutants are suspected to induce mutagenic transformations leading to cancer. Autophagy and apoptosis are two extensive stress responsive pathways that are initiated due to exposure to PAHs. Cellular stress can promote autophagy and apoptosis in multiple ways, including induction of autophagy/apoptosis sequentially, simultaneously, or in a mutually exclusive manner (Panda et al., 2015). In the cellular setting PAH exposure mediated carcinogenic tendencies are modulated in light of autophagy and apoptosis crosstalk is an emerging field of study which we have highlighted in this thesis.

While, apoptosis is a type I form of programmed cell death executed by caspases that culminate in the rapid removal of organelles and other cellular structures. Although apoptosis is the major mechanism of cell death in these disease processes, autophagy plays dual roles by mediating cytoprotection and cell death. Autophagy on the other hand is a self-catabolic pathway that degrades cellular macromolecules and organelles. It is regulated by autophagy-



related genes (Atg) that control the formation of autophagosomes, (cytoplasmic vesicles with a double membrane surrounding a cargo) and degraded through the lysosomal machinery (Mizushima et al., 2008; Ding et al., 2010; Arias et al., 2011). In addition to this “housekeeping” function, autophagy also plays an essential “adaptive” survival role by maintaining nutrient and energy levels during periods of metabolic starvation or stress (Bhutia et al., 2011; Bhutia et al., 2013).

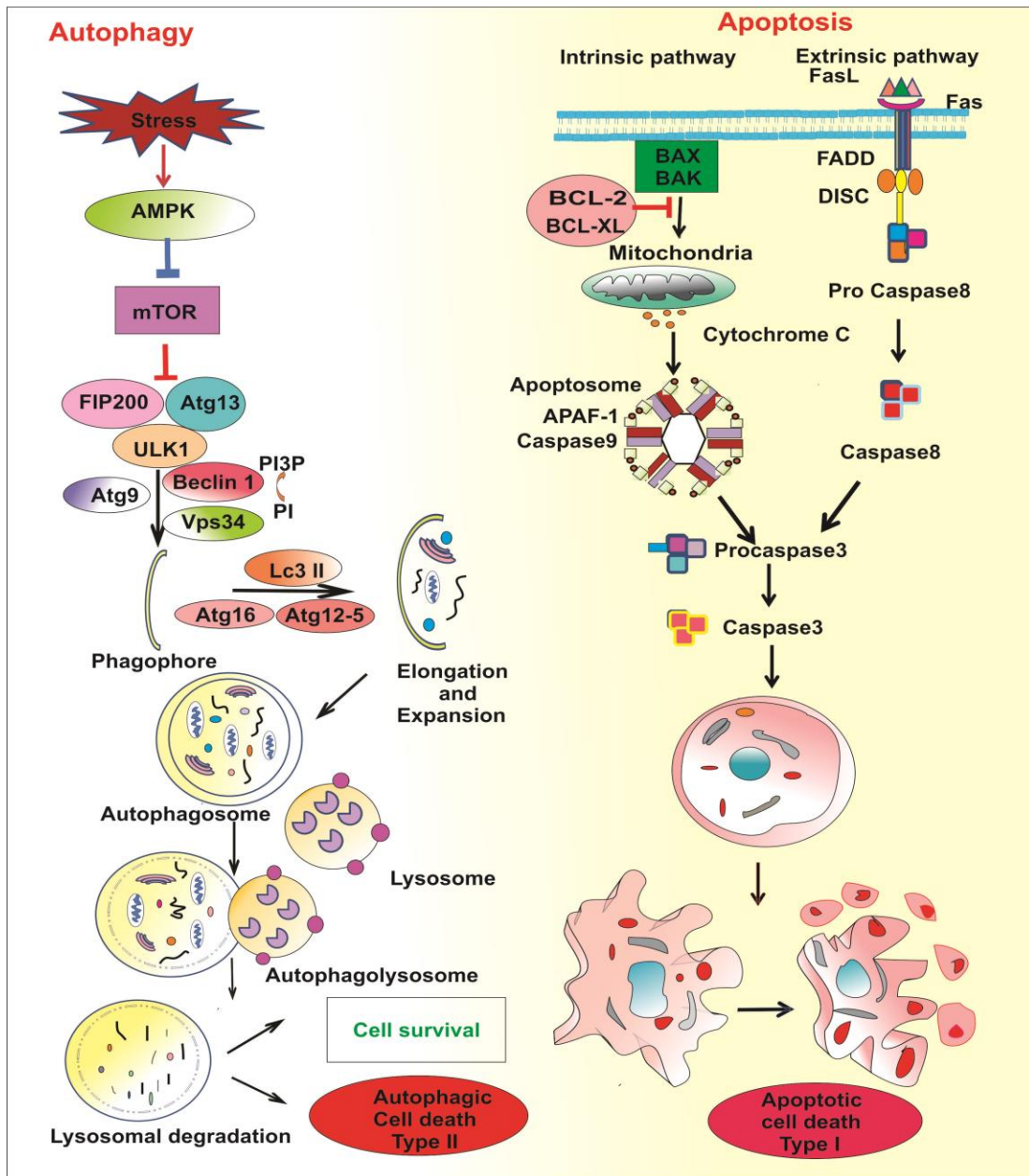


Fig.1.2. Apoptosis and Autophagy pathways

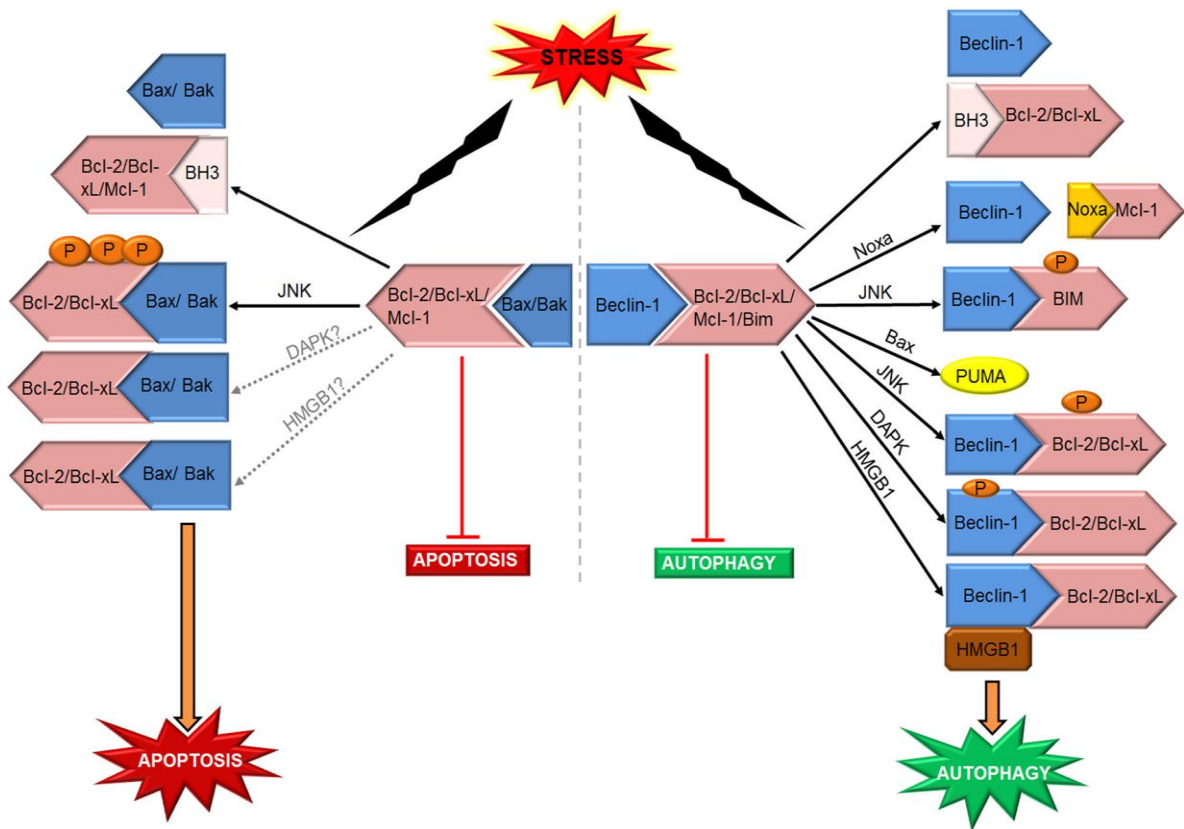
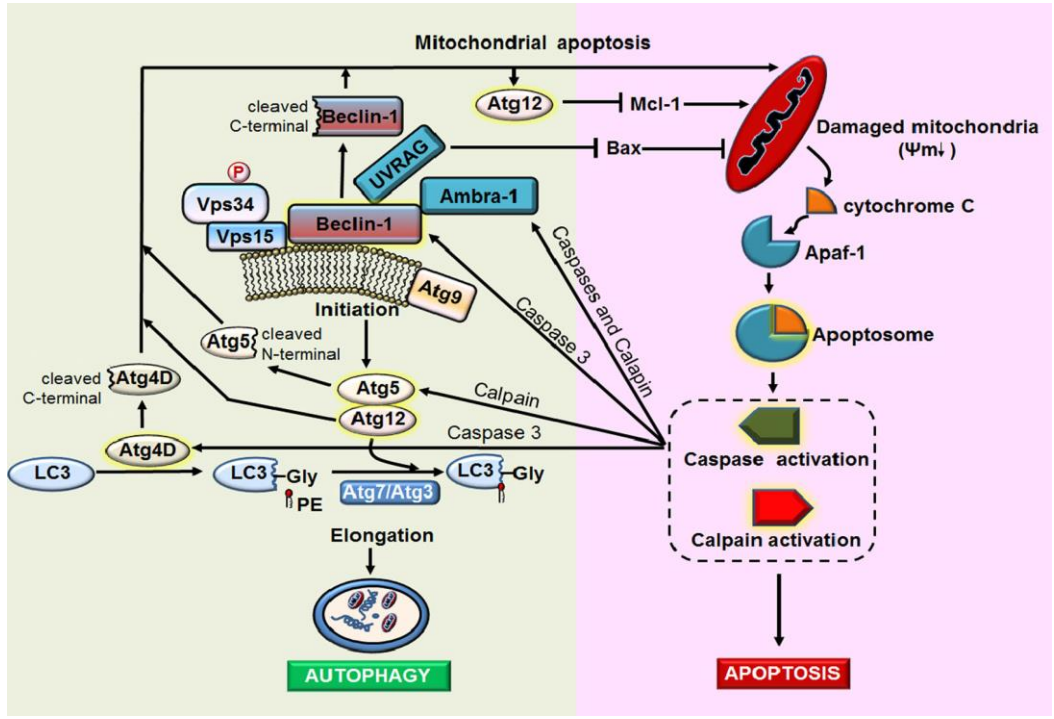


Fig.1.3. Connection between autophagy and apoptosis (Mukhopadhyay et al., 2014)



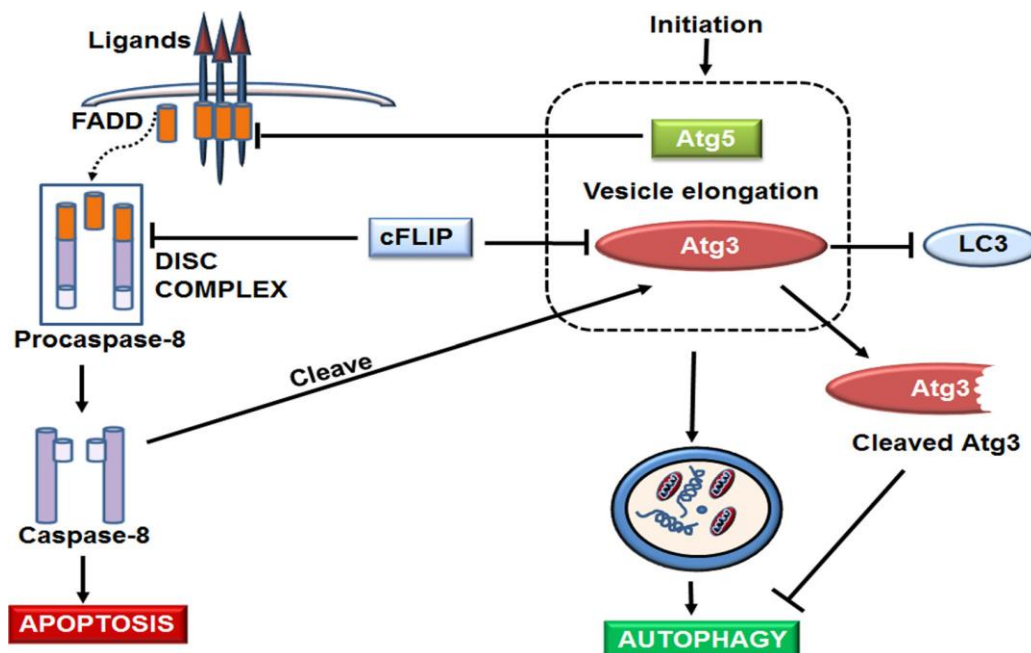


Fig.1.4. Connection between autophagy and extrinsic and intrinsic apoptosis pathways (Mukhopadhyay et al., 2014).

Cellular stress triggers a fascinating decision-making process in cells; they can either attempt to survive until the stress is resolved through the activation of cytoprotective pathways, such as autophagy, or can commit suicide by apoptosis in order to prevent further damage to surrounding healthy cells (Wang et al., 2015; Yang et al., 2015; Fiorito et al., 2011; Deng et al., 2013; Gannon et al., 2013). Although autophagy and apoptosis constitute distinct cellular processes with often opposing outcomes, their signaling pathways are extensively interconnected through various mechanisms of crosstalk (Fig.1.2.,1.3.) (Rubinstein et al., 2012; Mukhopadhyay S, Panda et al., 2014; Fernández et al., 2015). The physiological relevance of the autophagy–apoptosis crosstalk is not well understood, but it is presumed to facilitate a controlled and well-balanced cellular response to a given stress signal. Whether autophagy enhances or inhibits cell death in response to cellular stress is controversial. Furthermore, crosstalk occurs between the mediators of autophagy and apoptosis proved the interrelation between autophagy and apoptosis. In this thesis, we explore the various mechanisms by which autophagy and apoptosis regulate each other and define general paradigms of crosstalk on the basis of mechanistic features upon B[a]P treatment. The multiple layers of connectivity between autophagy and apoptosis that govern the delicate balance associated with cellular homeostasis along with various pathologies, such as cancer are highlighted in this work.

Chapter 2

Review of literature



2.1. Introduction

Human who live in urban areas near to industrial zones are exposed to high levels of particulate matters, including a variety of polycyclic aromatic hydrocarbons (PAHs). PAHs are aromatic hydrocarbons that have two or more single or fused aromatic rings with a pair of carbon atoms shared between rings (Baron et al., 2012; Stewart et al., 2010). They include benzo[a]pyrene (B[a]P), anthracene, 1,2-benzpyrene, dioxin, fluoranthene, benz[a]anthracene, and dibenzofuran; among them, benzo[a]pyrene (B[a]P) and dioxin are the most potent according to the Environmental Protection Agency. PAHs can impair human health by causing damage to the immune system, reduced fertility, developmental abnormalities, and respiratory damage; additionally, they promote the development of various types of cancer (Peluso et al., 2008; Tanyanon et al., 2012).

At the cellular level, PAHs are oxidized by many cytochrome P450 (CYP450) enzymes to several intermediates which binds to nuclear DNA. This binding results in mutation, replication errors, and apoptosis-mediated cell death. Furthermore, PAHs cause DNA damage and somatic mutations in normal cells, culminating in malignancy. They induce cellular toxicity by regulating the generation of reactive oxygen species (ROS), which mediate apoptosis. Moreover, most PAHs induce phosphorylation and the aggregation of the tumor suppressor protein p53, leading to the formation of DNA adducts followed by apoptosis (Kampa and Castanas, 2007). Interestingly, cellular toxicity-mediated cell death and immune suppression by industrial pollutants provide fertile ground for the proliferation of mutated cells, resulting in cancer growth and progression (Spinelli et al., 2006). This review is focused on the current state of research on PAHs from unwanted byproducts of incineration, uncontrolled burning, and automobile exhausts and their molecular mode of action for the initiation and development of cancer. Furthermore, it provides molecular insight into possible new therapeutic approaches to inhibit PAH-mediated cell death and carcinogenesis.

2.2. Cytochrome P450 induction is mediated by aryl hydrocarbon receptor

Polymorphism in *CYP* genes can affect the capacity to convert precarcinogens into carcinogens, which is an important factor contributing to individual susceptibility to cancer development (Rodriguez-Antona and Ingelman-Sundberg, 2006). CYP450s are monooxygenase enzymes that include a heme group responsible for the binding of molecular oxygen to iron. Human CYP450s are primarily membrane-associated proteins located either in the inner membrane of the



mitochondria or the endoplasmic reticulum of cells (Williams et al., 2000). Presently, more than 57 active human *CYP450* genes and 58 pseudogenes have been identified (Nelson et al., 2004). There are innumerable *CYP450* types. For example, *CYP1A1* is expressed extra-hepatically, and *CYP1A2* and *CYP1B1* are mainly expressed in the liver, skin, and brain, indicating a very different basal regulation, despite shared induction via the aryl hydrocarbon receptor (AHR) (Moffat et al., 2011). *CYP1A1* and *CYP1B1* are the most important human P450 enzymes involved in the metabolic activation of PAHs and PAH dihydrodiols to carcinogenic intermediates, whereas *CYP1A2* activates aromatic amines. For example, B[a]P, released from various industrial activities, is first oxidized by *CYP1A1* or *CYP1B1* to phenols, such as 3-hydroxy-B[a]P and 9-hydroxy-B[a]P, and epoxides (e.g., B[a]P-7,8-epoxide) (Jiang et al., 2005; Das et al., 2014). The most well-studied PAH, B[a]P, is transformed *in vivo* to BP-7,8-epoxide by *CYP1A1* through the CYP/EH pathway. Furthermore, BP-7,8-epoxide is later oxidized to form BP-7,8-dihydrodiol, by EH followed by the final step of *CYP1A1*-catalyzed hydroxylation to form the carcinogen BP-7,8-dihydrodiol-9,10-epoxide (BPDE). Among the abundant metabolites identified, BPDE most effectively forms DNA adducts and serves as a putative carcinogen (Gao et al., 2011). Similarly, dioxins, especially 2,3,7,8-tetrachlorodibenzo-*para*-dioxin (2,3,7,8-TCDD), are activated by *CYP1B1* and *CYP1A1* (Jeyabalan et al., 2011). There are approximately 75 types of PCDDs (polychlorinated dibenzo-*p*-dioxins); among them, 2,3,7,8-tetraCDD is the most significant due to its high toxicity and its persistence. Thus, 2,3,7,8-tetraCDD and 2,3,7-triCDD are converted into 8-OH-2,3,7-triCDD by cytochrome P450 (Shinkyō et al., 2003). The major metabolite of 2,3,7,8-tetraCDD observed in dog and rat species is 8-OH-2,3,7-triCDD, and the glucuronide conjugate of 8-OH-2,3,7-triCDD was experiential in the case of rat hepatocytes treated with 2,3,7,8-tetraCDD (TCDD) (Kasai et al., 2004).

B[a]P and TCDD bind to cytosolic AHR, which exists in a latent state as a multiprotein complex containing a heat shock protein 90 (HSP-90) dimer and the co-chaperone protein X-associated protein 2 (XAP2) (Beischlag et al., 2008). Upon binding with ligand, AHR undergoes a conformational change that exposes its N-terminal nuclear localization sequence, facilitating the nuclear translocation of the AHR–xenobiotic (ligand) complex. The translocated HSP90-bound AHR subsequently dissociates from the HSP90 complex by binding to a structurally allied nuclear protein, AHR nuclear translocator, which forms a heterodimer with



AHR. This heterodimer is capable of binding to a xenobiotic-responsive element with the sequence 5'- T/G/TCGTGA/CG/TA/T-3', which can induce the transcription of several CYP enzymes that are significant in the metabolism and bioactivation of PAHs (Murray et al., 2014) (Fig.2.1.). In addition, AHR has a role in cell proliferation, differentiation, cell–cell adhesion, cytokine expression, and mucin production, facilitating tumor progression (Tsay et al., 2013). In A549 cells, AHR activation increases the expression of several E2F1 target genes that are involved in cell cycle control, such as proliferating cell nuclear antigen (Watabe et al., 2010). TCDD increases vascular endothelial growth factor expression through AHR in bronchial epithelial cells, which might contribute to angiogenesis (Tsai et al., 2015).

2.3. Mechanisms by which polycyclic aromatic hydrocarbons affect cellular processes

A common cellular mechanism by which most of the PAHs exert adverse effects is their propensity to act directly as pro-oxidants of lipids and proteins or as free radical generators, promoting oxidative stress and the induction of inflammatory responses (Kampa and Castanas, 2007). Free radicals (reactive oxygen and nitrogen species) are injurious to cellular lipids, proteins, and nuclear or mitochondrial DNA, inhibiting their normal function, as well as interfering with the signaling pathways within cells.

2.3.1. Free radicals, oxidative stress, and genotoxicity with PAHs

Free radicals and ROS inflictors are mostly derived from metabolite derivatives in the human body or from external sources, such as exposure to PAHs. During PAH exposure, oxidative stress arises when there is an imbalance between ROS formation and individual antioxidant activity, potentially leading to the damage of lipids, proteins, and macromolecules, such as DNA and RNA (Rao and Kumar, 2015). For moderate levels of oxidative stress, nuclear factor (erythroid-derived 2)-like 2 (Nrf2), a protective response pathway member, is activated, resulting in mitogen activated protein kinases (MAPK) and nuclear factor kappa light chain enhancer of the activated B cell (NF- κ B) (a redox-sensitive transcription factor)-induced pro-inflammatory responses (Kang et al., 2012; Sandberg et al., 2014). Nrf2 regulates the expression of innumerable cytoprotective genes that function to detoxify reactive species produced during metabolic reactions owing to ambient air pollutants, highlighting the important role of Nrf2 in the defense against air pollutant-induced toxicity (Rubio et al., 2010). Sustained activation of NF- κ B pathway is involved in some forms of cancer, such as leukemia, lymphoma, colon



cancer, and ovarian cancer (Hoesel and Schmid, 2013). These diseases manifest at a certain age determined by genetic and environmental factors. Initiation and proliferation of cancer typically involves chromosomal defects and oncogene activation. For high levels of oxidative stress, the perturbation of the mitochondrial permeability transition pore and the electron transfer chain cause apoptosis, autophagy, and necrotic cell death. ROS cause strand breaks, alterations in guanine and thymine bases, and sister chromatid exchanges, and may inactivate tumor suppressor genes within tumor cells or increase the expression of proto-oncogenes (Khaitan and Dwarakanath, 2009) (Fig.2.2.).

2.3.2. PAHs forms adducts with DNA, lipids, and protein

PAHs interact with cellular macromolecules, such as DNA, lipids, or protein, in the target tissue, which causes damage (Fig.2.2.). Unrepaired DNA adducts can cause mutations in somatic cells that initiate carcinogenesis. In chemical carcinogenesis, the formation of carcinogen–DNA adducts is a critical step and is considered an important biomarker during cancer initiation. For example, after activation by CYP450, B[a]P converts into activated derivatives containing epoxide groups, which tend to react with atoms that are electron-rich, such as the amino nitrogen found in the DNA base guanine. The reaction of the epoxide group with guanine causes the B[a]P to bond covalently to DNA, thereby forming a DNA-carcinogen complex called a DNA adduct (Tarantini et al., 2009; Einem Lindeman et al., 2011). TCDD-induced CYP1B1, which enhances estrogen metabolism and the formation of DNA adducts, seems to play an important role during human breast malignancy (Cavalieri and Rogan, 2006). DNA adduct formation depends on polymorphism in metabolic genes, such as CYP1A1, MspI, and GSTM1 null genotypes (Rojas et al., 2000). Associations between PAH exposure and the number of PAH-DNA adducts have been found, between coke oven exposure and PAH-DNA adducts in blood cells (Jedrychowski et al., 2013).

Lipids are good source of energy and are the main constituent of cellular membrane and tissue. However, several observations suggest that lipids are involved in carcinogenesis. About 50% of all cancer patients show cachexia, a syndrome in which lipids are easily peroxidized to lipid peroxides by free radicals (Fearon et al., 2012). For example, BPDE–lipid adduct formation was detected *in vitro* and *in vivo* after exposure to BPDE-I or B[a]P. The generation of the BPDE–lipid complex *in vitro* indicated that triglycerides (TG), including tripalmitin, triolein, and tristearin, are likely target lipids for BPDE-I. TGs play a crucial role in transporting fatty acids to



varied tissues during the biosynthesis of many lipids. They show positive reactions with BPDE. In contrast, cholesterol, phospholipids, and non-esterified fatty acids do not react with BPDE-I, an ultimate carcinogenic form of B[a]P that binds covalently to TGs. Formation of the BPDE-I-TG adduct occurs due to the covalent binding of position 10 of BPDE-I to the TG ester bonds

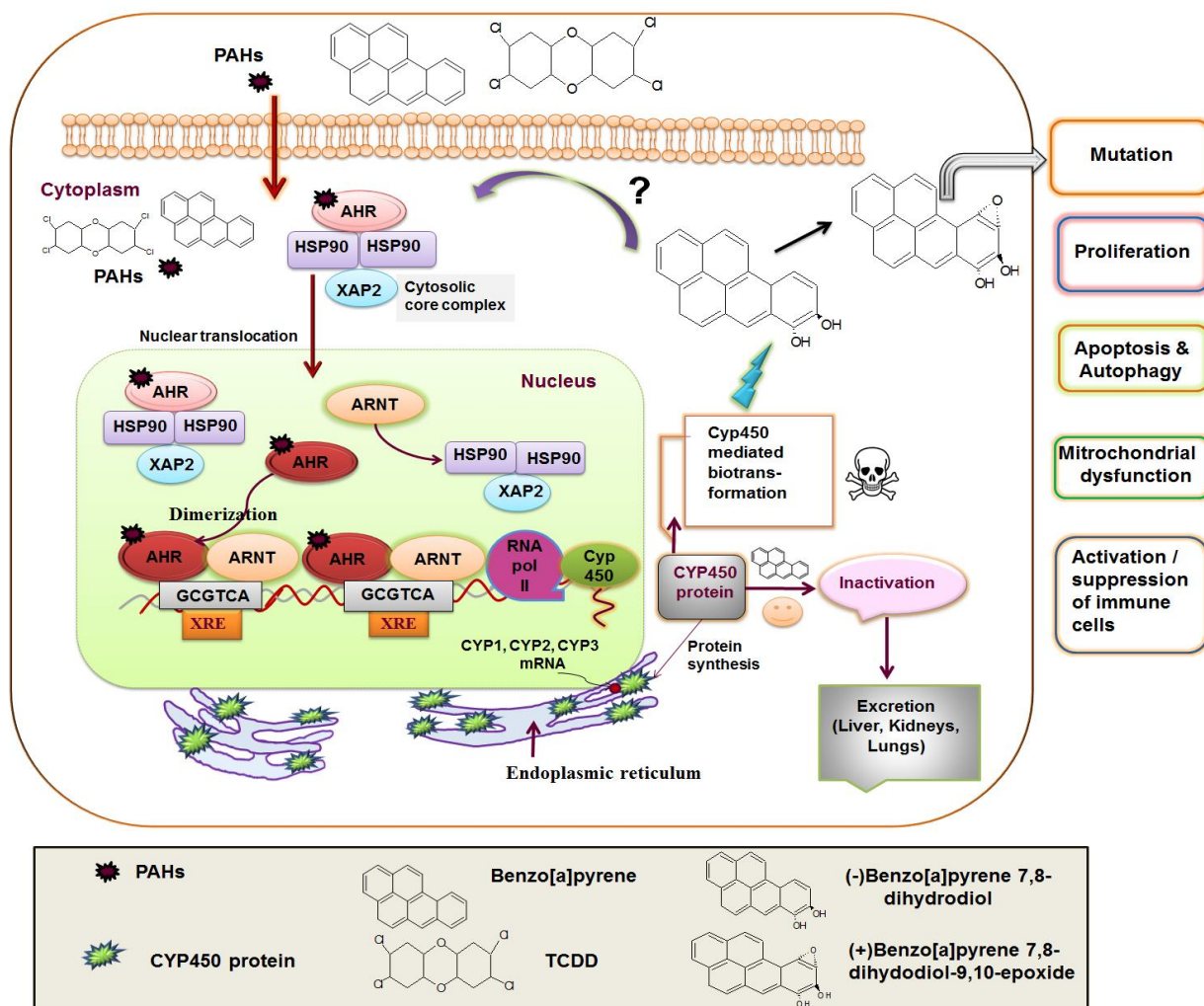


Fig.2.1. Schematic diagram of basic model of the molecular events associated with polycyclic aromatic hydrocarbons (PAHs) at cellular level. On binding a xenobiotic compound, the aryl hydrocarbon receptor (AHR) complex translocates to the nucleus and Aryl hydrocarbon receptor nuclear translocator (ARNT) mediates HSP90 displacement leading to the formation of AHR-ARNT heterodimer. This heterodimer is capable of binding to a xenobiotic responsive element (XRE) with the sequence 5'-T/G/TCGTGA/CG/TA/T-3'. The AHR-ARNT heterodimers can recruit co-activators leading to transcription of a wide diversity of genes, with the RNA polymerase II. The AHR target gene Cyp 450 is dependent on AHR activity for expression and is highly induced by AHR activation through multiple XRE. The Cyp450 specifically Cyp1, Cyp2 and Cyp3 metabolizes a number of pro-carcinogens, such as B[a]P and TCDD leads to mutation, rate of proliferation changes, apoptosis, autophagy,

mitochondrial dysfunction, activation and suppression of immune cells leading to cell toxicity and carcinogenesis. Interestingly, it has not yet been established whether the native or active PAHs bind with AHR and regulates cellular processes is not known.

between the glycerol portion and free fatty acids of TG. The BPDE-I-TG adduct is important evidence that lipids (especially in esterified form) can be directly damaged by reactive carcinogens (Godschalk et al., 2003). Lipids are abundant in human tissues and becomes susceptible to carcinogen exposure. If carcinogen-derived lipid damage occurs, it could be useful as an alternative to DNA or protein adducts (Phillips, 2002).

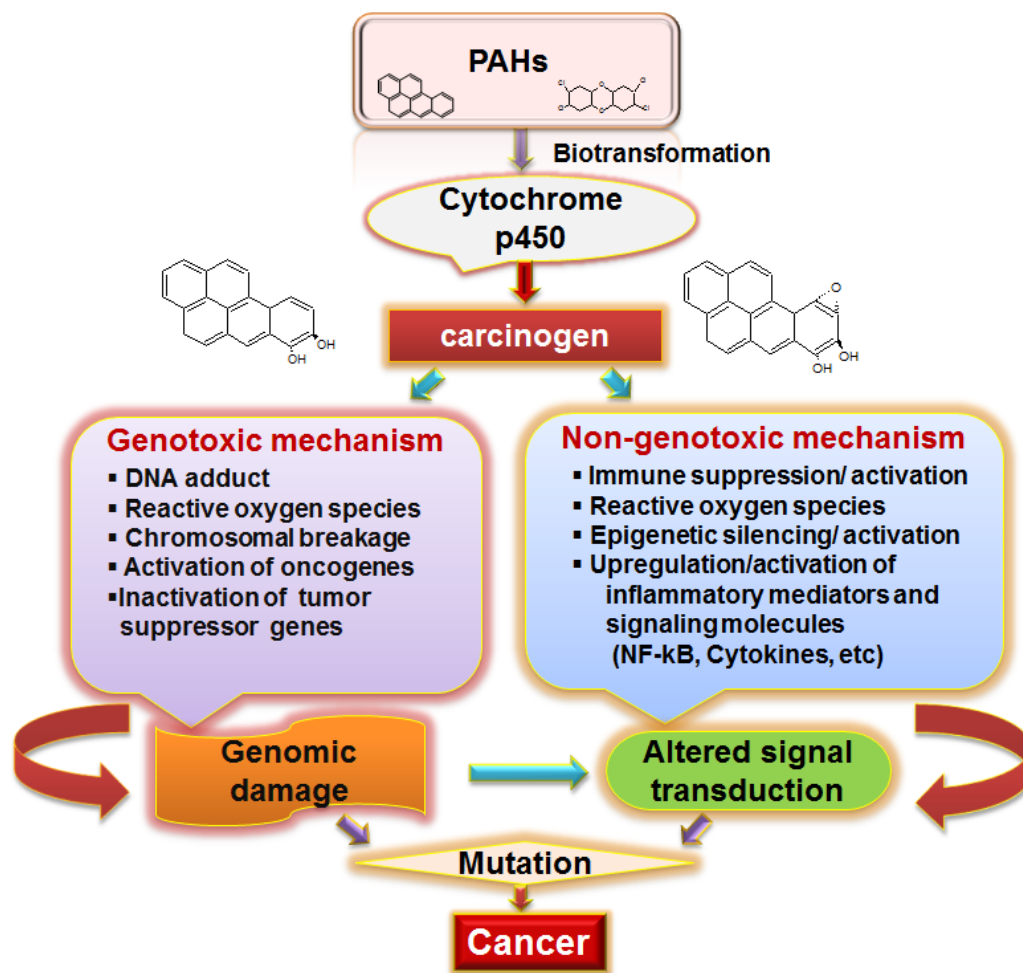


Fig.2.2. Role of activated PAHs on genotoxic and non-genotoxic effects. After activation by cytochrome P450, PAHs cause DNA damage and somatic mutations in normal cells. It can act directly as pro-oxidants of lipids and proteins or as free radical generators by promoting oxidative stress, lipid peroxidation and inducing inflammatory responses. Moreover, cellular toxicity mediated cell death and immune suppression by PAHs provide a fertile ground for proliferation of mutated cells that resulted in cancer growth and progression.

A study showed that protein adducts, including hemoglobin (Hb) adducts is formed via aromatic amines (e.g., 4-aminobiphenyl) in children (Richter et al., 2001). Hb adducts can be used as biomarkers of internal exposure and of environmental and occupational exposure (Begemann et al., 2001). The formation of carboxylic esters generated due to BPDE alkylation of one or more carboxylate groups in Hb has also been demonstrated. These studies have shown that ester adducts are the most abundant type formed by BPDE and are stable in native Hb. However, when the tertiary protein structure is disrupted, they release benzo[a]pyrene tetrols (BPTs), which are considered as typical marker of exposure to B[a]P. Benzo[a]pyrene diol epoxide adducts with Hb are measured to detect human exposure to environmental B[a]P released from traffic exhaust (Ogawa et al., 2006).

2.4. Mechanism of PAH-mediated carcinogenesis

2.4.1. PAHs and multistage characterization of carcinogenesis

Carcinogenesis due to chemical treatment is a complex, multistage process typically elapses between early events, including the initial carcinogen exposure, the onset of DNA damage, occurrence of mutations, and the subsequent appearance of a tumor (Chepelev et al., 2015). Initially, electrophilic metabolites interact with DNA, which may change the nucleotide sequence due to the misincorporation of a nucleotide opposite to the damaged base. Mutations occur when electrophilic chemicals or metabolites bind to DNA. The alteration in DNA structure causes the DNA sequence to be misread during cell replication, ultimately (Fig.2.3.).

Several lines of evidence support the role of PAH-DNA adducts in the transformation of normal cells to cancerous cells, including *in vitro* studies and those using animal models. The preeminent example is the role of PAH-DNA adducts in the development of human cancer. The distribution of BPDE and other PAH diol epoxide adducts has been mapped at the nucleotide level of p53 gene in PAH induced bronchial cells (Uccello et al., 2000). The strong sequence-specific formation of BPDE-DNA adducts in p53 of bronchial epithelial cells *in vitro* occurs at the same positions as well-known mutational hotspots in p53 found in DNA obtained from human lung cancer tissue. A high dosage of oral B[a]P (125 mg/kg/day) causes mutations in the mouse *Cyp1a1* gene, which results in immunosuppression and death within approximately 28 days (Johnson et al., 2008). Interestingly, in B[a]P-treated cells, the distribution of BPDE-N2-



dG adducts in the p53 tumor suppressor gene is highly correlated with p53 mutational hotspots found in lung tumors from cancer patients. These studies provide compelling evidence that environmentally induced BPDE-N2-dG adducts inactivate p53 via mutagenesis, thereby contributing to lung cancer in humans. Tumor localisation varies upon exposure route of the chemical carcinogen. Inhalation of B[a]P often induces lung cancer, and oral administration leads to tumors in various organs and tissues, including the gastrointestinal tract, liver, lungs, and mammary glands (Benford et al., 2010). Moreover, the effects of B[a]P on cancer metastasis and progression have been studied and the NF- κ B pathway is found to be a potential target. Specifically, the NF- κ B pathway may be related to adverse outcomes associated with the cumulative effects of B[a]P on human hepatocellular carcinoma metastasis (Ba et al., 2015). Wang et al. showed that B[a]P induces phosphorylation of ERK1/2 via phosphorylation and activation of Chk1, resulting in S phase accumulation of human H1355 lung cancer cells (Wang et al., 2015). Guo et al. validated that B[a]P increases breast cancer cell migration and invasion via upregulation of the ROS-induced ERK signaling pathway, and also promotes the activation of matrix metalloproteinase-9 (Guo et al., 2015).

Similarly, dioxins interact with AHR, which has a basic helix-loop-helix domain, and act as transcription factors after nuclear translocation, allowing the interaction of dioxins with DNA. The receptor-ligand complex binds to specific sites on DNA, altering the DNA structure and the transcription of a number of genes. TCDD is regarded as one of the most potent carcinogens ever tested in animal bioassays, and bioaccumulates in broad animal taxa (Yang and Rhim, 1995). In rodents, dioxin was reported to act more than a hepatocarcinogen by causing thyroid cell adenomas, squamous cell carcinomas of nasopharynx, as well as several types of fibrosarcomas. Malignant transformation has also been observed in immortalized human keratinocyte cell lines after a week of exposure to TCDD and in six subsequent subcultures (Ray and Swanson, 2004). Pavanello et al. recently showed that the shortening of telomeric length in peripheral blood occurs in workers unprotected from PAH exposure was predicted to lung cancer risk (Pavanello et al., 2010).

2.4.2. DNA damage and genetic mutations associated with PAHs

Generally, DNA damage forms the first step in the carcinogenic process. Chemical carcinogens can cause the formation of carcinogen-DNA adducts or induce other modifications to DNA, such



as oxidative damage and alterations to the DNA ultrastructure (e.g., DNA strand breakage, DNA-strand crosslinking, chromosomal rearrangements, and deletions). Although cells possess mechanisms to repair many types of DNA damage, they are never fool-proof and are not always completely effective. Transcription of the mutated templates ultimately leads to the synthesis of altered proteins (Fig.2.2. and 2.3.).

The industrial activity in the city of Leon, Mexico is related to shoe manufacturing. The working environment in the region is contaminated by rampant usage of organic solvents. The incidence of nuclear aberrations is significantly higher in exposed individuals than in unexposed individuals (or, than in a control group). Assays of micronuclei and other nuclear anomalies are a valid, practical, and easy way to measure genetic instability induced by genotoxic agents. Micronuclei are extra-nuclear bodies composed of chromosomes or chromosomal fragments that failed to be incorporated into daughter nuclei at mitosis (Zalacain et al., 2005). Micronuclear formations are resulted due to chromosomal damages related to carcinogenesis (Crasta et al., 2012).

It is generally agreed that several mutations are necessary to convert a normal cell into a cancer cell that is capable of uncontrolled growth. The formation of stable PAH-DNA adducts can lead to the induction of mutations that activate proto-oncogenes (Rybicki et al., 2006). Activation of the H-ras proto-oncogene may be involved in tumor initiation in mouse skin by various carcinogenic PAHs (Godschalk et al., 2003). Nucleotide transversion within codons 12 (G-T) or 61 (A-T) of cellular H-ras have frequently been identified in response to exposure to carcinogenic PAHs, such as B[a]P. Similarly, tumor suppressor genes are inactivated during carcinogenesis. Mutations in p53 gene was found in animal tumors and in a wide variety of human cancers. Approximately 50% of patients in those areas had a relatively rare G to T transversion at codon 249 (Hsu et al., 1991).

There is a growing interest in the relationships among carcinogenic exposures, the risk of cancer at specific sites, and mutation spectra in cancer-related genes (i.e., oncogenes and tumor suppressor genes). Strong and selective formation of adducts by 7,8,9,10-tetrahydrobenzo[a]pyrene at guanines in CPG sequences (i.e., -C-phosphate-G-) has been found at codons 157, 248 and 273 of the p53 gene, which are mutational hotspots in lung cancer (Schuller et al., 2011). Therefore, methylated CpG dinucleotides are a target for chemical carcinogens in cancer genes. Moreover, epidemiological studies have shown that paternal



exposure to organic solvents containing PAHs escalates the risk of childhood brain tumors in the offspring (Cordier et al., 2004).

2.5. PAHs act as modulators of cell death (apoptosis and autophagy)

Cell death by apoptosis occurs via the coordinated action of many different gene products. Particulate pollutants are considered to be potent oxidants, and induction of the intrinsic apoptosis pathway may be associated with oxidative stress generated from organic compounds (i.e., PAHs and nitro-PAHs/ketones/quinones) as well as inorganic compounds adsorbed on the surfaces of particles (Andersson et al., 2009). For example, B[a]P induces apoptosis-like cell death mediated via the mitochondrial pathway in a p53-dependent manner in hepatic cells and macrophages (Van Grevenynghe et al., 2004).

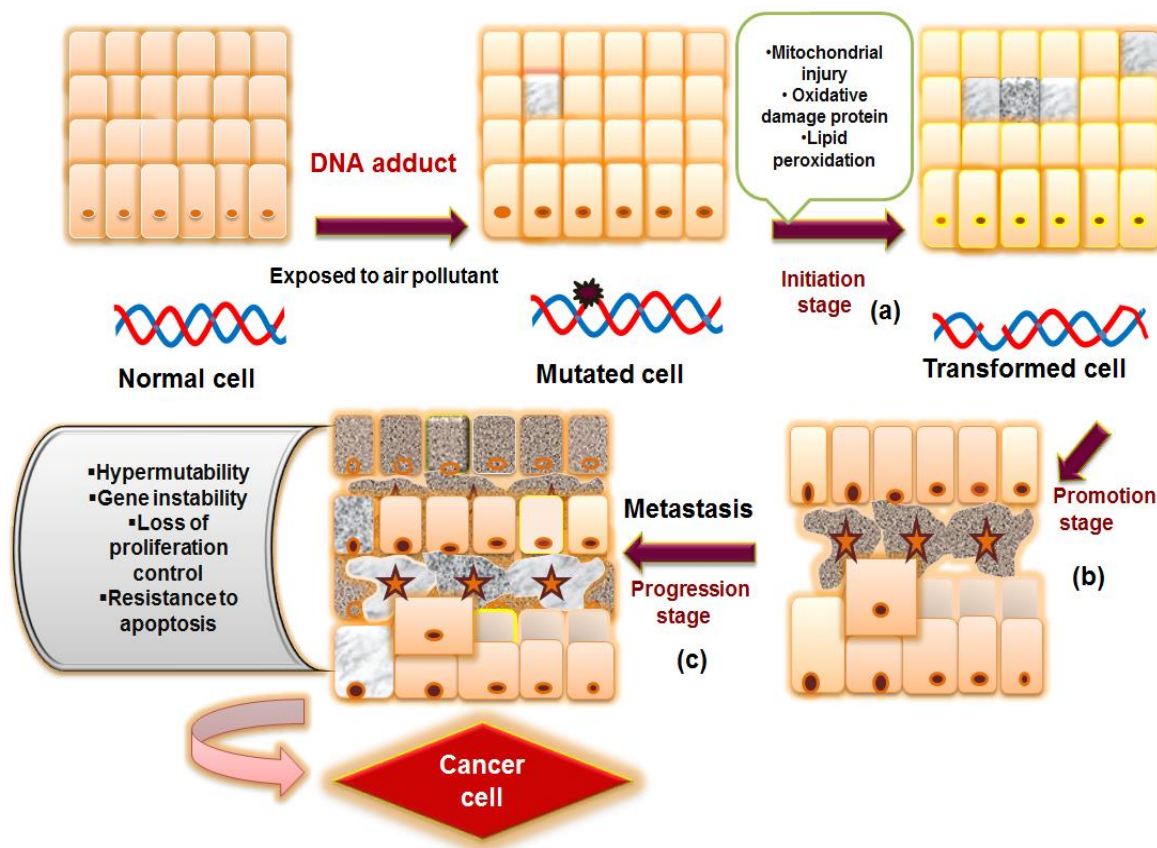


Fig.2.3. Chemical carcinogenesis is a multistep process. PAHs after activation with cytochrome P450, in normal cell DNA adduct formation take place, which plays a role in carcinogenesis; main stages of carcinogenesis: (a) Initiation stage- is based on DNA mutation which inflict DNA damage in a variety of ways, altering or removing individual bases and triggering breaks in one or both DNA strands, (b) Promotion stage-initiated cell is stimulated to proliferate, (c) Tumor progression stage, further mutations and epigenetic changes in gene expression generate

variant cells exhibiting enhanced growth rates on other aggressive properties that give assured cells a selective advantage to proliferate their companions and become the predominant cell population in the tumor formation.

Moreover, a low concentration of B[a]P induces apoptosis in the rat hepatic epithelial F258 cell line through multiple pathways. In addition to the activation of the p53 apoptotic pathway, the production of H₂O₂ during B[a]P metabolism is responsible for early NHE1 activation, which results in intracellular alkalinization. Both the p53 and NHE1 pathways induce mitochondrial dysfunction, which is responsible for the late phase of ROS production and secondary intracellular acidification (Huc et al., 2007). Interestingly, B[a]P-7,8-dihydrodiol is linked to the activation of AHR and the induction of CYP1A1, leading to the formation of BPDE-2, which induces apoptosis in the human HepG2 cell line (Roh et al., 2012). Moreover, B[a]P induces apoptosis in keratinocytes through oxidative and nitrosative stress, which is accompanied by complex changes in eNOS phosphorylation and changes in the Akt and MAPK pathways (Bölck et al., 2014). Aluminum and B[a]P exert synergistic effects on neural cells to induce apoptosis, and this effect is characteristic of neurodegenerative diseases (Jinzhu et al., 2015). Similarly, TCDD-induced apoptosis is accompanied by p53 accumulation and an imbalance of Bax/Bcl2. The induction of apoptosis by TCDD through the modulation of Bcl2 and Bax, release of cytochrome c, and subsequent caspase 3 activation and increased apoptosis after TCDD exposure has been demonstrated in several cell types, such as T-cells (Kobayashi et al., 2009), dendritic cells (Singh et al., 2009), and pituitary cells (Huang et al., 2005).

It is generally accepted that the inhibition of apoptosis plays a role in the carcinogenic process. Loss of apoptosis can affect tumor initiation, progression, and metastasis, and mutations in many cancer-related genes can disrupt the apoptotic pathway. TCDD was reported to show antagonistic effects in various well reported instances of DNA damage-induced apoptosis in a human mammary epithelial cell line (Park and Matsumura, 2006) and in rat hepatocytes (Chopra et al., 2009). TCDD is reported to inhibit apoptosis initiated by EGF withdrawal in a normal human mammary epithelial cell line (Davis et al., 2000). Generally, activation mediated by EGFR and IGF-receptor, and their cognate signaling pathways act as a potential mechanism of mammary tumor promotion and progression. TCDD inhibits DNA fragmentation and suppresses intensification in phosphorylation of p53. Interestingly, TCDD trigger genotoxic damage by p53 pathway in rat liver, both *in vitro* and



in vivo (Paajarvi et al., 2005). In human MCF-10A mammary epithelial cells, TCDD protects cells from apoptosis induced by a variety of stimuli (Park and Matsumura, 2006). TCDD inhibits apoptosis induced by genotoxic treatment, both *in vitro* and *in vivo* in innumerable models of human, rat, and mouse origin (Chopra et al., 2009). In addition, TCDD at a low concentration induces cell death by autophagy in Madin-Darby bovine kidney cells (Fiorito et al., 2011). At higher concentrations, it induces protective autophagy along with apoptosis through ROS generation in SH-SY5Y cells. Additionally, the inhibition of autophagy with 3-methyladenine significantly improves TCDD-mediated apoptosis (Zhao et al., 2015).

2.6. Activation and suppression of immune cells with PAHs

There exists a high prevalence of allergy-based diseases in individuals residing in industrial belts. Allergic diseases epitomize a major health problem and are linked to affluence and a modern lifestyle. Workers from different industries show alterations in the immune response, including the innate and adaptive systems. For example, people who work in stainless steel welding show alterations in phagocytic activity as well as cellular and humoral immunity. B[a]P can stimulate IL-8 gene expression in A549 lung epithelial cells with the induction of NF- κ B activation. Overexpression of I κ B α inhibits 1-NP, which induces the transcription of IL-8. This indicates that PAH-induced IL-8 regulation may be mediated by NF- κ B (Gentner and Weber, 2011). Moreover, TCDD can act directly on peritoneal macrophages, resulting in increases in tumor necrosis factor (TNF) production (Nohara et al., 2000). Accordingly, air particle exposure leads to an influx of neutrophils to tissues, which can be directed by numerous chemotactic mediators and which can increase the release of cytokines such as IL-8, TNF, and IL-1 β (Saber Hosnijeh et al., 2012).

In contrast, a study has shown that PAHs inhibit the differentiation of human monocytes into macrophages, as demonstrated by endocytosis, phagocytosis, LPS-triggered production of TNF α , and stimulation of allogeneic lymphocyte proliferation (Song et al., 2004). Similarly, exposure to TCDD, which induces AHR activation, leads to the suppression of both humoral and cellular immune responses and results in increased susceptibility to various types of infections (Stevens et al., 2009). TCDD also suppresses T cell-dependent B cell antibody production, persuades thymocyte loss, thymocyte proliferation arrest, and premature emigration of T-cell progenitors, and inhibits the CD8⁺ T cell response to influenza infections, indicating a role of AHR activation in the suppression of T cell-mediated immunity. It also increases the



toxicity of lipopolysaccharides on mice by enhancing the production of TNF- α and IL-1 by macrophages (Sulentic and Kaminski, 2011). Additionally, it decreases survival and enhances IFN- γ production in mice infected with influenza by an AHR-independent mechanism in bone marrow-derived cells (Neff-LaFord et al., 2007). In mice, dimethylbenzanthracene, B[a]P and methylcholanthrene suppress antibody production against both T-dependent and T-independent antigens. Indirect evidence has shown that children and adults with B cell-pertinent primary immunodeficiency syndromes exhibit reduced circulating immunoglobulins, and are prone to recurrent infections and allergic diseases. This leads to an eminent risk for non-Hodgkin lymphoma, and the increased occurrence of non-Hodgkin lymphoma has been reported in TCDD-exposed individuals. It is assumed that exposure to low and moderate levels of industrial pollutants generate a strong immune response, which results in allergic diseases. However, high doses of PAHs in an industrial area are associated with immune suppression by altering B- and T-cell maturation or function, and this regulates cancer progression. Moreover, TCDD can induce regulatory T cell production, suggesting that the existence of endogenous AHR ligands enhances regulatory T cell production in the tumor microenvironment (Funatake et al., 2008).

2.7. Modulation of cytochrome P450: Novel options for cancer therapeutics

Cytochrome P450 enzymes, especially isozymes of the P450 families 1, 2, and 3, are responsible for the metabolism of a wide assortment of PAHs with reactive intermediates, leading to many cellular and molecular alterations that mediate carcinogenesis. Prospective strategies targeting P450 inhibition could improve potential cancer preventative and therapeutic agents and the development of new selective inhibitors of these enzymes is a great challenge. Clinical studies and *in vitro* experiments have demonstrated that the combined administration of anticancer drugs and CYP enzyme inhibitors affect the efficacy of cancer therapy drugs. Anticancer bioactive compounds, including flavonoids, polyphenols, and several derivatives from fruits, contain a large number of CYP enzyme inhibitors that might have protective effects against PAH-mediated carcinogenesis. For example, resveratrol, an anticancer compound found in several fruits, including raspberries, blueberries, cranberries, peanuts, and some species of pine trees, inhibits CYP1A1 in humans and has a protective function against tumor formation and carcinogenesis (Chun et al., 2005). Interestingly, 2,4,3',5'-tetramethoxystilbene (2,4,3',5'-TMS), a methoxy



derivative of resveratrol, significantly suppresses 7-ethoxyresorufin-*O*-deethylase (EROD) activity and *CYP1A1* and *CYP1B1* induction by TCDD, and induced apoptosis in human tumor cells, including HepG2, MCF-7, and HL-60 cells (Han et al., 2011). Similarly, capsaicin, a constituent of peppers that inhibits 3-methylcholanthrene (3-MC) induces CYP1A1 through the activation of C/EBP β and blocks the AHR signaling pathway (Poon et al., 2013). The consumption of fruits and vegetables is chemopreventive, and naringenin, a citrus flavonoid, suppresses *CYP1B1* expression at the transcriptional level induced by 7,12-dimethylbenz(a)anthracene (DMBA) by antagonizing xenobiotic-responsive element binding in MCF-7 cells (Hidaka et al., 2004). Pineapple juice contains bromelain, which degrades CYP2C9 and acts as a potent inhibitor in liver microsomes (Fenneteau et al., 2010). In another study, furanocoumarins from grape fruits and from the juice of other fruits, such as banpeiyu, pomegranate, star fruit, and black berries, were also found to inhibit CYP3A (Fujita et al., 2003; Hidaka et al., 2006). The anticancer agent β -lapachone, a quinone isolated from lapacho trees, was shown to inhibit all CYP isozymes tested, including CYP1A2, CYP2A6, CYP2C8, CYP2C9, CYP2C19, CYP2D6, and CYP3A4 (Kim et al., 2006).

Fruits and vegetables consumption along with clinically administered drugs may cause interactions between bioactive agents in fruits and vegetables and drugs by pharmacokinetic regulation, which results in an upsurge in toxicity or a decrease in therapeutic effect (Rodríguez-Fragoso et al., 2011). Future research regarding the chemoprevention associated with flavonoids and other dietary phenolics should be highlighted as therapeutic agents.

2.8. Scope of present investigation

PAHs are considered new members of the growing group of harmful air pollutants, creating havoc in our ecological balance and promoting carcinogenesis. B[a]P is the most potent according to the Environmental Protection Agency. The B[a]P has been the source of increasing concern in the human health due to wide-spread dispersion in the environment and the adverse health effects including carcinogenesis associated with PAHs exposure. The B[a]P induces cellular toxicity through regulation of the generation of reactive oxygen species (ROS) mediated apoptosis. Moreover, B[a]P induces phosphorylation and aggregation of tumor suppressor protein p53 leading to the formation of DNA adduct followed to apoptosis. In addition, B[a]P is



oxidised by many cytochrome P450 enzymes to several intermediates which have the ability to bind to the nuclear DNA covalently and this binding result in the mutation, replication error and apoptosis mediated cell death. This thesis is mainly focused on elucidating the mechanism of B[a]P-mediated cellular toxicity and elucidating the further scope for the development of potential inhibitors against environmental air pollutants. In addition, this thesis is embodied with another discovery, *Bacopa monneiri* (BM) plant extract as an inducer of protective autophagy, which may directly contribute to the antioxidant promoting potential of BM on B[a]P induced cell death through Beclin-1 dependent autophagy activation.

Objective of the research

The following objectives are investigated to study the mechanisms of benzo[a]pyrene mediated apoptotic and autophagic cell death and its prevention.

1. In vitro mutagenic and genotoxic effects of native airborne particulate matter and its clinical significance.
2. Prediction and validation of apoptosis through cytochrome P450 activation by benzo[a]pyrene.
3. Benzo[a]pyrene mediated mitochondrial stress induces autophagy-dependent cell death.
4. Cytoprotective activity of *Bacopa monneiri* against benzo[a]pyrene induced apoptosis through modulation of autophagy.



Chapter 3

In vitro mutagenic and genotoxic effects of native airborne particulate matter and its clinical significance



Abstract

Epidemiologic studies have shown that airborne particulate matter (PM) exposure has both acute and chronic effects on human health. Here, we examined the potential adverse health effects of PM using data collected in the urbanized Rourkela City, Odisha, India. The PM was found to contain benzo[a]pyrene and other unidentified molecules, which had significant mutagenicity potential as demonstrated with the Ames test. We studied the effect of PM on immortalized human keratinocyte (HaCaT) cells and PM-induced DNA damage and pro-apoptotic signaling. Our study showed that the generation of reactive oxygen and nitrogen species after PM exposure could induce cellular oxidative stress and apoptosis. An increase in 7-ethoxyresorufin-O-deethylase (EROD) activities was observed in a dose-dependent manner in the presence of PM. Moreover, genetic and pharmacological inhibition of cytochrome P450 1B1 (CYP1B1) resulted in suppression of PM-induced apoptosis in HaCaT cells, confirming the crucial role of CYP1B1 in PM-induced apoptosis. Blood analysis by immunophenotyping and the comet assay did not show significant differences between samples obtained from people from industrial and non-industrial zones, in terms of alternations in immune cells and DNA damage activity, indicating that PM did not affect the people living in Rourkela City. In summary, this study provides an indication of potential environmental issues in Rourkela City and the preventive management required in the future to improve human health.

Keywords: Particulate matter; Cytochrome P450; Apoptosis; DNA damage; Reactive oxygen and nitrogen species



3.1. Introduction

Particulate matter (PM) is the component of air pollution believed to be responsible for many adverse health effects; the health impact depend on the pollutant type and concentration, length of exposure, other coexisting pollutants, and individual susceptibility. Most studies involving PM have often represented particles with mass concentration smaller than 10 μm (PM_{10}) or 2.5 μm ($\text{PM}_{2.5}$). Moreover, the metal content and the presence of polycyclic aromatic hydrocarbons (PAHs) and other organic components, such as endotoxins, mainly contribute to PM toxicity (Valavanidis et al., 2008; Barakat-Haddad et al., 2012).

PM, from industries and other different exhausts, is associated with adverse health effects, and numerous epidemiological studies have revealed increased morbidity and mortality due to PM (Pope et al., 2006; Beyea et al., 2013; Strak et al., 2013). These health effects include damage to the immune system, reduced fertility, developmental, respiratory, and other health problems. Moreover, it is thought to aggravate chronic respiratory and cardiovascular diseases, alter host defenses, damage lung tissue, and presumably contributes to cancer in addition to resulting in premature death (Brook et al., 2004; Atkinson et al., 2014). The PM fraction of air pollution contains a number of constituents that may increase the generation of reactive oxygen species (ROS) by a variety of reactions, such as transition metal catalysis, metabolism, redox cycling of quinones, and inflammation. PM causes oxidative damage to DNA, including guanine oxidation, which is mutagenic. In addition, PAHs and volatile organic compounds (e.g., benzene) may be metabolically activated to reactive species that form bulky adducts on the DNA. The particulate pollutants are considered potent oxidants, and the induction of the intrinsic and extrinsic pathways of apoptosis may be associated with oxidative stress generated by the organic compound (i.e., PAHs, nitro-PAHs/ketones/quinones) as well as inorganic compounds adsorbed on the surface of particles (Xia et al., 2004; Anderson et al., 2012; Jin et al., 2014). Moreover, PAHs, like benzo[a]pyrene (B[a]P) and dioxin, which are activated by cytochrome P450 (CYP450), play a role in the induction of DNA damage, reactive oxygen and nitrogen species, apoptosis, immune alternations, and cancer.

Here, we investigated the potential adverse health effects of PM collected in urbanized Rourkela, an industrial city in the state of Odisha, India. Rourkela is surrounded by a giant steel plant, several medium-scale industries like cement, refractories, sponge iron, explosive, and



chemical plants, and many smaller-scale industries. A survey of the regional transport office revealed that more than 1,50,000 small and heavy vehicles are registered in the industrial complex (Naik, 2005). In this study, PM from Rourkela was characterized by fluorescence spectroscopy and nuclear magnetic resonance (NMR), and the mutagenicity potential was deciphered by Ames test. The cytotoxic and apoptotic inducing activity of PM was demonstrated in immortalized human keratinocyte (HaCaT) cells. Moreover, our study showed that the generation of ROS and reactive nitrogen species (RNS) after PM exposure can induce cellular oxidative stress and apoptosis. The data showed that the biological activity of PM, including apoptosis, was regulated by CYP450. In addition, we showed that PM present in an industrial zone in Rourkela had no effect on the blood cells of people living in Rourkela.

3.2. Materials and methods

3.2.1. Chemicals and reagents

Benzo[a]pyrene (B[a]P), 2,3,7,8-tetrachlorodibenzo-*p*-dioxin (TCDD), dimethyl sulfoxide (DMSO), 3-[4,5-dimethylthiazol-2-yl]-2,5-diphenyltetrazolium bromide (MTT), and clotrimazole (CTZ) were procured from Sigma (USA). The "cluster of differentiation" CD markers and annexin V were from BD Bioscience, and the Caspase-Glo assay kit was purchased from Promega (USA). The CYP1B1 small interfering RNA (siRNA) and control siRNA were obtained from Santa Cruz Biotechnology (USA). Glass microfiber filter paper was purchased from Quartz Microfiber (USA), and *Salmonella typhimurium* (29629) was obtained from ATCC (USA).

3.2.2. Study areas

Rourkela, an industrial city, was selected as a study area in the present research work, with sampling from the area of the Indira Gandhi Park and the academic complex of (National Institute of Technology) NIT Rourkela. It is one of the most important industrial cities in the Sundargarh district of the State of Odisha in India and has a population of more than 4,00,000. Blood samples were collected on a volunteer basis from people in the non-industrial zone and from people exposed to PM in the industrial zone in Rourkela. The institutional ethics committee at NIT Rourkela approved the protocol for blood collection.



3.2.3. Sampling and analysis of particulate matter from Rourkela

Air was drawn through a size-selective inlet and through a 20.3 × 25.4-cm filter. The filter collected particles with an aerodynamic diameter less than the cut-off of the inlet. Air was drawn through a filter and into a covered housing by a high flow rate blower at 1.1 to 1.5 cum/min, which allowed suspended particulate matter with diameter < 10 μm (Stokes equivalent diameter) to collect on the filter surface. During this period, the diurnal air sampling time was nominally 8 h. Particles with diameters of 0.1 to 10 μm were collected on glass microfiber filters.

3.2.4. Fluorescence spectroscopy

The fluorescence spectrum was measured using a spectrofluorometer (Horiba, USA) with a pulsed xenon lamp for excitation, an optical light conductor, and a measuring probe. Fluorescence spectra were obtained with scanning λ_{max} from 380 to 650 nm to detect the presence of B[a]P in PM by comparing the spectra with a standard curve constructed using different concentrations of B[a]P (Patra, 2003).

3.2.5. NMR analysis

The PM in air pollutants was separated using preparative thin layer chromatography (TLC) with an n-hexane: ethyl acetate (95:5 v/v) solvent mixture. A light yellow colored compound, which is visible in the UV spectrum, was separated out and dissolved in chloroform-d ($^2\text{H}_2\text{CCl}_2$), and the ^1H NMR spectrum was determined. High-resolution ^1H NMR spectra were recorded on a 400 MHz Bruker spectrometer in $^2\text{H}_2\text{CCl}_2$. Samples (1 mg/ml in $^2\text{H}_2\text{CCl}_2$) were degassed and sealed under an atmosphere of argon. Chemical shifts are reported in ppm downfield from tetramethylsilane (Me, Si). The central resonance of $^2\text{H}_2\text{CCl}_2$ was used as an internal reference (Zhang et al., 2011).

3.2.6. Ames test

The mutagenicity of PM was tested by the well-accepted Ames test using His⁻ *Salmonella typhimurium*. We performed the plate incorporation assay with PM collected from Rourkela. The number of His revertants was counted and the mutagenic ratio (MR) was calculated as the ratio between the mean number of revertants on plates treated with a sample and the mean number of negative control plates. A sample was considered mutagenic when the MR and a clear dose–response relationship were observed. The number of revertants was evaluated and quantified.



3.2.7. Cell culture

The HaCaT cells and mouse macrophage cells (RAW 264.7) were obtained from the National Centre for Cell Science, Pune, India, and cultured in Dulbecco's Modified Eagle's Medium with high glucose (DMEM/high glucose), supplemented with 10% heat-inactivated fetal bovine serum (FBS) containing 1% penicillin-streptomycin. The cells were maintained at 37°C in a humidified atmosphere with 5% CO₂. All media, supplements, and antibiotics were purchased from Invitrogen Bangalore, India.

3.2.8. Cell viability by the MTT assay

HaCaT cells were harvested from maintenance cultures in the logarithmic phase and were counted with a hemocytometer using Trypan blue solution. HaCaT (1×10⁵ cells/well) were cultured in a 96-well plate at 37 °C and exposed to various concentrations of PM for 72 h. Next, MTT solution (5 mg/ml) was added and incubated for 4 h; the resultant formazan crystals were dissolved in DMSO and the absorbance was measured in a microplate reader (Perkin Elmer) at 595 nm. All experiments were performed in triplicate, and the relative cell viability is expressed as percentage relative to the untreated control cells (Das et al., 2014).

3.2.9. Annexin V staining

HaCaT cells were trypsinized after 48 h PM treatment and washed with phosphate-buffered saline (PBS). The cell pellets were incubated with annexin V and propidium iodide in binding buffer and analyzed by flow cytometry (Becton Dickinson Immunocytometry Systems, USA). (Das et al., 2014).

3.2.10. Caspase assays

HaCaT cells were seeded in 6-well plates and treated with PM for 48 h. After the treatment, caspase activity was measured using the Caspase-Glo assay, according to the manufacturer's instructions (Promega Corp., Madison, WI, USA).

3.2.11. CYP1B1 knockdown using siRNA

HaCaT cells were cultured in 60 mm plates and transfected with Lipofectamine 2000® reagent (Invitrogen) in the presence of siRNAs specific for human CYP1B1 or control siRNA. HaCaT cells 48 h after transfection were used for RNA extraction and apoptosis studies.

3.2.12. 7-Ethoxyresorufin-O-deethylase (EROD) assay

The ability of PM particles to induce CYP450 enzyme activity was evaluated in intact cells by measuring EROD activity. In 96-well plates, HaCaT cells were exposed to various



concentrations of PM for 24 h. Subsequently, HaCaT cells were washed with PBS buffer and incubated with EROD for 30 min. The fluorescence intensity, which was a result of conversion of ethoxyresorufin to resorufin by CYP450 enzymes, was measured using a microplate reader (Perkin Elmer) with excitation and emission wavelengths of 530 nm and 590 nm, respectively (Fernández et al., 2013).

3.2.13. ROS generation

To detect ROS, HaCaT cells were exposed to different concentrations of PM for 24 h. HaCaT cells were incubated with 2.5 µg/ml dihydrorhodamine 123 (DHR 123) in PBS for 30 min in the CO₂ incubator. DHR 123 is rapidly taken up by cells and converted to rhodamine 123 (Rh 123) in the presence of ROS. Cells incubated with DHR 123 were washed 3 times in PBS for 5 min, fixed for 30 min in 4% paraformaldehyde in phosphate buffer, washed again, and observed under an Olympus IX-71 fluorescence microscope, America INC. For flow cytometry analysis, HaCaT cells were harvested and suspended in PBS, and ROS generation was detected by measuring the fluorescence intensity at 530 nm FACScan flow cytometer (BD Biosciences, USA) (Loxham et al., 2015).

3.2.14. Nitric oxide (NO) determination

NO was quantified in the cell supernatant of RAW 264.7 cells 24 h after treatment with the PM. It was measured by adding 100 µl of Griess reagent [0.1% (w/v) naphthylethylene diamine HCl and 1% (w/v) sulfanilamide in 5% (v/v) phosphoric acid (vol. 1:1)] to 100 µl cell supernatant. After incubation for 20 min in the dark, the optical density was measured at 550 nm using a microplate reader (PerkinElmer).

3.2.15. Single cell gel electrophoresis

The comet assay was performed measure DNA damage. Briefly, HaCaT cell suspensions were pipetted onto the agarose-covered surface of a pre-coated slide. Then, the slides were submerged in a covered dish containing lysis solution overnight in the dark at 4 °C. After overnight lysis, slides were removed and submerged in rinse solution for about 20 min, and this wash was repeated three times to ensure removal of salts and detergent. Next, electrophoresis was performed by submerging the slide in fresh A2 electrophoresis solution for 25 min at a voltage of 0.6 V/cm. After electrophoresis, the slides were removed, rinsed, and neutralized in 400 ml of distilled water. Then, propidium iodide staining was performed and the slides were analyzed under a fluorescence microscope (Olympus IX-71). The cell images were analyzed



using CASP software (downloaded from www.casplab.com). All experiments were performed in triplicate (Panda et al., 2014).

3.2.16. Immunophenotyping by flow cytometry

Single cell suspensions of blood samples were collected voluntarily from people living in Rourkela under aseptic conditions. About 100 μ l of blood was added to lysis buffer, and the mixture was incubated for 15 min at room temperature. The suspension was centrifuged to obtain the cell pellet. The cell pellet was washed with PBS and CD markers containing antibodies against CD3-FITC, CD4-APC, CD8-PE, CD19-APC, CD45-PerCP, CD14-PE, and CD16-PE, and CD56-APC cells were measured using flow cytometry. The data were analyzed using Cell Quest Pro software on a FACS Calibur Becton-Dickinson flow cytometer (Birgisdottir. et al., 2013).

3.2.17. Statistical analysis

All data are given as the mean \pm SD. Experimental results were analyzed by Student's *t*-test. *P* values less than 0.05 were considered statistically significant when comparing treated and control samples. Box plots and histograms were used to see the distribution of variables. The *t*-test was performed to enumerate the difference between risk scores in the two populations from either the industrial or non-industrial zones.

3.3 Results

3.3.1. Characterization and mutagenic potential of PM from Rourkela

PM is composed of both fine and coarse particles. Coarse particles in PM are 2.5 to 10 μ m in diameter. Fine particles formed from gases and organic pollutants in the atmosphere are less than 2.5 μ m in diameter. The monitored air samples from Indira Gandhi Park and the academic complex of NIT of Rourkela contained 6.08 and 0.5 mg/m^3 PM, respectively, after 8 h of air sampling (Fig.3.1.A). Samples were extracted from the sampled filter strip by immersing them in acetonitrile and further extracted samples were dried in the rotary vacuum evaporator. The extracted samples were then stored at -80 $^{\circ}\text{C}$ until future use. The samples from an academic complex area of NIT Rourkela were prepared using the same method as the experimental sample and were used as a control in all experiments. Similarly, blanks (unexposed filters) were prepared using the same method except for sampling and were used as a negative control in the experiments.



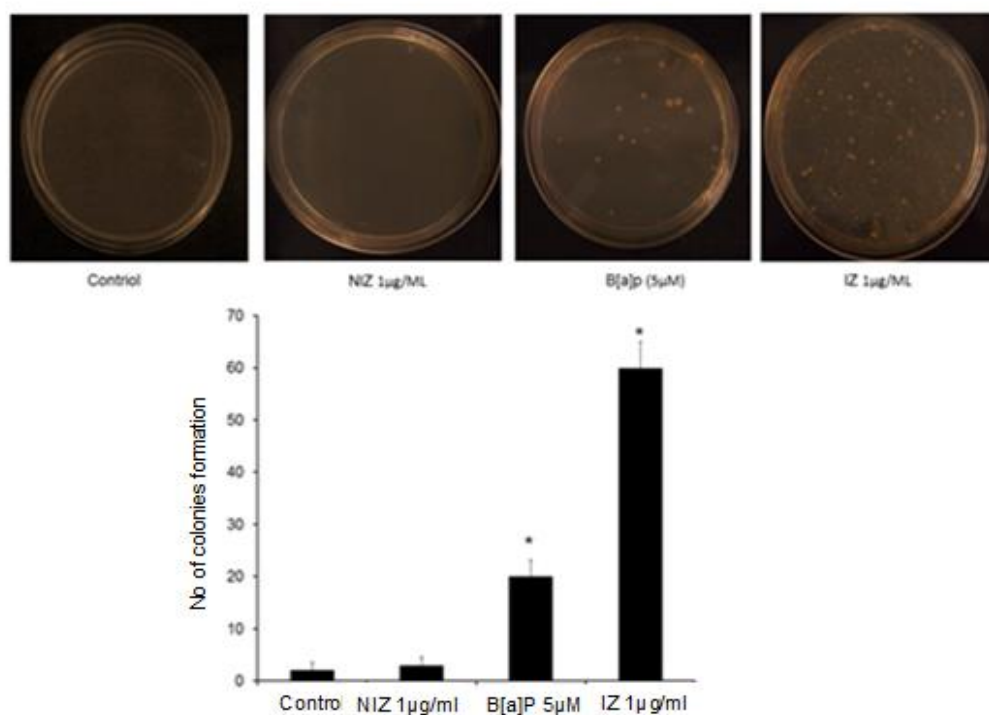
A**B**

Fig.3.1. The PM was collected from different sites of Rourkela city, Odisha with air sampler and glass microfiber filter paper and the mutagenicity of PM was tested by well accepted Ames test using His- *Salmonella typhimurium*. The number of His revertants colonies was counted, and the mutagenic ratio (MR) was calculated as

33



the ratio between the mean number of revertants on plates treated with a sample and the mean number of negative control plates (A and B).

The Ames *Salmonella*/mutagenicity assay is a short-term bacterial reverse mutation assay explicitly designed to detect a wide range of chemical substances that can produce genetic damage that can lead to gene mutations. Of the *Salmonella* tester strains grown on a minimal medium agar plate containing a trace of histidine, only the bacteria that revert to histidine independence (*hisC*) are able to form colonies. Here, we studied the mutagenic activity of PM collected from different areas of Rourkela. Our study showed that the control sample (non-industrial zone) had insignificant colony formation that was comparable to that for the negative control (blank). However, in the case of PM from the industrial zone of Rourkela, mutagenicity significantly increased (12.4-fold over the control) and was higher than that noted for B[a]P (positive control), indicating that PM contains different components with mutagenic properties and promotes colony formation (Fig.3.1.B). The presence of B[a]P in PM was confirmed by fluorescence spectroscopy and NMR, which was trustworthy with results for previously identified industrial zones (Fig.3.2.A and B).



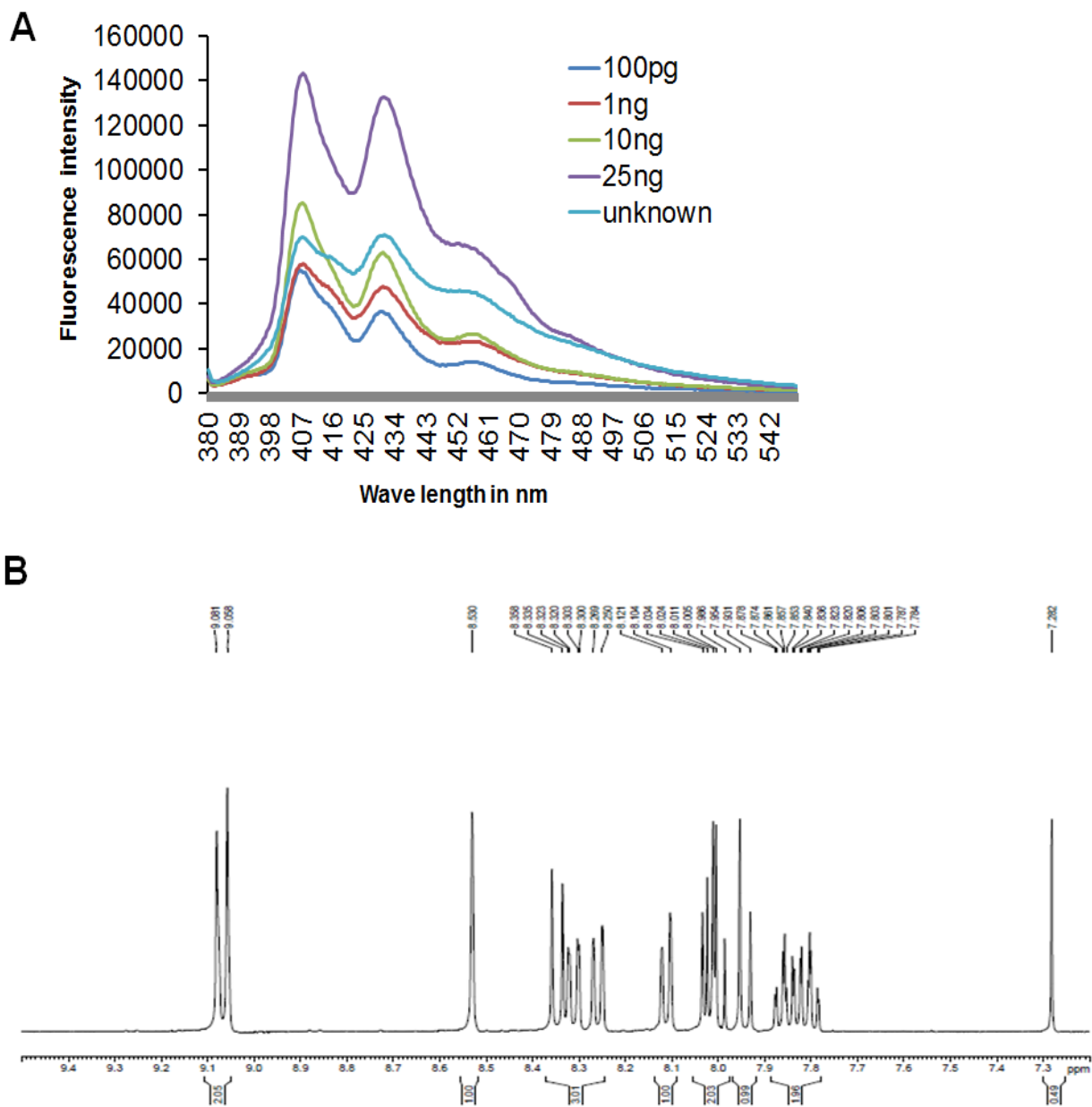


Fig.3.2. The presence of PAHs, including B[a]P and dioxin, in PM from the industrial zone was demonstrated by fluorescence spectroscopy and ^1H NMR. The data showed that B[a]P was present in industrial PM, but dioxin was not detected (A, B).

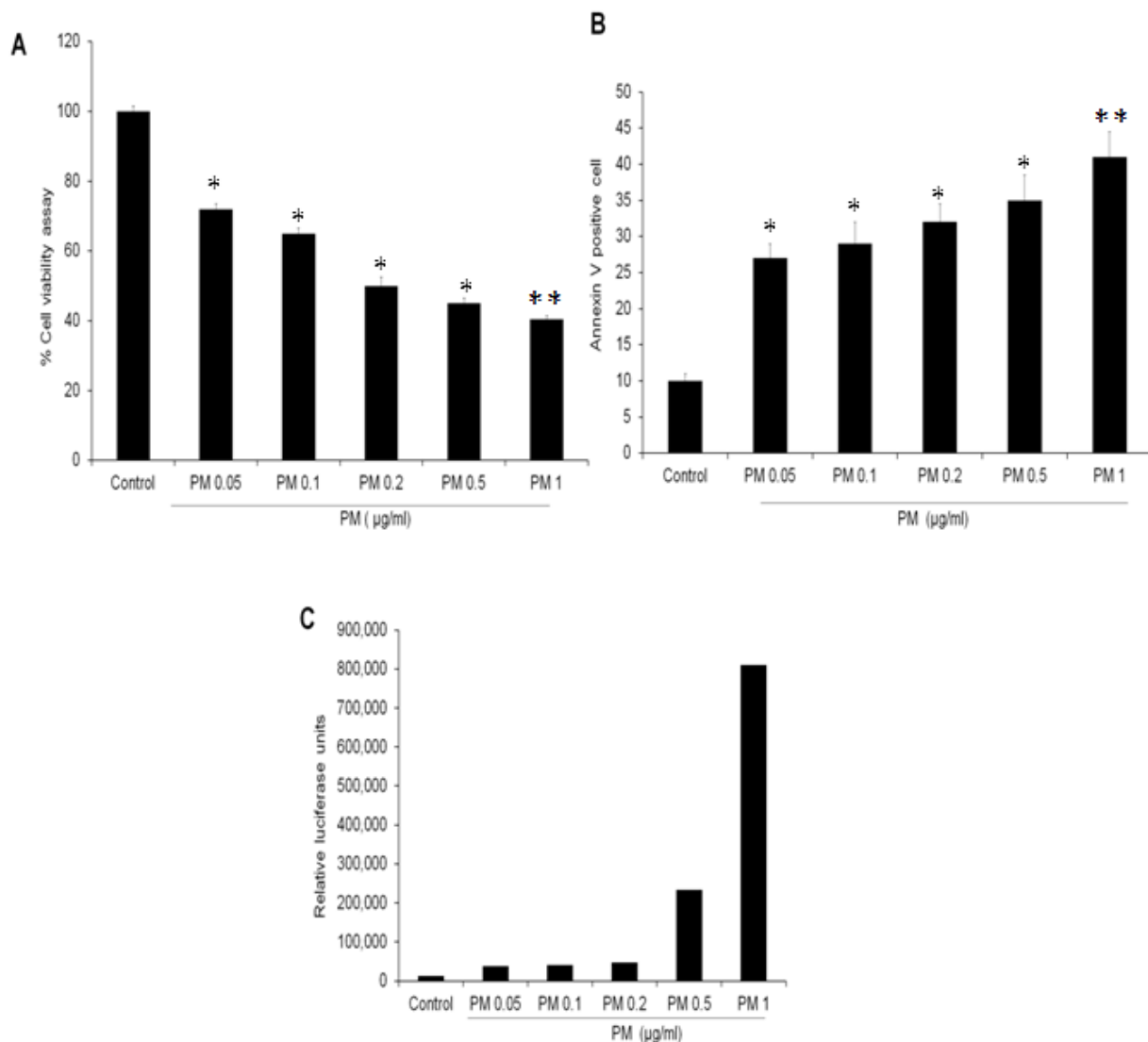


Fig.3.3. HaCaT cells were seeded into each of the 96 well plates and were treated with various concentrations of PM for 72 h and determined by MTT assay (A). The HaCaT cell was treated with PM for 48 h and apoptosis assay was performed by annexin V staining through flow cytometry (B) and analyzed for caspase 3 expression using caspase- Glo assay (C). Data reported as the mean \pm S.D. of three independent experiments and compared against PBS control.*P Values < 0.05 and **P < 0.01 values were considered significant.

3.3.2. PM-induced apoptosis in HaCaT cells

To investigate whether PM does have any cytotoxic effects on normal cells, HaCaT cells were exposed to different concentrations of PM (0.05, 0.1, 0.2, 0.5, and 1 µg/ml) for 72 h, and cell viability was measured by the MTT assay (Fig.3.3.A). Treatment with PM resulted in a decrease in the viability in a dose-dependent manner. We next studied whether the cell death induced by

PM was due to apoptosis and by examining annexin V staining by flow cytometry (Fig.3.3.B). The data showed that PM induced apoptosis in HaCaT cells and that the apoptosis percentage increased in a dose-dependent manner. Apoptosis is characterized by a well-organized sequence of cellular caspases in tandem to trigger the apoptotic pathway. In HaCaT cells, PM induced activation of caspase 3, the essential effector during apoptosis, as measured by the caspase 3/7 Glo assay (Fig.3.3.C), confirming the apoptosis inducing activity of PM collected from the industrial sector of Rourkela.

3.3.3. Generation of ROS and NO by PM

ROS and NO are usually potential factors related to mitochondrion-dependent cell injury and inflammation. To detect ROS production, DHR123 was used; DHR123 is rapidly taken up by cells and converted to Rh 123 in the presence of ROS. PM Treatment increased the fluorescence intensity (level of ROS) in HaCaT cells in a dose-dependent manner, compared to control, as demonstrated by flow cytometry and fluorescence microscopy (Fig. 3.4.A,B). In addition, we quantified NO production using mouse macrophages, which produces nitrite and nitrate in response to xenobiotic compounds. The data showed that PM induced the production of NO in a dose-dependent manner in the Raw 264.7 cell line, confirming the potential adverse effect of PM on human health (Fig. 3.4.C).

3.3.4. PM-induced DNA damage analyzed by the comet assay

HaCaT cells were treated with different concentrations of PM, and DNA damage was detected by the comet assay. Cell images were analyzed using Casp software (downloaded from www.casplab.com). Progressive DNA damage, reflecting the important genotoxic effect of PM, was demonstrated in a dose-dependent manner. The data showed that the percent of DNA in the tail (tail DNA %) and comet tail length were significantly higher than those for the control (Fig. 3.5. A-C).



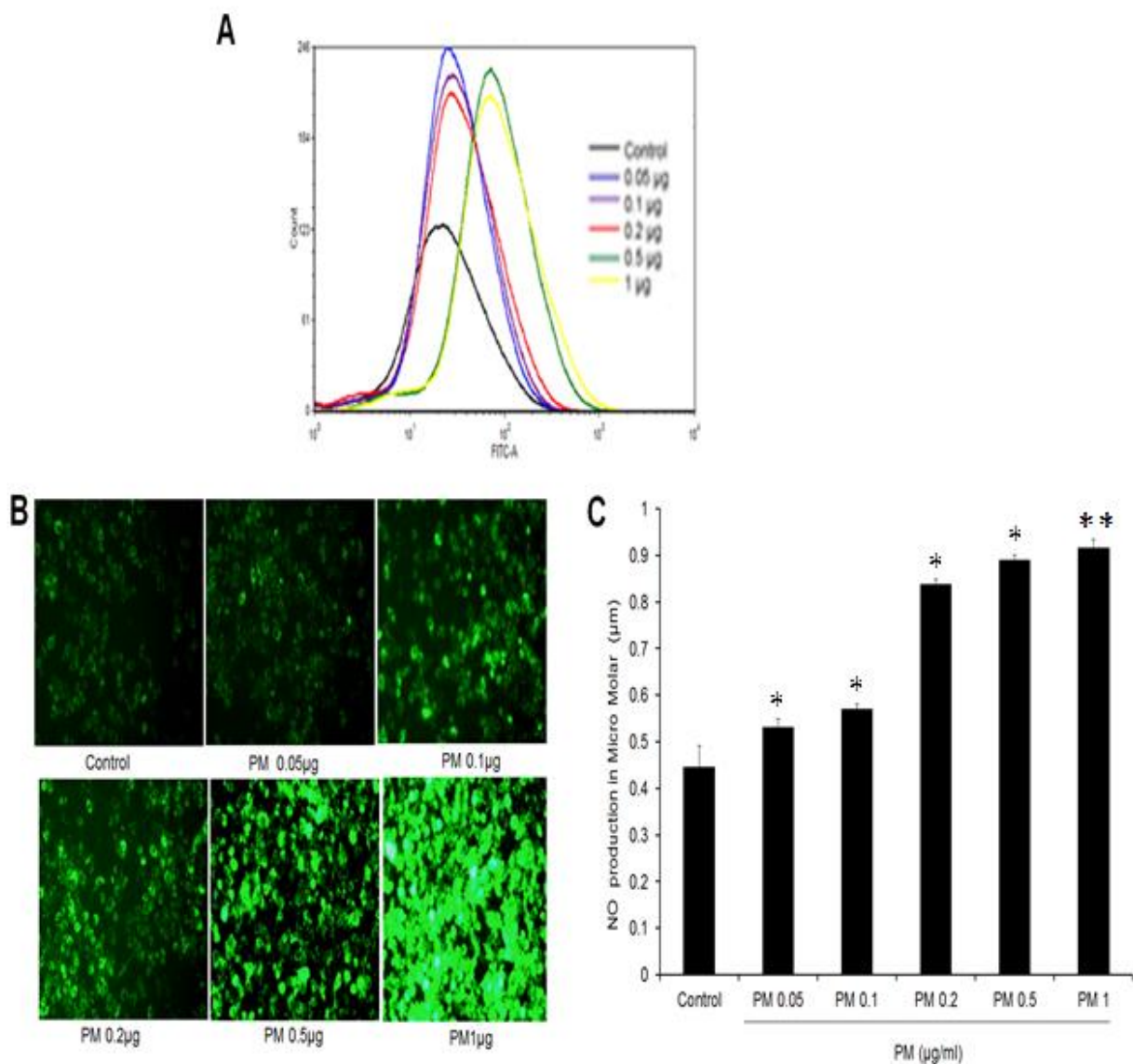


Fig.3.4. Generation of ROS and NO by PM. HaCaT cells were treated with different concentration of PM for 24 h and analyzed for ROS generation by DHR123 through flow cytometry (A) and fluorescence microscopy (B) (Olympus IX71, 400X). RAW 264.7 cells were treated with different concentration of PM for 24 h and nitric oxide production was quantified by using the Griess reagent(C).

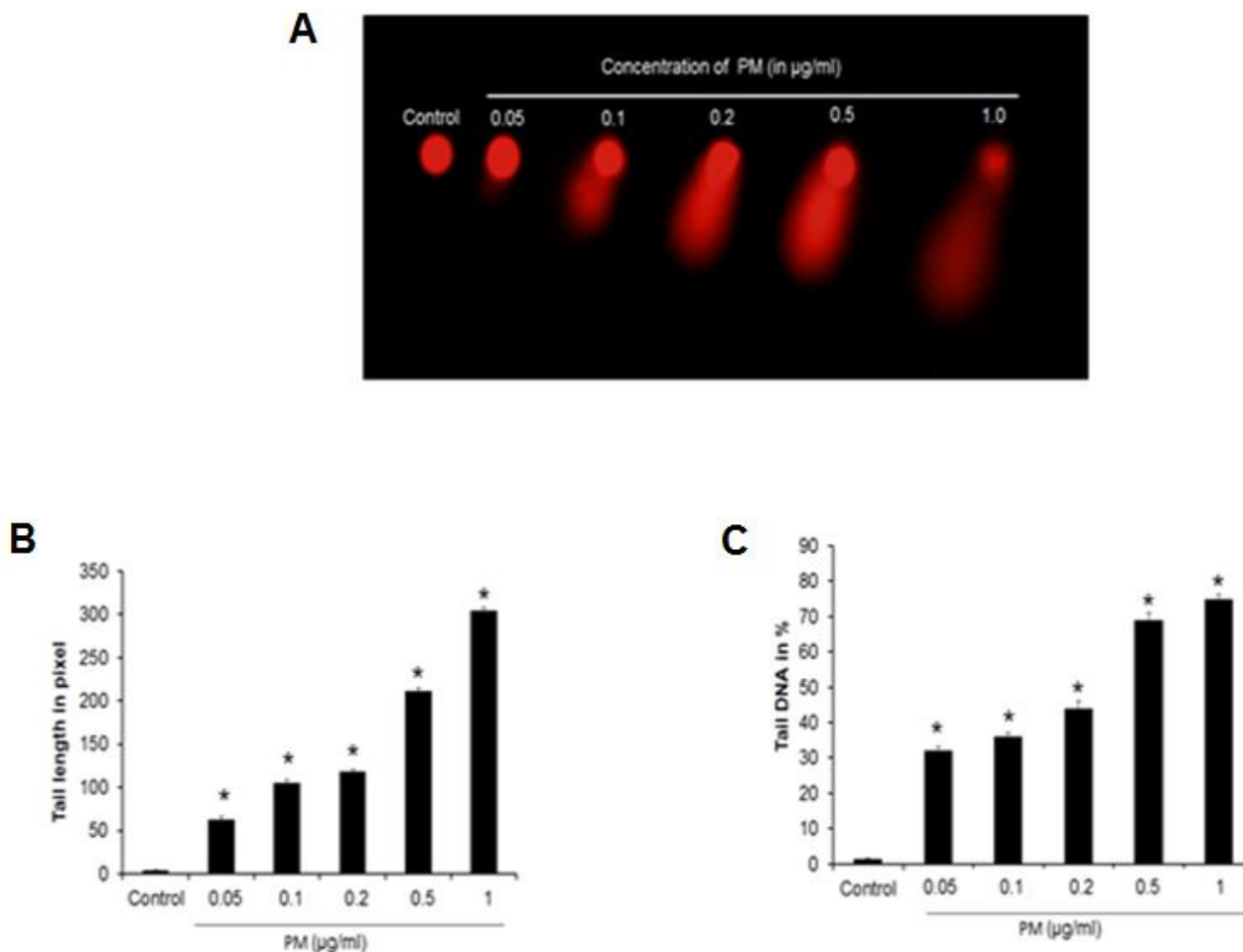


Fig.3.5. PM-induced DNA damage analyzed by the comet assay. HaCaT cells were treated with various doses of PM for 6 h and DNA damage was quantified by the comet assay. After propidium iodide staining, photographs were taken with a fluorescence microscope (Olympus IX71, 400X). Tail length and tail DNA content was measured using CASP software (* $P < 0.05$, compared with control).

3.3.5. Activation of CYP1B1 by PM and inhibition of PM-induced apoptosis by siCYP1B1 and CTZ

CYP450 activation by air pollutants plays a major role in PM-mediated biological phenomena. Here, the EROD assay, which measures combined activity of CYP450, was carried out in PM-treated HaCaT cells. An increase in EROD activity was observed in a dose-dependent manner in the presence of PM (Fig.3.6.A). PAHs present in industrial pollutants are metabolized by the CYP450 family, specifically CYP450 1A1 (CYP1A1) and CYP450 1B1 (CYP1B1), to reactivate

metabolites and induce toxicity. To investigate the potential involvement of CYP1B1 in PM-mediated apoptosis, the CYP1B1 gene was knocked down, and PM sensitivity was examined MTT assay and by measuring caspase-3/7 activity 48 h after treatment. The data showed that targeted CYP1B1 siRNA suppressed the expression of corresponding mRNA as compared to control siRNA, demonstrated by RT-PCR (Das et al., 2014). The CYP1B1 deficient cells exhibited enhanced cell viability after PM treatment as compared to those cells treated with control siRNA. Moreover, we performed the caspase-Glo assay in transfected HaCaT cells in the presence of PM, and the data clearly showed a very significant decrease in caspase 3/7 activity in cells with CYP1B1 knock down, as compared to cells treated with the control siRNA, indicating the specific role of CYP1B1 in PM-mediated apoptosis (Fig.3.6.B, C) (Das et al., 2014).

To further investigate and validate the potential involvement of CYP1B1 in PM-mediated apoptosis, CTZ, a known pharmacological CYP1B1 inhibitor, was used in our study. HaCaT cells were treated with PM in the presence or absence of CTZ, and apoptosis activity was quantified. The MTT assay showed that PM-induced cell death was significantly inhibited in the presence of CTZ as compared to in the absence of CTZ. Next, we performed the caspase-Glo assay in the presence of CTZ, and the data showed that caspase3 activity was very significantly decreased upon treatment with PM in presence of CTZ as compared to in the absences of CTZ (Fig.3.6.D,E).

3.3.6. Blood analysis for people living in Rourkela, by immunophenotyping and the comet assay

To establish the correlation between the *in vitro* activities of air effluent with clinical expression, we examined the blood from people living in the industrial and non-industrial sectors of Rourkela. The blood was collected from volunteer donors and analyzed by immunophenotyping and the comet assay to survey any change in immune cells and DNA damage in blood cells, respectively. The analysis was performed with blood samples from 55 people (35 men and 20 women), including 32 from industrial areas and 23 from around Rourkela City; the average (\pm SD) age of the study population was 35 ± 6.2 years. We did not observe any significant change in the lymphocytes ($p = 0.671$), B cells ($p = 0.104$), cytotoxic T cells ($p = 0.512$), helper T cells ($p = 0.396$), NK cells ($p = 0.675$), and monocytes ($p = 0.170$) in the blood samples from these two groups (Fig.3.7.A-F).



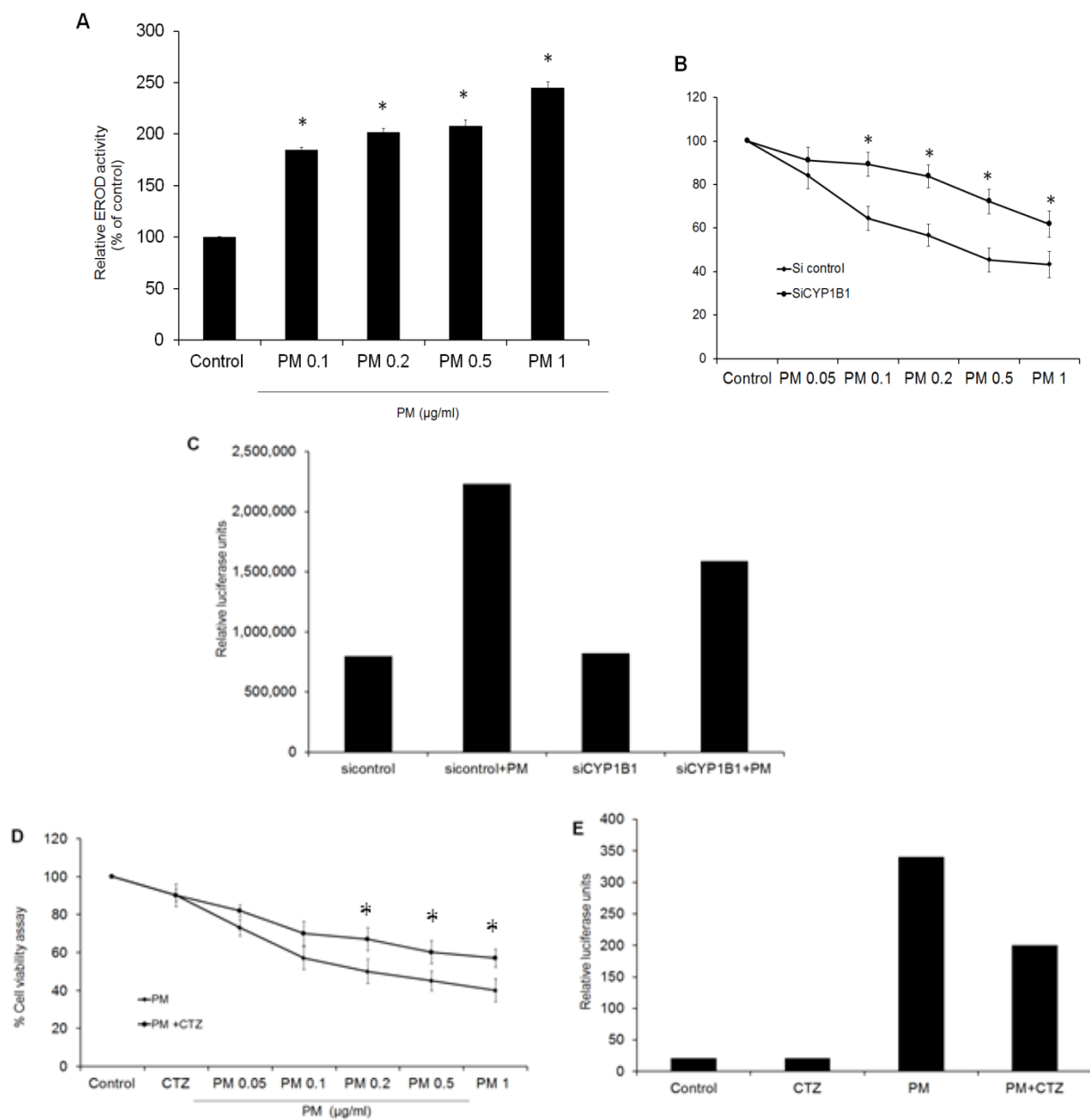


Fig.3.6. Role of cytochrome P450 in PM mediated apoptosis. HaCaT cells were treated with PM for 24 h and Ethoxyresorufin-O-deethylase (EROD) activity of PM was measured at 560 nm in microplate reader (A). HaCaT cells transfected with the indicated siRNA against CYP1B1 or were pre-treated with CTZ (5 µM) for 2 h followed by treatment of different concentration of PM and quantified for MTT assay after 72 h (B and D) and after 48 h apoptosis was quantified by caspase 3/7 Glo assay (C and E). Data reported as the mean ± S.D. of three independent experiments and compared against PBS control. *P Values < 0.05 and **P < 0.01 values were considered significant.

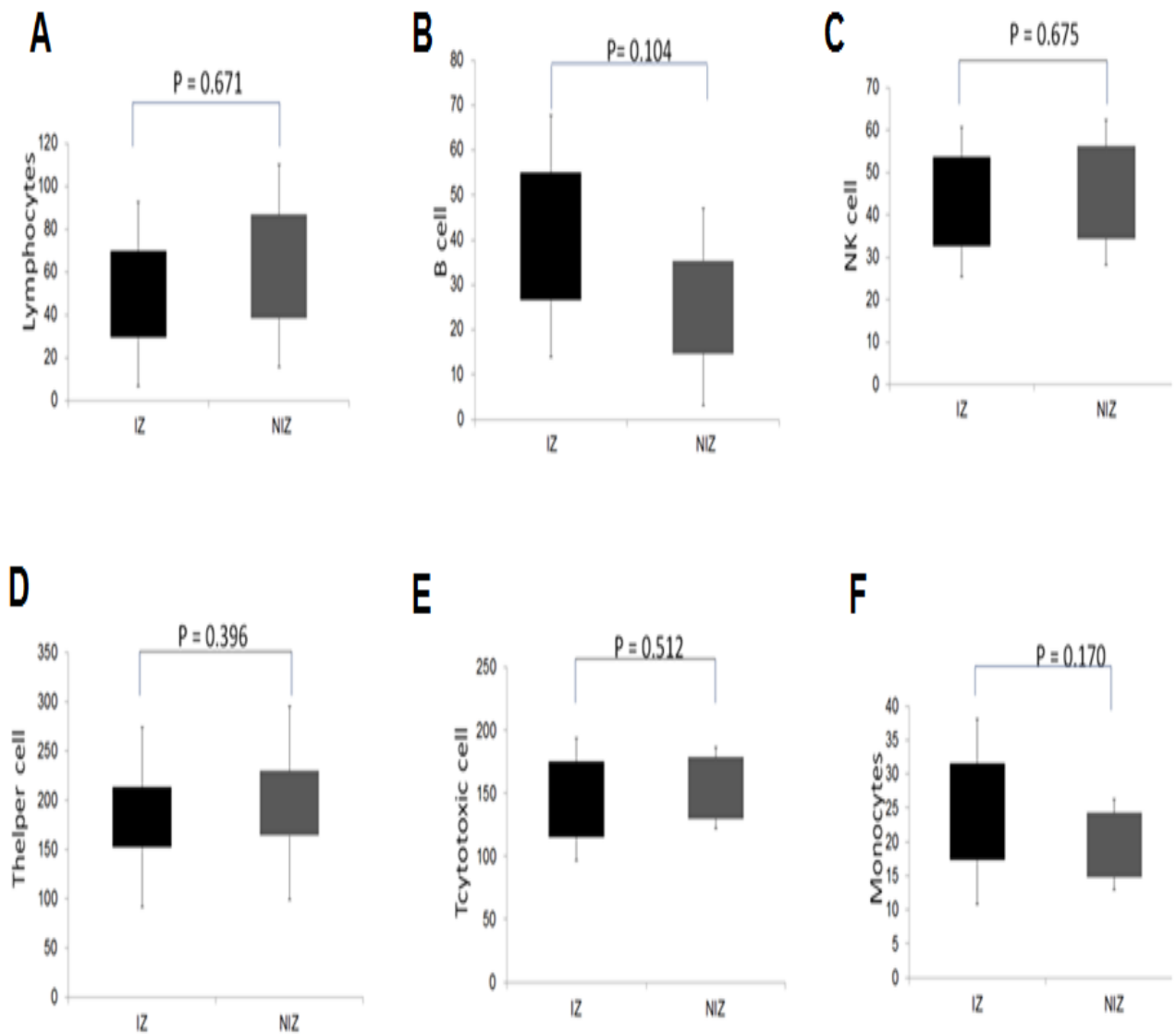


Fig.3.7. Analysis of immune cells from people of Rourkela city by box plot. Box plot comprising the CD marker expression of lymphocytes (A), B cells (B), cytotoxic T cells (C), helper T cells (D), NK cells (E) and monocytes (F) as determined by flow cytometry in people of industrial zone (n=32) and non-industrial zone (n=23) of Rourkela city.

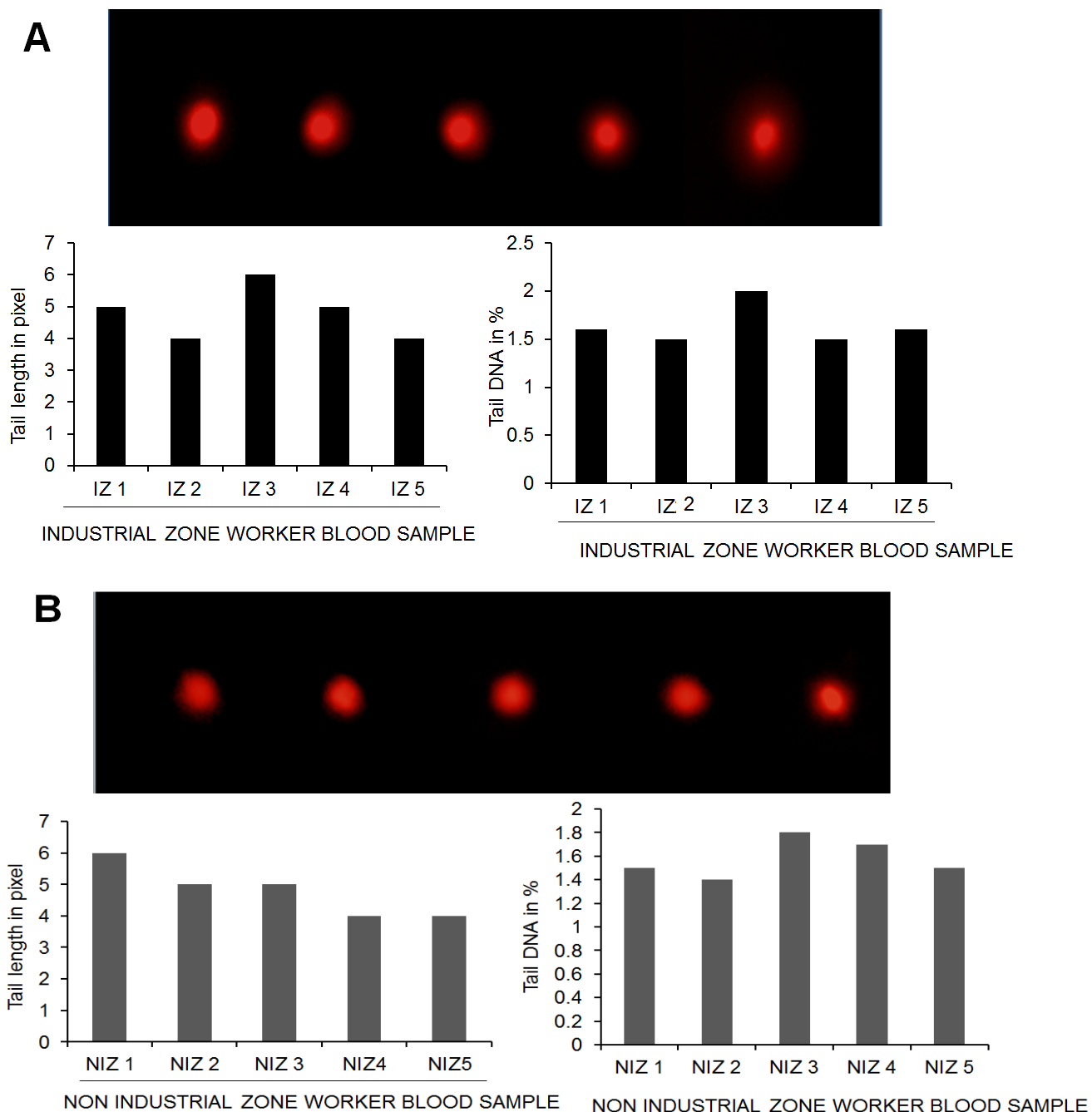


Fig.3.8. DNA damage analysis in blood of people of Rourkela city. Blood samples collected voluntarily from Rourkela city people under aseptic conditions and 100 μ l of blood were added in lysis buffer incubated for 15 min. The suspension was centrifuged to obtain cell pellet and analyzed for DNA damage by comet assay. Tail length and tail DNA content was measured using CASP software (* $P < 0.05$, compared with control).

3.4. Discussion

Abundant studies have reported that PM-related air pollution is a problem in many cities and towns, and it appears to be the component of air pollution most consistently associated with

adverse health effects. PAHs are significantly associated with enhanced mortality from respiratory and cardiovascular diseases, exacerbation of allergies, asthma, chronic bronchitis, and respiratory tract infection in many industrial cities (Li et al., 2003; Yu et al., 2014; Jung et al., 2014). Moreover, the World Health Organization (WHO) estimates that inhalation of PM is responsible for 500,000 excess deaths each year worldwide. The role of cellular participants and the mechanisms involved in the response to PM exposure have been identified. In our study, an air quality monitoring program was designed to collect the gaseous and particulate air pollutants from two sites (in front of Indira Gandhi Park and the academic complex of NIT Rourkela) of the industrial city Rourkela. The presence of B[a]P in PM was confirmed by fluorescence spectroscopy and NMR, which was consistent with results for previously identified industrial zones. Furthermore, we studied the mutagenic activity of PM with the Ames test, which determines if substances are capable of inducing mutations and has become an important procedure in safety assessment.

PM has been reported to induce many biological phenomena, including apoptosis, DNA damage, and oxidative stress. For instance, mitochondrial signaling and oxidative stress have been reported to mediate PM-induced apoptosis in the human CF bronchial epithelium (Kamdar et al., 2008; Marangolo et al., 2001). Accordingly, our study showed that the generation of ROS after PM exposure could induce cellular oxidative stress and apoptosis. Another study reported the induction of IL-8 and ROS in human respiratory epithelial cells exposed to PM; in agreement with this study, our data indicate that PM induced NO and ROS production, which might be related to the inflammatory response and carcinogenesis (Becker et al., 2005; Garcon et al., 2006). Recently, amorphous nanosilica was found to induce endocytosis-dependent ROS generation and DNA damage in human keratinocytes (Nabeshi et al., 2011). In this regard, one of the most important changes induced by PM was DNA damage, as reported by the comet tail formation and the level of DNA damage has been correlated with mutagenicity and tumor formation in experimental models (Upadhyay et al., 2003; Sánchez-Pérez et al., 2009). The DNA damage induced by PM₁₀ and its constituents involves the formation of DNA double-strand breaks (Soberanes et al., 2006).

Air pollutants, especially PAHs after activation of CYP450, can act directly as pro-oxidants of lipids and proteins or as free radical generators by promoting oxidative stress and lipid peroxidation and inducing inflammatory responses (Fu et al., 2012; Giannapas et al.,



2012). Our findings support that B[a]P and other unidentified PAHs present in the PM activated by CYP1B1 and induced apoptosis. Accordingly, inhibition of CYP1B1 by siRNA or pharmacologically with the inhibitor CTZ reduced PM-mediated cytotoxicity and apoptosis.

Conversely, our clinical data showed that the PM did not affect the blood cells of people living in Rourkela, as demonstrated by the results for comet tail formation and immunophenotyping analysis. These are potentially contradictory clinical data, which might be due to low exposure to PM and its bioavailability to cells during the entire human life-span; the effect is likely to appear after 30-40 years of exposure according to the chemical carcinogen hypothesis (Kleinsmith 2006). The effects also depend on age, the health condition, and genetic factors of the individual. For example, a polymorphism in the CYP genes could affect an individual's capacity for transforming PAHs into reactive metabolites, which is one of the important factors contributing to individual susceptibility toward the development of health problems and airborne disease (Preissner et al., 2013). In summary, this study focused on awareness of the source of the environmental problems in Rourkela and provided an indication on potential environmental issue for future preventive management to improve human health.



Chapter 4

Prediction and validation of apoptosis through cytochrome P450 activation by benzo[a]pyrene



Abstract

Polycyclic aromatic hydrocarbons (PAHs) processed by cytochrome P450 (CYP450) during metabolism is well reported to induce carcinogenesis. The present study has developed a new approach to examine apoptotic activity of a known PAH called benzo[a]pyrene (B[a]P), using protein–ligand and protein–protein interaction through *in silico* approach, followed by *in vitro* validation. *In silico* study showed that the conformational changes and energies involved in the binding of B[a]P to CYP1B1 was crucial with its target proteins. The data showed that activated B[a]P had high affinity to bind with aryl hydrocarbon receptor (AHR) with binding energy of -601.97 kcal/mol. Interestingly, B[a]P–CYP1B1 complex showed strong binding affinity for caspase -8, -9, -3 with binding energy of -625.5, -479.3 and -514.2 kcal/mol respectively. Moreover, the docking of specific caspase inhibitors in the complex showed weak interaction with low binding energy value as compared to B[a]P–CYP1B1 caspase complexes. To validate our *in silico* work, we showed B[a]P treated HaCaT cells triggered apoptosis with increase in caspase 8, caspase 9 and caspase 3/7 level. Further, *in vitro* work confirmed that B[a]P induced apoptosis was significantly suppressed in Ac-DEVD-CMK pre-treated cells. In addition, knockdown of CYP1B1 suppressed B[a]P induced apoptosis in HaCaT cells confirming a pivotal role of CYP1B1 in B[a]P induced apoptosis. Interestingly, through *in-silico* modeling, we screened clotrimazole as a potent CYP1B1 inhibitor which completely inhibited B[a]P mediated activation. This hypothesis was validated by MTT assay, caspase activation measurement and showed remarkable inhibition of B[a]P induced cell death; thereby, highlighting a potent therapeutic role for industrial pollution associated diseases.

Keywords: Benzo[a]pyrene, Cytochrome P450, Apoptosis, Ligand–protein, Protein–protein, Aryl hydrocarbon receptor



4.1. Introduction

Modern environment entail considerable exposure of humans against a wide array of potentially toxic compounds including polycyclic aromatic hydrocarbons (PAHs) which are generated by incomplete combustion and pyro-synthesis of various organic materials. Benzo[a]pyrene (B[a]P) is regarded as a carcinogenic compound among the group of PAHs (Conney et al., 1994; Shimada, 2006; Gao et al., 2011) and is listed as a Group 1 carcinogen by the IARC (International Agency for Research on Cancer). To become carcinogenic, PAHs must be metabolized by the cytochrome P450 (CYP450) family of monooxygenase especially CYP1A1 (cytochrome P450 1A1) and CYP1B1 (cytochrome P450 1B1) to reactivate diol-epoxide metabolites (Miller and Ramos, 2001; Arlt et al., 2008). Moreover, PAHs activate aryl hydrocarbon receptor (AHR) which plays an imperative role in mediating transcriptional regulation of target genes including CYP1A1 and CYP1B1 as well as several phase II enzymes. On binding with B[a]P, AHR becomes activated, translocate to nucleus and regulates transcription (Stolpmann et al., 2012). Cytochrome P450 enzyme (CYP1B1) are mainly expressed in liver, skin indicating different basal regulation but they share induction via the AHR (Moffat et al., 2011). B[a]P is oxidized by CYP450 during metabolism to produce toxic intermediate species such as B[a]P diolepoxide, leading to apoptosis induction and genotoxicity (Moorthy et al., 2003; Uno et al., 2004). Cells undergoing apoptosis ultimately exhibits nuclear condensation followed by internucleosomal DNA cleavage and activation of the caspase cascades. Caspases, the cysteine activated proteases are exemplified by caspase 8 and caspase 9 which are activated in extrinsic and intrinsic apoptosis respectively serve to activate caspase 3, the chief effector caspase (Salas and Burchiel, 1998; Lei et al. 1998; Chen et al., 2003; Holme et al., 2007; Xiao et al., 2007). With the increase in accessibility of molecular biological structures, docking approaches have become imperative tools in order to determine structure based rational molecule discovery and design. For a protein-receptor with known three dimensional structures, the ligand–protein docking challenge basically consists in predicting the bound conformation of a ligand molecule within the protein active site. For example, Adinarayana et al. showed that extracted DHFR protein (PDB id:2BL9) from protein data bank (PDB) used to assess the strength of affinity of different molecules towards ligand binding site and the extent of correlation between experimental values and computational docking score (Adinarayana and Devi, 2011). Likewise, Shalini et al. showed that *Ocimum sanctum* found as a potential herbal



drug for swine flu by docking the phytochemicals with the receptor PB1F2 by using HEX tool (Shalini and Kalivani, 2011) Docking is also used to predict protein–protein complexes, which are supportive in determining the quaternary structures of intrinsically multimeric proteins as well as to gain an insight of the protein interaction networks. Protein–protein interactions play a vital role in most essential cellular processes including signal transduction, cell regulation and immune response. Recently, Wang et al. predicted the three dimensional structure of human tyrosinase and simulated the protein–protein interactions between tyrosinase and its three binding partners (Wang et al., 2002). To understand the molecular mechanism of biochemical processes at the atomic level, a detailed structural model of the interacting complex is required. Computational tools are being adopted in conjunction with the wet lab techniques that generate high level of data as output (Hetenyi and van der Spoel, 2002; Huey et al., 2007; Xu et al., 2013).

Here, we studied the apoptotic prospective of B[a]P through protein–ligand and protein–protein interaction *in silico* and validated the study on human keratinocyte cell line (HaCaT). Our prediction showed that B[a]P was activated by CYP450 (CYP1B1), to induce multiple cellular effects related to activation of the AHR due to formation of toxic metabolites and this in turn activated caspases. Moreover, data showed that clotrimazole (CTZ) and siRNA against CYP1B1 could inhibit the B[a]P activation and suppressed the apoptosis as demonstrated in both *in silico* modeling and *in vitro* studies in HaCaT cells.

4.2. Materials and methods

4.2.1. Chemical and reagents

Benzo[a]pyrene, dimethyl sulfoxide(DMSO), 3-[4,5-dimethylthiazol-2-yl]-2,5-diphenyl- tetrazolium bromide (MTT), clotrimazole (CTZ) from Sigma, USA; caspase-3 Inhibitor III (Ac-DEVD-CMK) from Merck were purchased. The Annexin V and 7AAD kit from BD Bioscience and caspase-Glo assay kit for quantification of caspases were purchased from Promega, USA, CYP1B1 siRNA and control siRNA from SantaCruz Biotechnology, USA.

4.2.2. Cell culture

The immortalized human keratinocyte cell line (HaCaT) was obtained from National Centre for Cell Science, Pune, India and cultured in Dulbecco's modified Eagle's medium with high glucose (DMEM/high glucose), supplemented with 10% heat-inactivated fetal bovine serum (FBS) containing and 1% penicillin–streptomycin. The cells were maintained at 37°C in a



humidified atmosphere at 5% CO₂. All media, supplements and antibiotics were purchased from Invitrogen.

4.2.3. Cell viability by MTT assay

HaCaT cells were harvested from maintenance cultures in logarithmic phase and were counted by hemocytometer using trypan blue solution. HaCaT (1×10^4 cells/well) were cultured in a 96-well plate at 37°C, and exposed to varying concentrations of B[a]P for 72 h. After 72 h MTT solution (5mg/ml) were added, post 4 h incubation, the resultant formazan crystals were dissolved in dimethyl sulfoxide and the absorbance was measured by a microplate reader (Perkin Elmer) at 595 nm. All experiments were performed in triplicate, and the relative cell viability was expressed as percentage relative to the untreated control cells (Bhutia et al., 2010).

4.2.4. Annexin V and propidium iodide staining

It was performed using a FACScan (Becton Dickinson Immunocytometry Systems). After 48 h B[a]P treatment HaCaT cells were washed with phosphate buffer saline and then centrifuged at 1200 rpm for 5 min at room temperature. Cell pellets were incubated with Annexin V and propidium iodide in binding buffer and analysed by flow cytometer.

4.2.5. Caspase assays

HaCaT cells were seeded in 6 well plates and were treated with B[a]P for 48 h. After treatment, caspase activity was measured using caspase-Glo assay following the manufacturer's protocol (Promega Corp., Madison, WI) (Bhutia et al., 2010).

4.2.6. CYP1B1 knockdown using small interfering RNA

HaCaT Cells were cultured in 60 mm plates and transfected at 80% confluence with Lipofectamine 2000 ® reagent (Invitrogen), in the presence of 100 nM of siRNAs specific for human CYP1B1 or control siRNA. HaCaT cells were used 48 h after transfection for RNA extraction and apoptosis studies (Stolpmann et al., 2012; Bhutia et al., 2010).

4.2.7. RNA extraction and semiquantitative RT-PCR

Total RNA from HaCaT cells were harvested by using RNeasy kit from Qiagen following manufacturer's instruction. The cDNA was synthesized using 2 µg of total RNA with reverse transcriptase enzyme following manufacturers' instruction. RT-PCR was used to study the expression of mRNA for CYP1B1 and GAPDH (internal control). The respective primers (Sigma) and conditions were as follows: for CYP1B1, sense 5'CAA CCG CAA CTT CAG CAA CT-3' and antisense 5'-CAG GAC ATA GGG CAG GTT G-3' (annealing at 62 °C, 35



cycles); for GAPDH, sense 5'-CAC AAT GCC GAA GTG GTC GT-3' and antisense 5'-TCA CCA TCT TCC AGG AGC GA-3' (annealing at 62 °C, 35 cycles) (Yang et al., 2010). Amplified products were separated by electrophoresis on 1.5% agarose gel and visualized using gel document system (BioRad) after ethidium bromide staining.

4.2.8. *In silico* study

Chemical structure of benzo[a]pyrene was obtained from ChEMBL data bank (Chemical Entities of Biological Interest). The structures of cytochrome P450 and various extrinsic, intrinsic apoptotic pathway proteins were retrieved from PDB for docking analysis. Chimera 1.6.2 and Swiss PDB Viewer were used in intermediate steps of *in silico* studies and visualize the molecules. SWISS-MODEL server (<http://swissmodel.expasy.org>) was used for automated comparative modelling of three dimensional (3D) protein structures of AHR. The stereo chemical property was checked by Ramachandran plot using PROCHECK (Soriano-Ursúa et al., 2009; Khobragade et al., 2011). AutoDock 4.2 was used for protein–ligand docking analysis. HEX 6.3, docking software was used for studying protein–protein interactions. All caspases 8, 9, 3 inhibitors and clotrimazole structures were retrieved from Pub- Chem database. Interacting binding residues at the active site was visualized using Ligplus software. Besides Hex 6.3, visualization of protein–protein interaction was also done by Discovery studio Visualizer 2.5.

4.2.9. Statistical analysis

All data were given as the mean \pm S.D. Experimental results were analyzed by Student's t-test. $P < 0.05$ was considered as the level of significance for values obtained for treated compound to control.

4.3. Results

4.3.1. Benzo[a]pyrene activated by cytochrome P450: *in silico* approach

The ability to predict the conformations and energies involved in the binding of small molecules to proteins is quite crucial in ligand interactions. Docking helps in the identification of the low energy binding modes of a small molecules or ligands within the active site of known macromolecules or receptors. The docking study predictions provide a quantitative measure that supports the experimentally determined value. During metabolism the precarcinogenic moiety like B[a]P gets activated by members of the CYP450 enzyme family and becomes carcinogenic as reported (Bhutia et al., 2010; Conney et al., 1994). The CYP1B1 structure was retrieved from



protein data bank (PDB id: 3PM0). The PDB structure of CYP1B1 was complexed with a-naphthoflavone (ANF) (Miller and Ramos, 2001). In order to remove ANF bound to CYP1B1, Chimera 1.6.2 was used. After this energy minimization was done with the help of SPDBV 4.0.1 to achieve a stable structure. Subsequently, we evaluated docking of B[a]P with CYP1B1 in AutoDock and observed binding energy is -8.52 kcal/mol (Fig. 4.1.A–C; Table 1) (Wang et al., 2011; Morris et al., 2008). Furthermore, we visualized B[a]P binding sites at CYP1B1 cavity and found B[a]P was bound in a narrow slot – with active site like cavity above the surface of the heme moiety. We observed G329, F268, N265, F231, L264, D333, Q332 and N228 at active site of CYP1B1 which was consistent with reports from previous work (Miller and Ramos, 2001) showing hydrophobic and Vander- Waals interaction (Fig.4.1.D and E). From this analysis, we confirmed B[a]P bound with CYP1B1 at its active site and was converted to carcinogen.

Homology modeling for AHR was performed by automated homology modeling SWISSMODEL using their respective template downloaded from NCBI. The steepest descent energy minimization using the SPDBV 4.0.1 force field was done to regularize the protein structure geometry. The stereo chemical property was checked by Ramachandran plot using PROCHECK (Wang et al., 2011; Morris et al., 2008). Hex 6.3 used for docking CYP1B1–B[a]P complex showed high binding affinity towards AHR protein with binding energy -601.97 kcal/mol. B[a]P– CYP1B1 complex with AHR evidently showed interaction conformation with residue S91, R117, S119, S122, R124, V243, Q248, D417, V419, L134, S151, H155, Q156, F136 present at binding site (Fig.4.1.F and G). This interaction supported that biotransformation of B[a]P is regulated via AHR (Stolpmann et al.,2012) and B[a]P activates AHR with signal transduction events enhancing the toxicity of the B[a]P.

Table 4.1: Binding energy value for ligand–protein interaction.

Sl no	Ligand–protein interaction (AutoDock 4.2)	Binding energy value (ΔG kcal/mol)
1	B[a]P–cytochrome P450(CYP1B1)	-8.52
2	Caspase 8-AC-IEPD-CHO	-20
3	Caspase 9-pan caspase inhibitor	-8.48
4	Caspase 3-AC-DEVD-CMK	-13.4

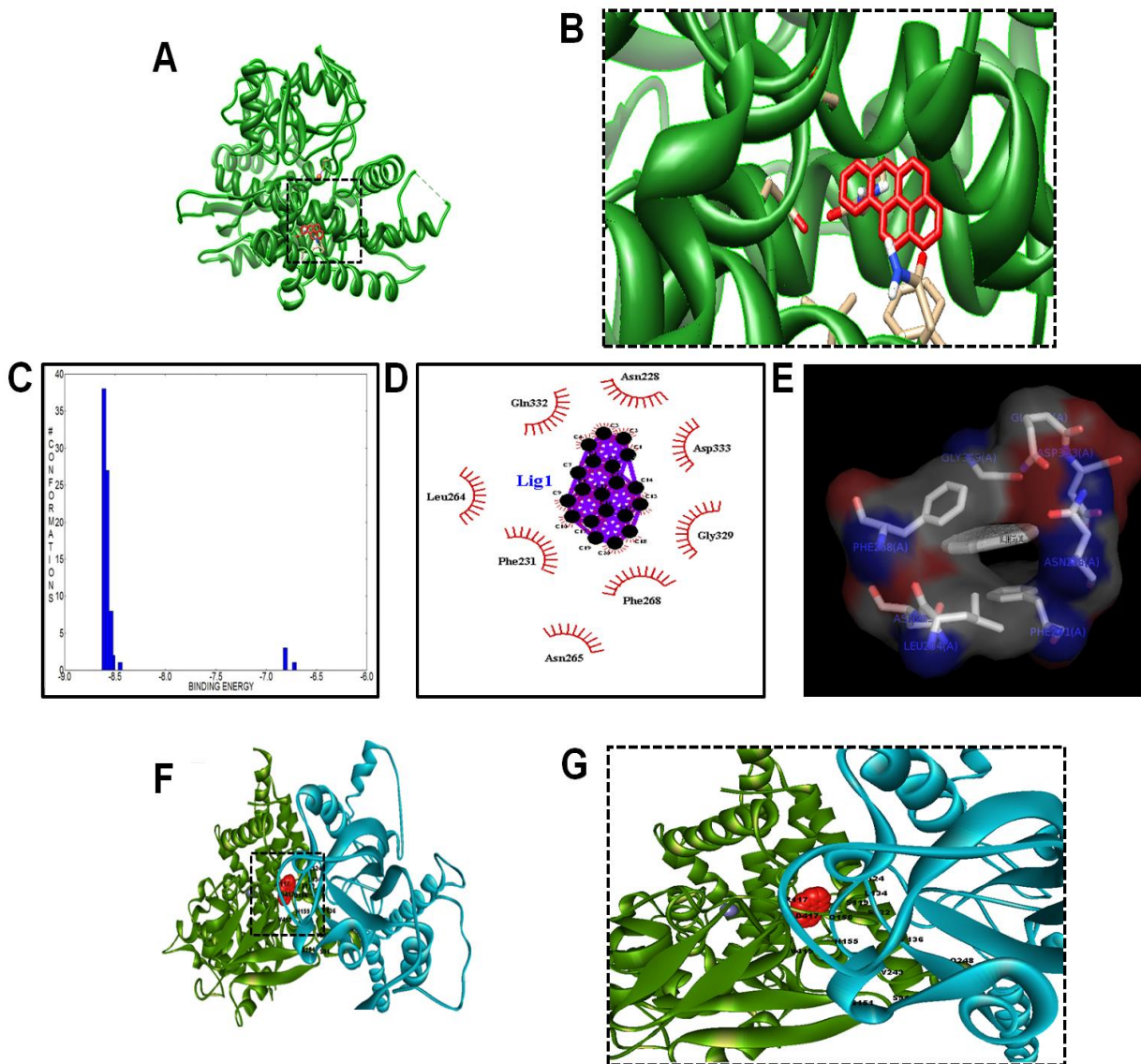


Fig.4.1. Benzo[a]pyrene activated by cytochrome P450 *in silico* approach: (A) B[a]P structure retrieved from chEBI and cytochrome P450 (CYP1B1) structure retrieved from PDB. Docking of B[a]P (Red) with CYP1B1 (Green) using AutoDock software was done and the complex was visualised through chimera 1.6.2. (B) Showing enlarge version of docking orientation of B[a]P binding at CYP1B1. (C) Binding energy graph of AutoDock 4.2 of B[a]P and CYP1B1. (D) Showing binding amino acids residues present at active site using Ligplot. (E) Using Pymol to visualize binding pattern and residue. (F) Docking of B[a]P (Red)-CYP1B1 (Green) complex with AHR (Blue) using HEX 6.3 and Discovery studio Visualizer 2.5 was used to visualize the interaction. (G) Binding interaction B[a]P (Red)-CYP1B1 (Green) complex with AHR (Blue) enlarged to visualize showing interaction

conformation with residue present at binding site S91, R117, S119, S122, R124, V243, Q248, D417, V419, L134, S151, H155, Q156, F136.

4.3.2. Benzo[a]pyrene induced apoptosis in human skin keratinocytes

Skin serves as the first line of immune defence against xenobiotic exposure. We investigated whether B[a]P does have any cytotoxic effect on human skin keratinocytes HaCaT cells. HaCaT cells were exposed to various concentration of B[a]P (0.5 μ M, 1 μ M, 2.5 μ M, 5 μ M and 10 μ M) for 72 h and the cell viability was measured by MTT assay. Treatment with B[a]P significantly resulted in decrease of the viability in a dose dependent manner (Fig.4.2.A). Based on this result of cytotoxic concentrations, we next studied whether the cell death induced by B[a]P was due to apoptosis. The mode of cell death induced by B[a]P was examined with Annexin V staining by flow cytometry and showed apoptosis was induced by B[a]P in HaCaT cells (Fig.4.2.B). Apoptosis is initially characterized by morphological features, such as chromatin condensation, nuclear fragmentation, and membrane blebbing (Padhye et al., 2009; Nathwani et al., 2010; Greene et al., 2013). One of the biochemical hallmarks of apoptosis is the cleavage of chromatin into nucleosomal fragments, a DNA fragmentation assay was performed to detect genome digestion. HaCaT cells showed DNA fragmentation in dose dependent manner (Fig.4.2.C). This results indicated that the B[a]P induced apoptosis in HaCaT cells.

Table 4.2: Binding energy value for protein–protein interaction.

Sl no	Protein–protein interaction (Hex 6.3)	Binding energy value (Δ G kcal/mol)
1	Benzo[a]pyrene–cytochrome P450-AHR	-601.97
2	Benzo[a]pyrene–cytochrome P450-caspase 8	-623.5
3	Benzo[a]pyrene–cytochrome P450-caspase 9	-479
4	Benzo[a]pyrene–cytochrome P450-caspase 3	-514.2
5	Benzo[a]pyrene–cytochromeP450-caspase8-AC-IEPD-CMK	-195.5
6	Benzo[a]pyrene–cytochromeP450-caspase 9-Pan caspase inhibitor	-184.6
7	Benzo[a]pyrene–cytochromeP450-caspase 3-AC-DEVD-CMK	-192.4



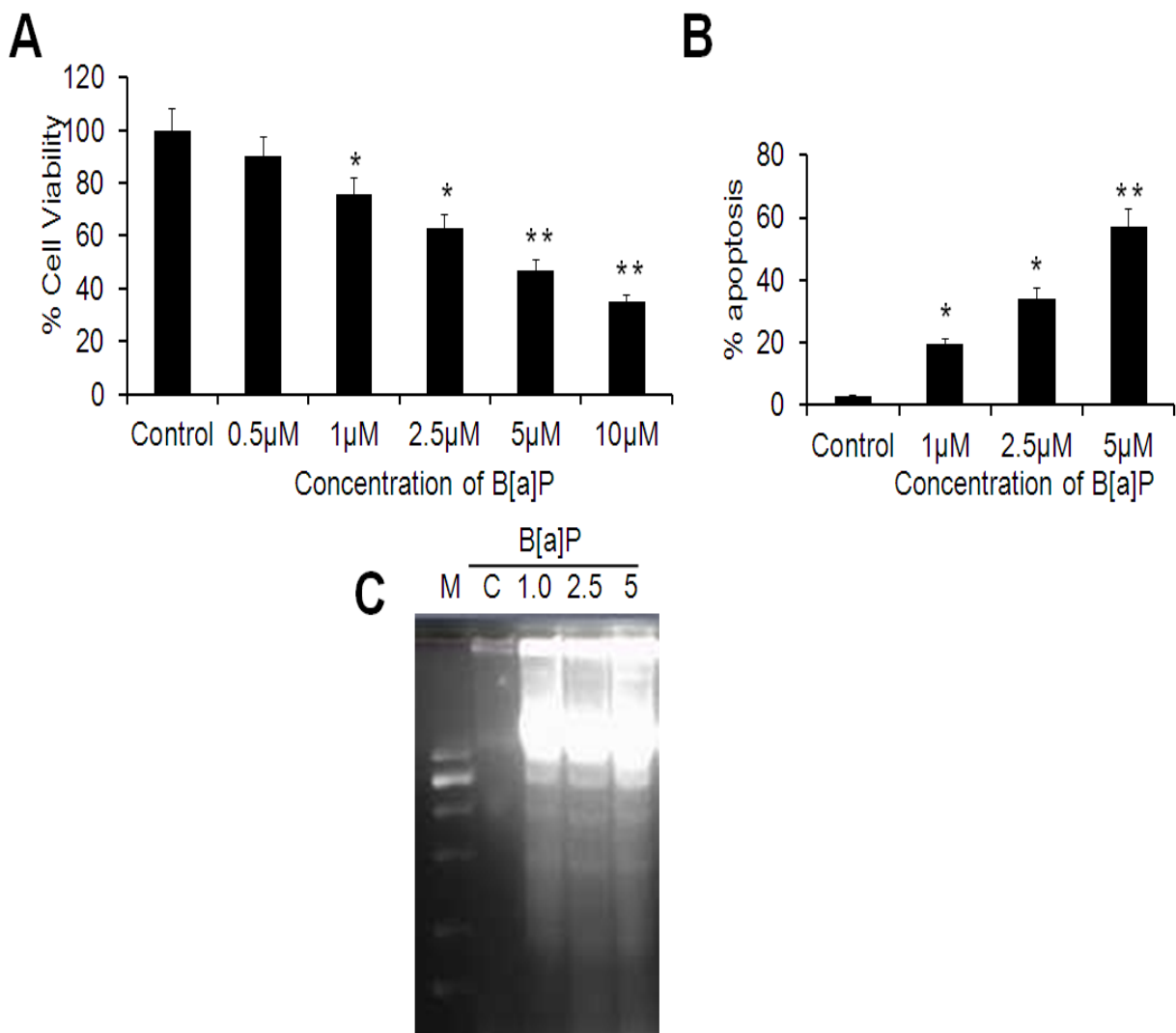


Fig.4.2. Benzo[a]pyrene induced apoptosis: (A) HaCaT cells were seeded into each of the 96 well plates and were treated with various concentrations of B[a]P for 72 h and determined by MTT assay. (B) Quantification of the apoptotic cell population with Annexin V staining by flow cytometric analysis after B[a]P treatment of cells for 48 h. Data reported as the mean \pm S.D. of three independent experiments and compared against PBS control. *P Values < 0.05 and **P < 0.01 values were considered significant. (C) The genomic DNA was isolated and separated on 1.5% agarose gel electrophoresis. DNA fragmentation was measured by ethidium bromide staining. This was representative of three experiments.

4.3.3. Benzo[a]pyrene induced activation of intrinsic and extrinsic caspase activation

Protein–protein interaction is deliberated with different apoptosis pathway proteins like caspase 8, 9 and 3. After evaluating the complex structure of CYP1B1–B[a]P complex, we again docked various apoptosis proteins like caspase 8, 9 and 3. The structures of the human caspase 8 (PDB: 2C2Z), 9 (PDB: 1NW9) and 3 (PDB: 2XZT) were retrieved from protein data bank. Caspase 8, 9 and 3 structures were also attached with different inhibitor ligands. Chimera 1.6.2 facilitated removal of ligand and extracted pure structure of caspase 8, 9 and 3. Hex 6.3 was used for protein–protein interaction. Hex 6.3 is a widely used technique based on Fast Fourier transform (FFT) based method to perform the global searches. FFT-based method of searching allows the evaluation of many docked conformations on a grid using a correlation type scoring function (Thornberry et al., 1997). CYP1B1–B[a]P complex showed high binding affinity towards apoptosis protein (Fig.4.3.A). The docking results were ordered by energy value and lowest energy value docking showed stable binding complex. Here the energy ranges of stability were determined by set of Emin value (minimum binding energy). The lowest minimum energy depicts highest affinity between the proteins. Fascinatingly, B[a]P–CYP1B1 complex showed strong binding affinity for caspases with binding energy -625.5, -479.3 and -514.2 kcal/mol for caspase 8, caspase 9 and caspase 3 respectively (Fig.4.3.A–C). B[a]P–CYP1B1 complex with caspase 3 evidently showed interaction conformation with residues present at binding site H140, R130, N319, L264, F247, L317, K275, L277, C220, R278. The binding residue we predicted for B[a]P–CYP1B1 and caspase 8 are P370, I369, N267, G368, Q366, S127, D223, Y448, I297, E445. The residues present at binding sites of B[a]P– CYP1B1 complex with caspase 9 are S119, F120, K358, A11, S122, G182, N184, V364, S361, Y363. To determine the effect of B[a]P on both intrinsic and extrinsic activation of caspases in HaCaT cells, caspase Glo assay was performed after 48 h of B[a]P treatment. The data showed that caspase 8, 9 and 3 were increased with increasing the concentration of B[a]P. These data clearly showed that B[a]P showed apoptotic cell death by the involvement of caspase 8, caspase 9 and caspase 3/7 in HaCaT cells (Fig.4.3.D).

4.3.4. Caspase inhibitors suppressed the B[a]P mediated apoptotic death

Next, we aimed to demonstrate the role of caspase inhibitors in B[a]P induced apoptosis. Accordingly an enzyme inhibitor is a molecule that binds to enzyme and decreases their



activity. The binding of an inhibitor can stop a substrate from entering the enzyme active site and hinder the enzyme from catalyzing its reaction. Inhibitor for caspase 8, 9 and 3 retrieved

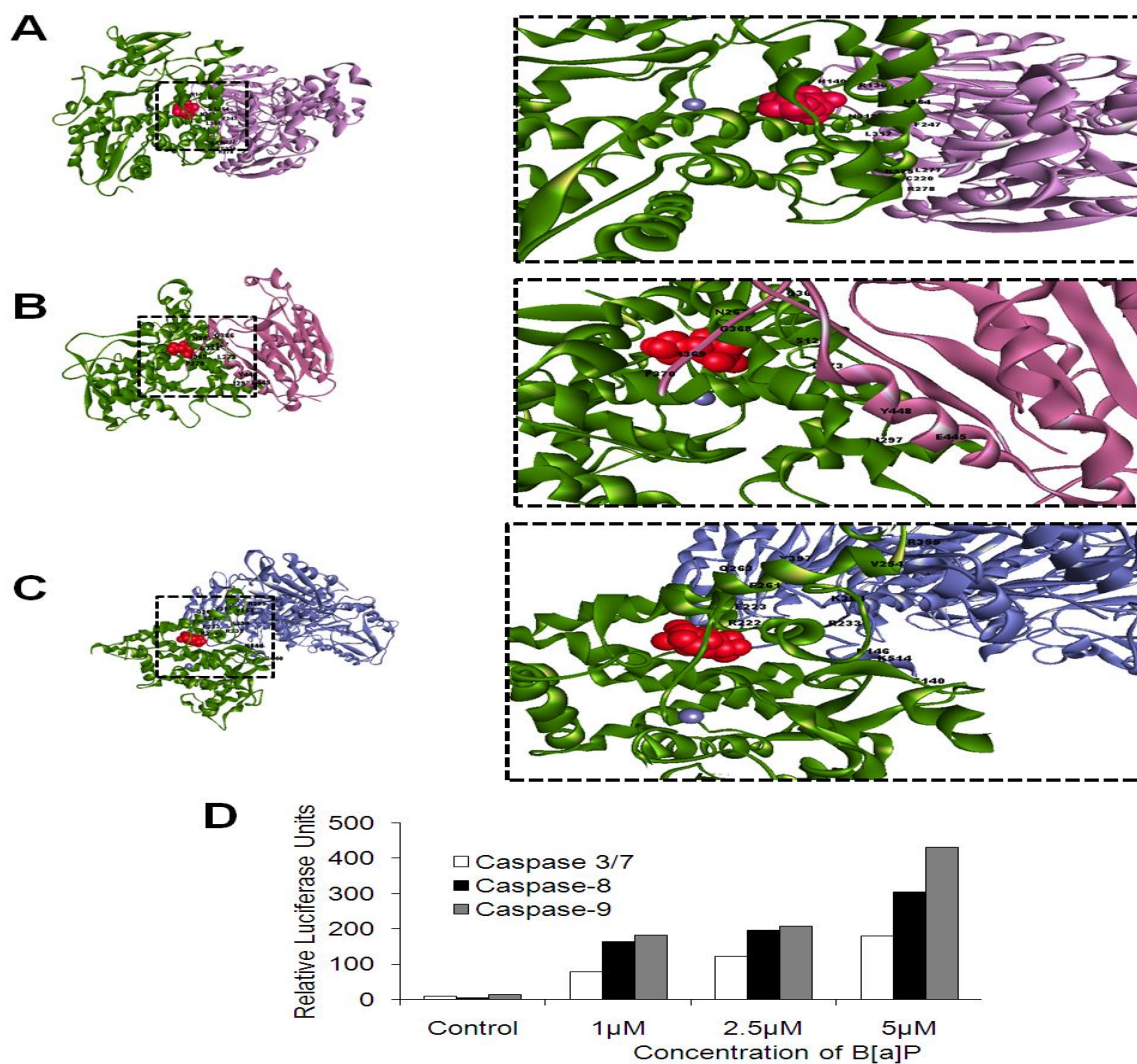


Fig.4.3. Benzo[a]pyrene induced activation of intrinsic and extrinsic caspase activation: (A) Docking of B[a]P (Red)–CYP1B1 (Green) complex with caspase3 (Purple) using HEX 6.3 and Discover studio Visualizer 2.5 was used to visualize the interaction with residues present at binding site H140, R130, N319, L264, F247, L317, K275, L277, C220, R278.(B) Binding interaction of B[a]P (Red)–CYP1B1 (Green) complex with caspase8 (Pink) enlarged to clearly showing interaction conformation with residues present at binding site P370, I369, N267, G368, Q366, S127,D223, Y448, I297, E445. (C) B[a]P (Red)–CYP1B1 (Green) complex with caspase 9 (Cyan blue) with enlarge conformation view and residues present at binding sites are S119, F120, K358, A11, S122, G182, N184,

V364, S361, Y363. (D) HaCaT cells were treated with B[a]P for 48 h followed by analysis of caspase 3, caspase 8 and caspase 9 expression using caspase-Glo assay and this was representative of 3 independent experiments.

from Pubchem as they contain calculated properties and description, which helped in searching and filtering of chemical structure. The ligands were downloaded as xml files from Pubchem. These xml files were converted into the 3D structure using open Babel software. In addition, selective inhibitor, Ac-DEVD-CMK (CID-9959259)-caspase3, Ac- IEPD-CHO (CID-16760476)-caspase8 and pan caspase (CID- 644195)-caspase 9 were docked using AutoDock 4.2 (Fig.4.4.A–E). Binding energy of caspase 3 and Ac-DEVD-CMK was -13.4 kcal/ mol). The caspase inhibitor complex were again interacted with B[a]P and CYP1B1 complex. According to our docking result they showed less and weak affinity interaction (Fig. 4.4.F, H). Energy value was shown to be much less than B[a]P–CYP1B1-caspases complex. This *in-silico* study showed that caspase inhibitors could decrease B[a]P induced apoptosis.

The *in silico* study was validated *in vitro*, using caspase 3 inhibitor Ac-DEVD-CMK. HaCaT cells treated with B[a]P in presence of Ac-DEVD-CMK showed increased in caspase 3/7 activity compared with the DMSO treated group. The caspase 3/7 activity were significantly decreased in presence of Ac-DEVD-CMK (50 μ M) in B[a]P induced apoptosis. Addition of caspase 3 inhibitor resulted in a lesser but statistically reduced rate of apoptosis and this *in vitro* caspase inhibition was comparable with *in-silico* data (Fig. 4.4.G).

4.3.5. CYP1B1 deficiency decreased B[a]P induced apoptosis

To investigate potential involvement of CYP1B1 in B[a]P mediated apoptosis, the CYP1B1 gene was knocked down and B[a]P sensitivity was examined by MTT and caspase-3/7 assays 48 h after treatment. The data showed that targeted CYP1B1 siRNA suppressed the expression of corresponding mRNA as compared to sicontrol demonstrated by RT-PCR (Fig.4.5.A). The CYP1B1 deficient cells exhibited enhanced cell viability toward B[a]P as compared to sicontrol (Fig. 4.5.B). Moreover, we performed caspase-Glo assay in transfected HaCaT cells in presence of B[a]P and data clearly showed that caspase 3/7 activity was very significantly decreased in CYP1B1 knocked down with respect to sicontrol group (Fig. 4.5.C) indicating specific role of CYP1B1 in B[a]P mediated apoptosis.



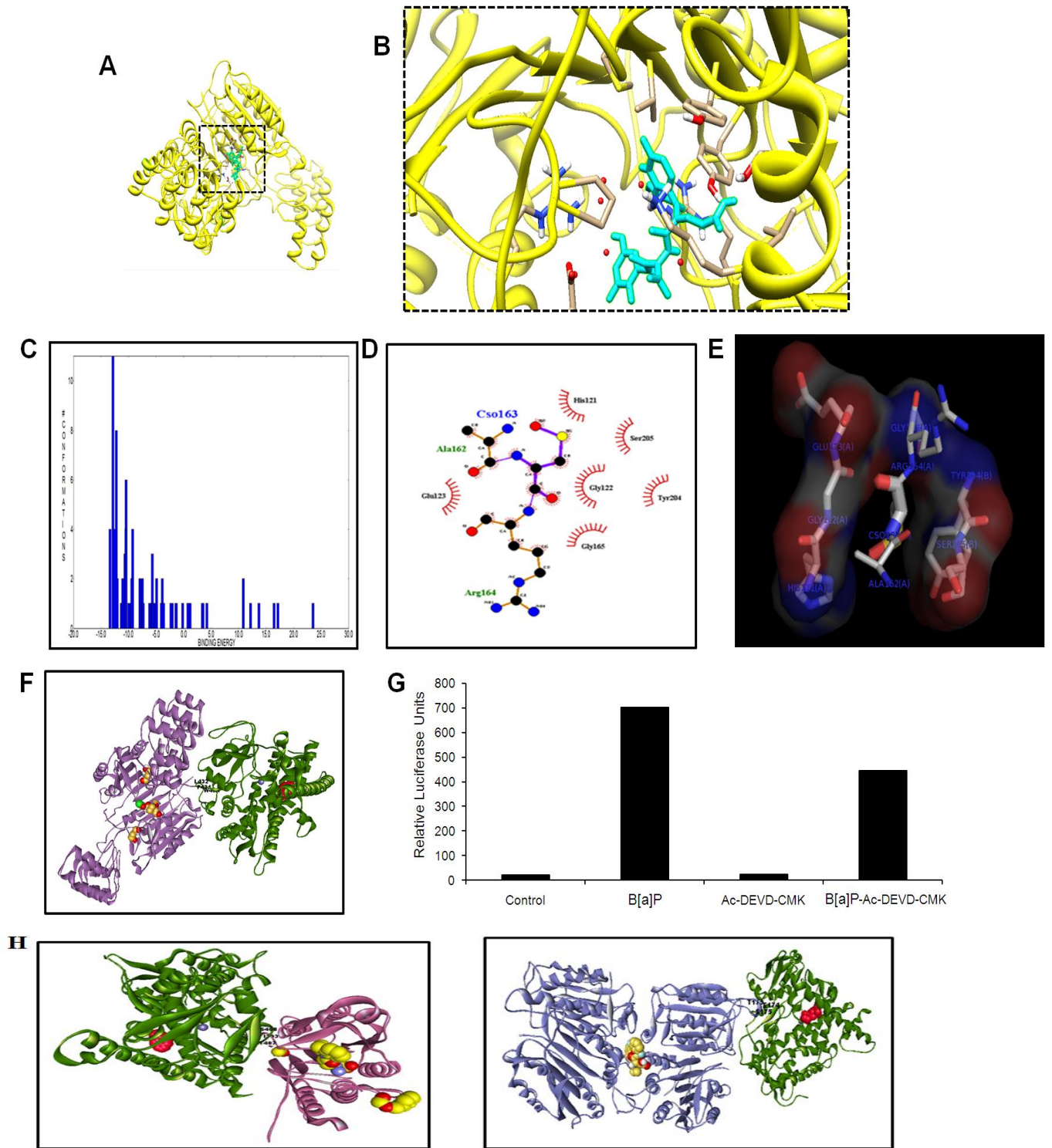


Fig.4.4. Inhibition of B[a]P induced apoptosis by caspase inhibitor: (A) Ac-DEVD-CMK (Sky blue) caspase 3 inhibitor bound in a contracted active site of caspase 3 (Yellow). (B) The image was magnified to show binding

conformation. (C) Binding energy graph of AutoDock 4.2 of Ac-DEVD-CMK and caspase 3. (D) Showing binding of amino acids residues were H121, S205, G122, Y204, G165 and E123 using Ligplot. (E) Using Pymol to visualize binding residue. (H) B[a]P (Red)–CYP1B1 (Green) complex with caspase3 (Purple)–AC-DEVD-CMK (Yellow) inhibitor complex showing weak interaction. (I) HaCaT cells were pre-treated with 50 IM of AC-DEVD-CMK for 2 h and then treated with 5 IM B[a]P for 48 h and caspase 3 activity was determined by caspase 3 Glo assay. (H) Benzo[a]pyrene–cytochromeP450-caspase8-AC-IEPD-CMK and Benzo[a]pyrene–cytochromeP450-caspase 9-Pan caspase inhibitor.

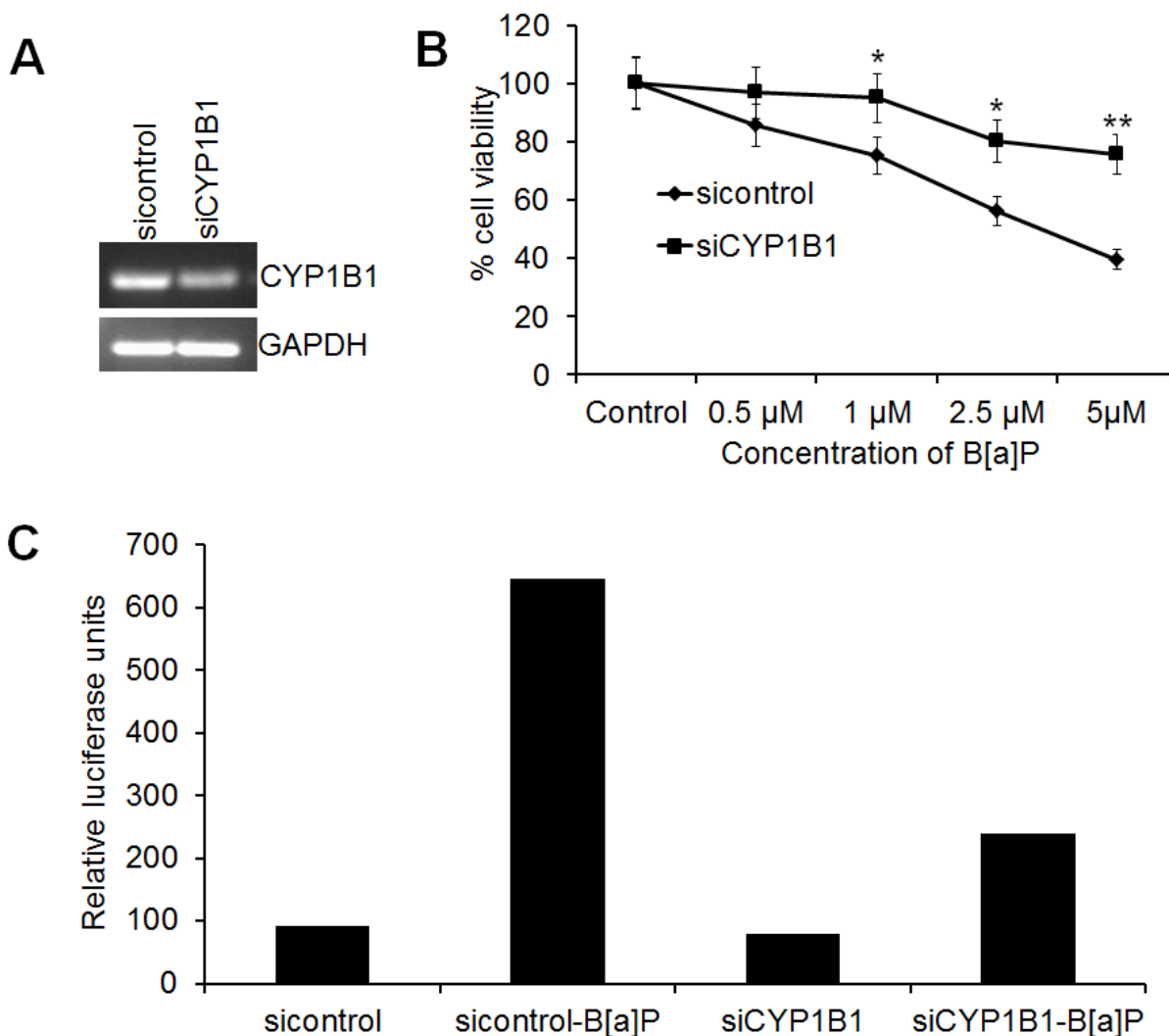


Fig.4.5. Clotrimazole potent inhibitor of cytochrome P450 playing crucial role in inhibit activity of B[a]P: (A) computational model showing clotrimazole (CTZ) (Purple) bound in a narrow active site of CYP1B1 (Green) using AutoDock 4.2. (B) The image was enlarged to clearly show binding conformation using chimera 1.6.2. (C) Binding energy graph of AutoDock 4.2 of CTZ and CYP1B1. (D) Showing binding amino acids residues present at

active site using Ligplot. (E) Using Pymol to visualize binding patten and residue. (F) HaCaT cells were pre-treated with CTZ (5 IM) for 2 h followed to B[a]P (5 IM or other) treatment and quantified for MTT assay after 72 h and caspase 3 expression after 48 h by caspase 3/7 Glo assay. Data reported as the mean \pm S.D. of three independent experiments and compared against PBS control. P Values < 0.05 and $P < 0.01$ values were considered significant.

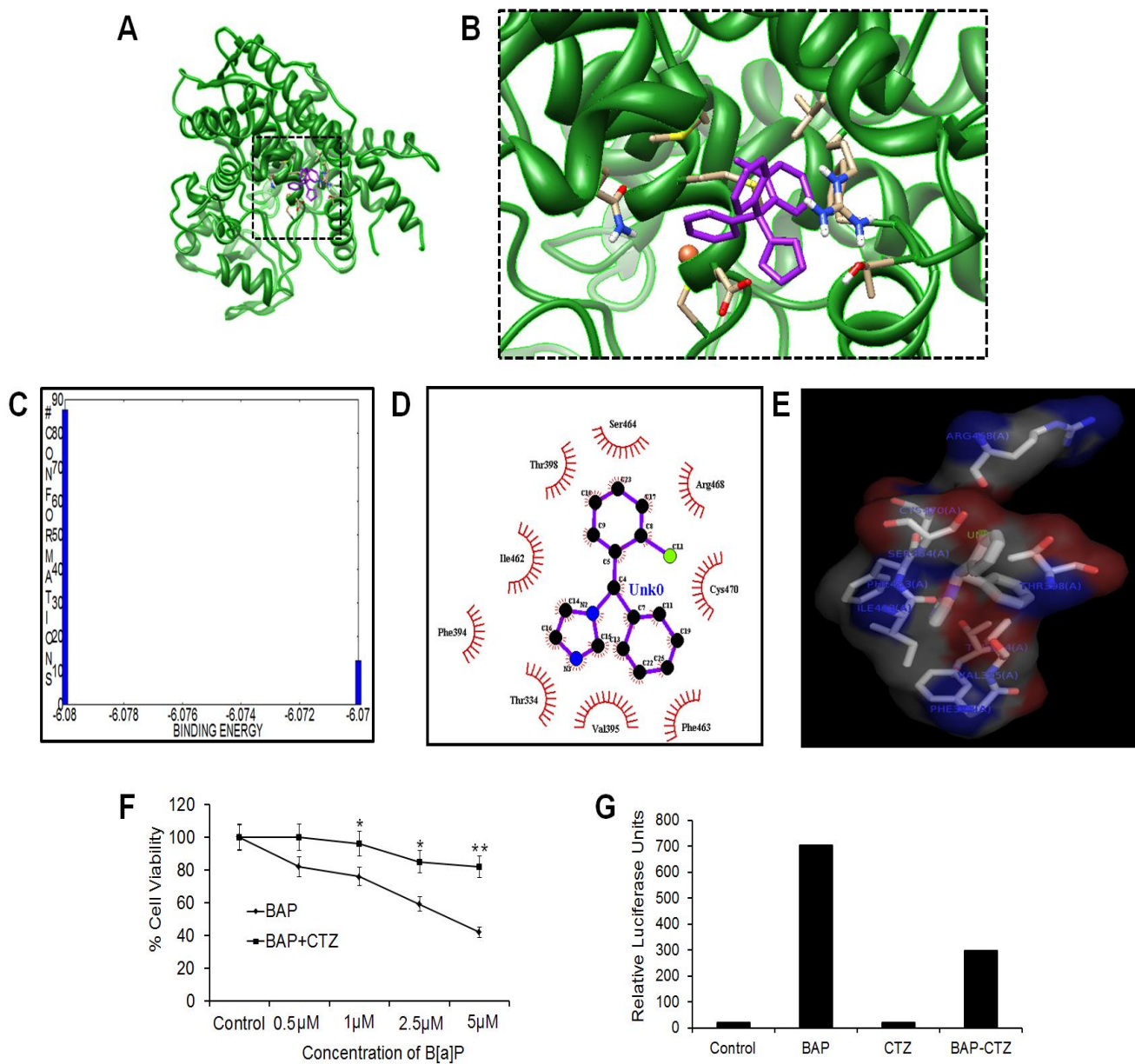


Fig.4.6. Clotrimazole potent inhibitor of cytochrome P450 playing crucial role in inhibit activity of B[a]P: (A) computational model showing clotrimazole (CTZ) (Purple) bound in a narrow active site of CYP1B1 (Green) using AutoDock 4.2. (B) The image was enlarged to clearly show binding conformation using chimera 1.6.2. (C) Binding energy graph of AutoDock 4.2 of CTZ and CYP1B1. (D) Showing binding amino acids residues present at active site using Ligplot. (E) Using Pymol to visualize binding patten and residue. (F) HaCaT cells were pre-treated

with CTZ (5 μ M) for 2 h followed to B[a]P (5 μ M or other) treatment and quantified for MTT assay after 72 h and caspase 3 expression after 48 h by caspase 3/7 Glo assay. Data reported as the mean \pm S.D. of three independent experiments and compared against PBS control.* P Values < 0.05 and**P < 0.01 values were considered significant.

4.3.6. Clotrimazole potent inhibitor of cytochrome P450 playing crucial role in inhibit activity of benzo[a]pyrene

To elucidate possible mechanism of B[a]P activation by CYP1B1 which induced different apoptosis pathways, we screened different types of available pharmacological CYP1B1 inhibitors. CTZ was identified as a potent inhibitor of B[a]P activated CYP1B1 to restrain apoptosis. CTZ is one of a family of imidazole-derived antimycotic agent which inhibits CYP1B1 mediated reaction. We observed CTZ bound at active site of CYP1B1 hydrophobic and Van der Waals interactions (Fig.4.6.A and B) with binding energy -6.03 kcal/mol using AutoDock 4.2 (Fig.4.6.C). The residues like S464, T398, F394, I462, T334, V395, F463, R468 and C470 were present at active site of CYP1B1 (Fig.4.6.D and E). The docking between CTZ–CYP1B1 complex and B[a]P showed no interactions between the complex and the ligand.

To investigate and validate the role of CTZ as CYP1B1 enzyme inhibitor, HaCaT cells were treated with B[a]P in presence of CTZ and apoptosis activity was quantified. The MTT assay showed that B[a]P induced cell death was very significantly inhibited in presence of CTZ as compared to only B[a]P (Fig.4.6.F). Next, we performed caspase-Glo assay in presence of CTZ and data showed that caspase 3 activity was very significantly decreased with treatment of B[a]P in presence of CTZ as compared to B[a]P alone. Our data clearly showed that CTZ could suppress the activity of B[a]P by inhibiting CYP1B1 (Fig.4.6.G). As CYP450 play important role in both biosynthesis and oxidative degradation of many physiological and foreign compounds, inhibition of CYP1B1 by CTZ could have important role in carcinogenesis.

4.4. Discussion

Abundant studies have been reported about carcinogenic and mutagenic effects of B[a]P and have been well documented in human, animals and other mammalian cell systems (Wass et al., 2011). B[a]P itself is an inert, hydrophobic molecule. As already discussed B[a]P becomes carcinogenic when metabolised by the CYP450 family of monooxygenases. It has been hypothesized that polymorphism in the CYP genes could affect the individual capacity in converting precarcinogens into carcinogens which is one of the important contributing factor to



individual susceptibility towards cancerous development (Tokiwa et al.,1993). CYP1A1 and CYP1B1 have been shown to be the most important human P450 enzymes in the metabolic activation of PAHs to carcinogenic intermediates (Roberts-Thomson et al., 1999; Luch et al., 1999). Here, we developed docking as an approach to study activation of PAHs and its signalling mechanisms through ligand–protein and protein–protein interactions which could provide an opportunity for understanding and formulating the active compound could be used as a tool for monitoring environment pollutants. Interestingly, we observed that B[a]P bound with CYP1B1 at its active site whereas water and glucose molecule showed no interaction with CYP1B1. This indicated that interaction between B[a]P and CYP1B1 was specific and binding at active site was required for activation. Previous study showed that vitamin D upon binding with CYP450 gets activated (John et al., 2010; Prosser and Jones, 2004). Another previous report showed that molecular docking and conformational sampling studies of the Ca²⁺ loaded caspase-3/calbindin-D28K interaction were performed in order to isolate potentially crucial intermolecular contacts. Residues in the active site loops of caspase 3 and EF-hands 1 and 2 of calbindin- D28K were shown to be critical to the interaction (Schuster, 2011). In addition, it showed that three series designed novel heterocyclic azoles derivatives containing pyrazine (5a–5k, 8a–8k and 11a–11k) were synthesized and their biological activities were evaluated as potential telomerase inhibitors (Bobay et al., 2012). Recently, Stolpmann et al. showed that B[a]P was a strong activator of the aryl hydrocarbon receptor (AHR) and the biotransformation of B[a]P was regulated via AHR. Our data deciphered that CYP1B1–B[a]P show high affinity of binding towards AHR which could associate in AHR activation and transcription regulation to convey toxic effects on cells. Next, the *in-silico* work showed B[a]P induced apoptosis. B[a]P– CYP1B1 complex then showed binding affinity towards caspase 8, 9 and 3. On contrary B[a]P alone did not show any types of interaction with different types of caspases. This indicated that the active metabolites from B[a]P–CYP1B1 complex as the end products of B[a]P metabolism may directly activate the signalling pathway including apoptosis signalling cascade. Moreover, several previous study showed that the inert and inactive B[a]P initially oxidized by CYP1A1 or CYP1B1 to phenols, such as 3-hydroxy-B[a]P and 9-hydroxy- B[a]P, and epoxides B[a]P-7,8-epoxide, which serves as a substrate for a second CYP-dependent oxidation, generating toxic BPDE-2. B[a]P-r-7,t-8-dihydrodiol-t-9,10-epoxide (BPDE-2) (Zhang al., 2012; Nordling et al., 2002; Shimada and Fujii-Kuriyama, 2004; Jiang et al., 2005). Our finding also



support that inhibition of CYP1B1 by siRNA approach and CTZ suppressed the B[a]P induced caspase activation followed to apoptosis. Caspases the key executioner of apoptosis is critical to the cellular commitment to apoptotic cell during B[a]P mediated death. The *in silico* study demonstrated that B[a]P–CYP450 showed high binding affinity towards caspase 8, 9 and 3 as indicated from lowest energy value. Our data showed that caspase 3 inhibitor Ac-DEVD-CMK bound in active site of caspases and presence of caspase inhibitors with B[a]P–CYP1B1 showed enhanced energy value suggesting lower binding affinity. So it was clearly demonstrated that B[a]P was an inactive state but during catabolism it was catalyzed by CYP450 family enzymes (CYP1B1) and induced apoptosis. This result of apoptosis was further confirmed performing Annexin V binding and DNA fragmentation assay evidently provided idea B[a]P induced apoptosis in HaCaT cell by dose dependent manner. The mechanism of apoptosis inhibition can occur by either direct caspase 3/7 inhibitor (Ac-DEVD-CMK) or inhibitor of the conversion of procaspase-3 to the active form (Huang et al., 2012; Cid et al., 2003; Barnoy et al., 2005). As B[a]P activated by CYP1B1 and induced apoptosis, sequentially we validated the hypothesis with inhibition of CYP1B1 complex by CTZ. Analysis of active binding sites showed that B[a]P and CTZ were bound at different sites on CYP1B1 and it clearly elaborated that binding of CTZ irreversible changed the configuration of CYP1B1. This leads to change in the active site of B[a]P and data showed that binding of B[a]P with CYP1B1 was completely abrogated in presence of CTZ. Similarly, study also showed a remarkable suppression of B[a]P induced cell death in presence of CTZ. Moreover, the CTZ was deciphered to be effective in reducing cytotoxicity induced by other PAH released from industrial pollutants. Interestingly, the specificity of the inhibitory effect of low concentration CTZ has been evaluated for different rat liver P450 (Walters et al., 2009; Turan et al., 2001) demonstrating blocking the activation of PAH by CTZ could have therapeutic benefits from several diseases including allergy and cancer.



Chapter 5

Benzo[a]pyrene mediated mitochondrial stress induces autophagy-dependent cell death



Abstract

Benzo[a]pyrene (B[a]P), known polycyclic aromatic hydrocarbon has been found to induce cytotoxicity through apoptosis. In the present study, we documented that B[a]P induced autophagy-dependent cell death through the canonical pathway in HaCaT cells. B[a]P was found to induce autophagy in HaCaT cells as determined by acridine orange staining, GFP-LC3 puncta cells and LC3-II accumulation. We examined that B[a]P activated by CYP1B1 and aryl hydrocarbon receptor (AHR) was associated with induction of autophagic cell death. Inhibition of autophagic death with siBeclin-1 as well as inhibiting apoptosis by overexpression of Bax^{-/-} could not alter the cell death suggesting that B[a]P independently induced autophagic and apoptotic death in HaCaT cells. The colocalization study showed mitochondria interacted with the lysosome and induced mitophagy in B[a]P treated cells. B[a]P declined the ATP/AMP ratio, resulting in diminished cellular metabolism and activation of AMP kinase, which induced AMPK/mammalian target of rapamycin-dependent autophagy. Interestingly, pretreatment of methyl pyruvate (MP) restored ATP production and reduced GFP-LC3 puncta formation in B[a]P treated HaCaT cells. Further, we showed that B[a]P was found to deplete oxygen consumption and ATP generation in mitochondria and activated reactive oxygen species (ROS) production to induce mitochondrial toxic autophagy in HaCaT cells. Additionally, B[a]P mediated ROS generation was suppressed by pretreatment of MP in HaCaT cells, confirming a role for energy alternation in B[a]P mediated autophagic cell death. In conclusion, the present study revealed distinctive aspects as to how B[a]P contributes to cellular toxicity and identified as an inducer of mitophagy dependent cell death.

Keywords: Benzo[a]pyrene, autophagic cell death, mitochondrial stress, ATP depletion, mitophagy



5.1. Introduction

Benzo[a]pyrene (B[a]P) belongs to a class of polycyclic aromatic hydrocarbons (PAHs) that serve as micropollutants in the environment. It is produced during the incomplete combustion of organic materials like wood and tobacco smoke, vehicle exhaust, residential heating, electric power, industrial source (Cirla et al., 2007). B[a]P contributes to approximately 50 % of the total carcinogenic potential of the PAH group. The occupational exposure, for instance, is associated with lung, bladder, oral cavity, esophagus, hematolymphatic, skin, lip, pharynx and larynx cancers (IARC 2012) (Li et al., 2007; Hakami et al., 2008; Chen et al., 2013; Labib et al., 2012). B[a]P causes cytotoxic, teratogenic, genotoxic, mutagenic, and carcinogenic effects in various tissues and cell types in organisms (Nebert, 1989; Ellard et al., 1991). Cytochrome P450 catalyses the hydroxylation at a vacant position of an aromatic ring is deliberated to be the hallmark for the instigation of carcinogenesis, through the formation of highly reactive alteration products that can induce oncogenic mutations in experimental animals and humans (Wei et al., 1996; Luneva et al., 2000; Arlt et al., 2008; Androutsopoulos et al., 2009). The transcriptional activation of the CYP1A1 gene is facilitated by the binding of environmental pollutants and inhalation chemicals, particularly substrates of the CYP1A1 enzyme, to the cytosolic receptor AHR and is also intermediated by its translocation to the nucleus and subsequent formation of a dimer, which interacts with the corresponding xenobiotic response elements (XRE) to stimulate transcription located in the promoter region of AHR target genes such as CYP1A1 and CYP1B1 (Hankinson et al., 1995;Beischlag et al., 2008;Tsay et al., 2013; Murray et al., 2014). B[a]P and its metabolites cause DNA damage and can affect numerous cellular processes leading to carcinogenesis. In addition, other effects have also been described including epigenetic modification, cell cycle changes, inappropriate cell death and survival, disturbed metabolism and gene expression.

Although environmental toxicant and xenobiotic- induced cell death has been extensively investigated, little attention has been paid to the role of cellular protective mechanisms in environmental toxicant and xenobiotic-induced cell death and tissue injury. In addition to cell death, autophagy may also be a cell survival mechanism where old and damaged cell material and organelles are degraded by lysosomal hydrolases. Autophagy is an evolutionarily conserved catabolic process where a cell self digests its cytoplasmic contents (the



expression derives from Greek; “auto” – self and “phagia” – eating), and it is a crucial adaptive response that recycles energy and nutrients during starvation or stress (Mizushima et al., 2008; Yin et al., 2008; Ding et al., 2010; Arias et al., 2011; Bhutia et al., 2011; Bhutia et al., 2013; Panda et al., 2015). The role of autophagy in normal cellular homeostasis, the intricate relationship between cellular stress and the stimulation of autophagy, and the identification of specific xenobiotics capable of modulating autophagy, point to the importance of the autophagic process in toxicology. Autophagy is a conserved catabolic process whereby cellular components are degraded by engulfment into autophagosomes. Autophagosomes fuse with lysosomes, which contain hydrolytic enzymes that break down cellular components. Mitophagy insinuate the degradation of mitochondria through autophagy (Haouzi et al 2002; Kim et al., 2007; Garrido-Maraver et al., 2015). In this study, within a research project aimed to investigate the importance of autophagy in homeostasis, the close relationship between cell stress and autophagy, and the documentation of environmental stressors and xenobiotics that are capable of modulating autophagy, all underscore the prominence of this cellular process to the field of toxicology.

5.2. Materials and methods

5.2.1. Chemical and reagents

Benzo[a]pyrene, dimethyl sulfoxide (DMSO), 3-[4-5-dimethylthiazol-2-yl]-2,5-diphenyl tetrazolium bromide (MTT), Methyl pyruvate, acridine orange from Sigma, USA. Fetal bovine serum (sterile-filtered, South American origin), minimal essential medium (MEM), Dulbecco's minimal essential medium (DMEM), antibiotic-antimycotic (100X) solution, LysoTracker red, MitoTracker Green and Lipofectamine 2000[®] were purchased from Invitrogen, USA. The caspase-Glo assay kit for quantification of caspases were purchased from Promega, USA, siRNA for Beclin-1, AHR, CYP1B1 and control siRNA from SantaCruz Biotechnology, USA.

5.2.2. Cell culture

The immortalized human keratinocyte cell line (HaCaT) was obtained from National Centre for Cell Science, Pune, India and cultured in Dulbecco's modified Eagle's medium with high glucose (DMEM/high glucose), supplemented with 10% heat-inactivated fetal bovine serum (FBS) containing and 1% penicillin–streptomycin. The cells were maintained at 37 °C in a humidified atmosphere at 5% CO₂. All media, supplements and antibiotics were purchased from Invitrogen (Das et al., 2014).



5.2.3. Cell viability by MTT assay

HaCaT cells were harvested from maintenance cultures in logarithmic phase and were counted by hemocytometer using trypan blue solution. HaCaT (1×10^4 cells/well) were cultured in a 96-well plate at 37 °C, and exposed to varying concentrations of B[a]P for 72 h. After 72 h MTT solution (5mg/ml) were added, post 4 h incubation, the resultant formazan crystals were dissolved in dimethyl sulfoxide and the absorbance was measured by a microplate reader (Perkin Elmer) at 595 nm. All experiments were performed in triplicate, and the relative cell viability was expressed as percentage relative to the untreated control cells (Das et al., 2014).

5.2.4. Caspase assays

HaCaT cells were seeded in 6 well plates and were treated with B[a]P for 48 h. After treatment, caspase activity was measured using caspase-Glo assay following the manufacturer's protocol (Promega Corp., Madison, WI) (Bhutia et al., 2010; Das et al., 2014).

5.2.5. Measurement of autophagy

HaCaT cells were cultured with B[a]P for 48 h, washed with PBS and then detection of late autophagic vesicles was done by staining with 0.5 µg/ml of acridine orange for 15 minutes. The media was discarded and the cells were washed with PBS for three times and observed using an inverted fluorescent microscope (Panda et al., 2014).

HaCaT cells were transfected with pEGFP-LC3 (Addgene plasmid 11546, Jackson et al., 2005) and 48h after transfection, HaCaT cells were incubated in presence of BM for 48 h and the level of autophagy was quantified by counting the mean number cells with puncta fluorescence to autophagosome formation (Panda et al., 2014; Mukhopadhyay et al., 2014b).

5.2.6. Measurement of Mitochondrial ROS

Mitochondrial ROS was measured by MitoSox (Invitrogen) in a fluorescence microscope. After specific treatment, HaCaT cells were incubated with MitoSox in incomplete media for 30 min in the CO₂ incubator. Cells were then washed 3 times in PBS and live cell imaging was performed in fluorescence microscope.

5.2.7. Measurement of cellular ATP level

Determination of cellular ATP level from cellular lysates was done following the protocol of the ENLITEN[®] ATP Assay System Bioluminescence kit from Promega (Madison, WI, USA).



5.2.8. Western blotting analysis

HaCaT cells were treated with B[a]P before proteins were extracted. Cell extracts were prepared in cell lysis buffer, and equal amount of proteins were resolved by SDS-PAGE and then transferred onto PVDF membrane. Protein level in each band was evaluated using antibody against LC3, ATG5, Beclin-1, total AMPK, phospho-AMPK, phospho-mTOR, phospho-S6K, CYP1B1 and AHR protein levels were performed as described previously (Mukhopadhyay et al., 2014b).

5.2.9. Plasmids, Small interfering RNA and transfection

1×10^6 HaCaT cells were cultured in 60 mm petriplate and transfected with an 80 % confluency using Oligofectamine reagent (Invitrogen) following manufacturers protocol. HaCaT cells were transfected with specific siRNA by using Lipofectamine 2000, following the manufacturer's instructions. CYP1B1 siRNA(sc-44546) sc-44546A: Sense: CAGCUCGAUUCUUGGACAATT, Antisense: UUGUCCAAGAAUCGAGCUGTT; sc-44546B: Sense: GGAAACUUGCCAAUAAGAATT, Antisense: UUCUUAUUGGCAAGUUUCCTT; sc-44546C: Sense: CAAGAUUGGUCUCCCAUAUTT, Antisense:AUAUGGGAGACCAAUCUUGTT, AHRsiRNA (sc-29654) sequence Sense: UACUCCACCUCAGUUGGCTT, Antisense: GCCAACUGAGGUGGAAGUATT (all sequences are provided in 5' → 3' orientation) and control siRNA (sc-37007) were from SantaCruz Biotechnology, Dallas, TX. After 48 h of transfection cells were treated with B[a]P and autophagy and apoptosis was studied (Bao et al., 2015).

5.2.10. Visualization of mitophagy

After specific treatment, HaCaT cells were incubated with lysotracker red and mitotracker green at 37 °C for 30 minutes and followed to three times washing with incomplete media. The cells were observed at 200× magnifications under a confocal microscope (Mukhopadhyay et al., 2015).

5.2.11. Measurement of mitochondrial respiration rate and glycolysis study

In order to analyse the mitochondrial oxygen consumption rate (OCR), 1×10^5 HaCaT cells were seeded in a special respirometric plate. Following which B[a]P was treated for 2h and then OCR analysis was carried out in XF-24 Extracellular Flux Analyzer (Seahorse Bioscience, MA, USA) by following the protocol of (Santiago et al BBA 2014, PMID: 25038307). We determined aerobic glycolysis by determining enzymatic lactate as well as extracellular



acidification rate (ECAR), which is a substitute for lactate efflux rate in extracellular medium. After analysing the basal ECAR, maximal reserve capacity analysis was done by oligomycin (1 μ M) treatment. ECAR was represented in milli-pH (mpH) units expressing the alternation in pH per min.

5.2.12. Statistical Analysis:

Data are represented as the mean \pm SE and analyzed for statistical significance using one-way ANOVA followed by Newman-Keul's test as a post hoc test. A *P* value of <0.05 was considered significant.

5.3. Results:

5.3.1. Autophagic cell death with benzo[a]pyrene in HaCaT cells

Skin act as the first line of immune defence against xenobiotic exposure. We investigated whether B[a]P does have any cytotoxic effect through induction of autophagy on human skin keratinocytes HaCaT cells. Initially, we stained the B[a]P treated HaCaT cells with a frequently used acidotropic dye, acridine orange and found out that there was a dose dependent increase of late autophagic vacuoles (Fig.5.1. A and B). The unique standard to analyze autophagy is to monitor conversion of microtubule associated light chain 3 (LC3) form I to LC3 II form which is manifested through the autophagic puncta formation. We transfected HaCaT cells with pEGFP-LC3 and found a dose dependent accrual of autophagic puncta 1, 2.5, and 5 μ g/ml B[a]P treated doses respectively (Panda et al., 2014). We also compared our results against a positive control using pEGFP-LC3 transfected cells in serum free media for 24 h, which showed an increase in autophagic puncta (Fig.5.1.C and D). Moreover, rise of B[a]P dosage resulted in alterations of cell morphology including cellular rounding patterns in pEGFP-LC3 transfected HaCaT cells was seen along with autophagy, specifying that there was a visibly evident death involved with autophagy. Hence, B[a]P may be regarded to trigger autophagic cell death. With this background, we demonstrate that B[a]P is capable of inducing both autophagic and apoptotic cell death. To rule out nonspecific aggregations of ectopically expressed GFP-LC3, we scrutinized changes in the expression of endogenous LC3 (Kabeya et al., 2000; Wu et al., 2006; Bhutia et al., 2010). HaCaT cells with B[a]P led to a rapid accumulation of the LC3-II form (corresponding to the characteristic lipidation of this protein during autophagosomes



formation) in a dose dependent manner compared with control and B[a]P-treated cells

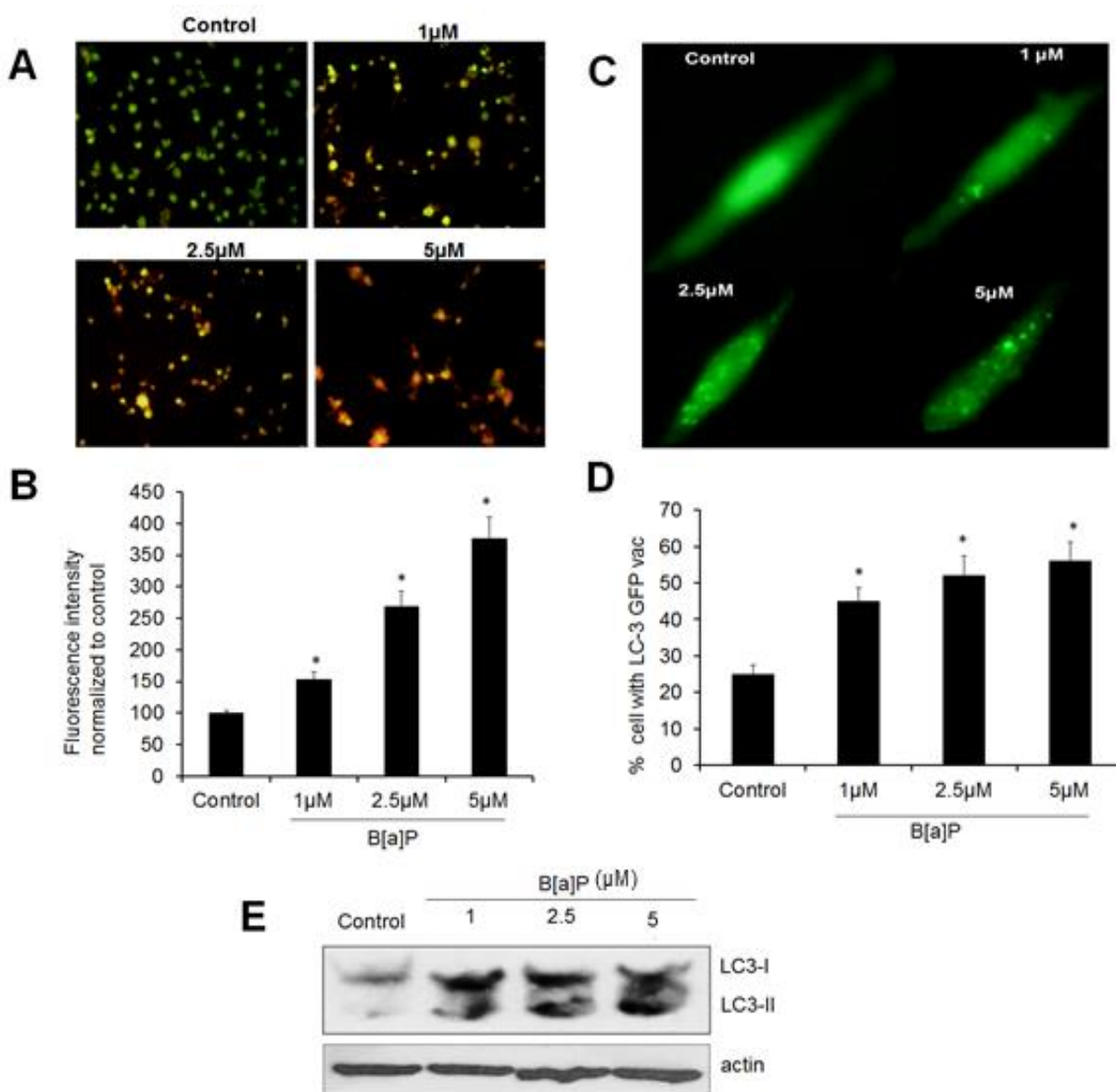


Fig.5.1. Benzo[a]pyrene induced autophagic cell death in HaCaT cells.(A) HaCaT cells were treated with different concentration of B[a]P (1, 2.5, 5 μM) for 24 h following that acridine orange staining was done for analyzing autophagic vesicles. (B) Red fluorescence intensity indicating the autophagic progression was quantified taking control as 100 arbitrary units. (C) HaCaT cells were transfected with GFP-LC3 for 48h followed by treatment with different doses of B[a]P as in (A), then GFP-LC3 puncta were enumerated to quantify autophagosome formation (D), at least 100 number of GFP-LC3 transfected cells were counted. (E) Accumulation of LC3-II was observed by Western blot after treating HaCaT cells with various doses of B[a]P for 24 h. Data are reported as mean ± SD of five different observations and compared against PBS control by using Student's t-test. *P* values <0.05 were considered significant (*significant compared to DMSO treated control).

(Fig.5.1.E). Autophagy can be mediated by the canonical pathway, in which Beclin-1 initiates the generation of the autophagosome by forming a multiprotein complex with class III phosphatidylinositol-3-kinase or hVps34. Simultaneously, autophagy can occur by the noncanonical pathway independent of Beclin-1 and hVps34 (Bhutia et al., 2010; Greene et al., 2012; Decuypere et al., 2013). In our study we analyzed the expression of Beclin-1 and ATG5 expression and found to increase in dose dependent manner (Fig.5.2.A). To determine pathway mediates B[a]P–induced autophagy, we used an siRNA approach to selectively knockdown essential autophagy (atg) genes, such as Beclin-1, and quantified GFP-LC3 punctate formation. The targeted siRNAs resulted in a substantial down-regulation of their corresponding encoded proteins (Fig.5.2.B). Among these genes, inhibition of Beclin-1 decrease the percentage of GFP-LC3–positive cells or LC3-II levels (Fig5.2.C).

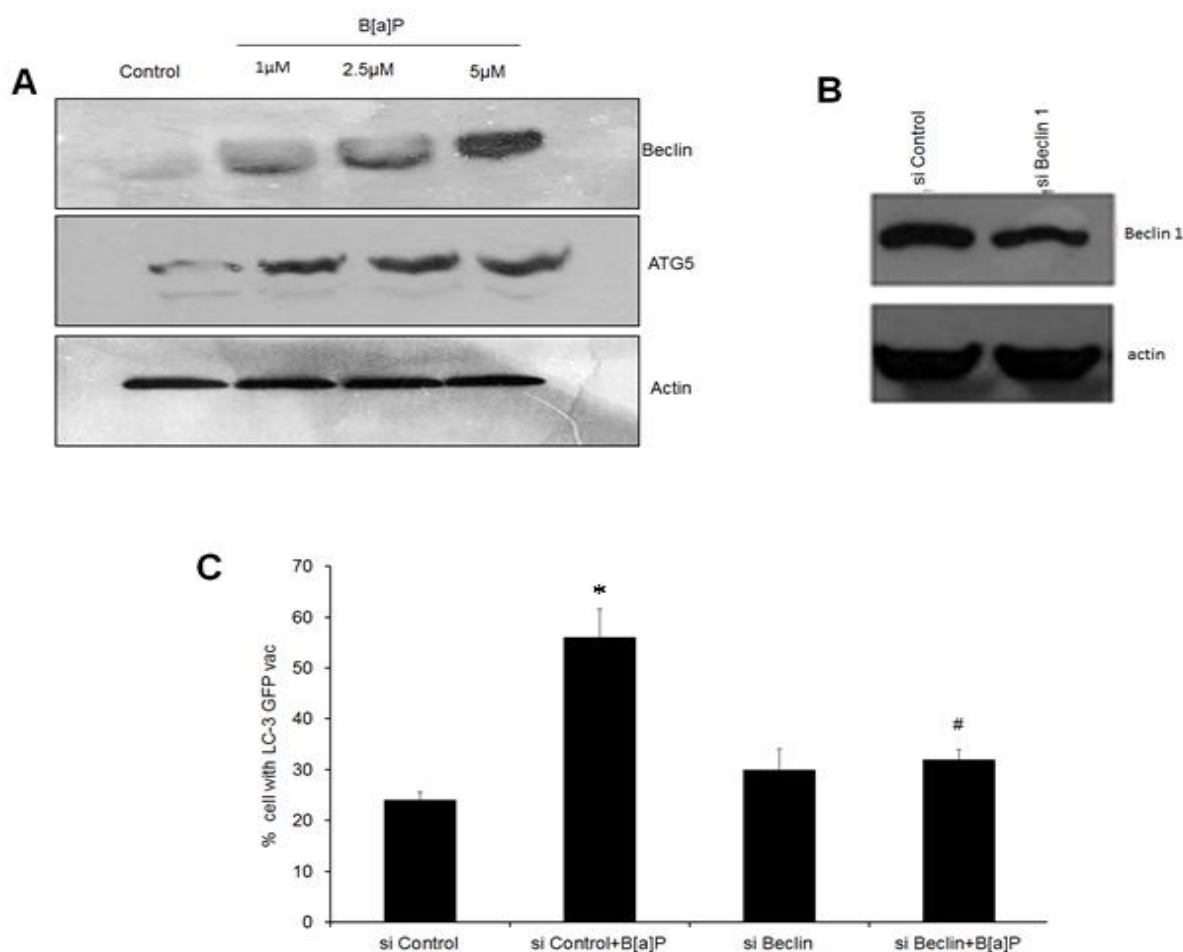


Fig.5.2. Benzo[a]pyrene induced autophagic cell death through the canonical pathway. (A) The expression of

Beclin-1 and ATG5 was determined by performing Western blot. (B) The siRNA transfected to selectively knockdown si Beclin (C) Percentage of GFP-LC3 puncta formation was quantified in siBeclin-1 knockdown cells treated with B[a]P (5 μ M) for 24h. *represents a statistically significant change in comparison to pcDNA (*P < 0.05).

5.3.2. Activated benzo[a]pyrene induced autophagic cell death

To investigate the potential involvement of CYP1B1 and AHR in autophagic cell death, HaCaT cells were transfected with siRNA against CYP1B1 and AHR for 48 h and autophagy was quantified pEGFP-LC3 puncta formation. The CYP1B1- and AHR-knockdown cells showed a decrease in autophagic puncta in B[a]P-treated cells as compared to sicontrol (Fig.5.3.A and B). (Stolpmann et al., 2012).

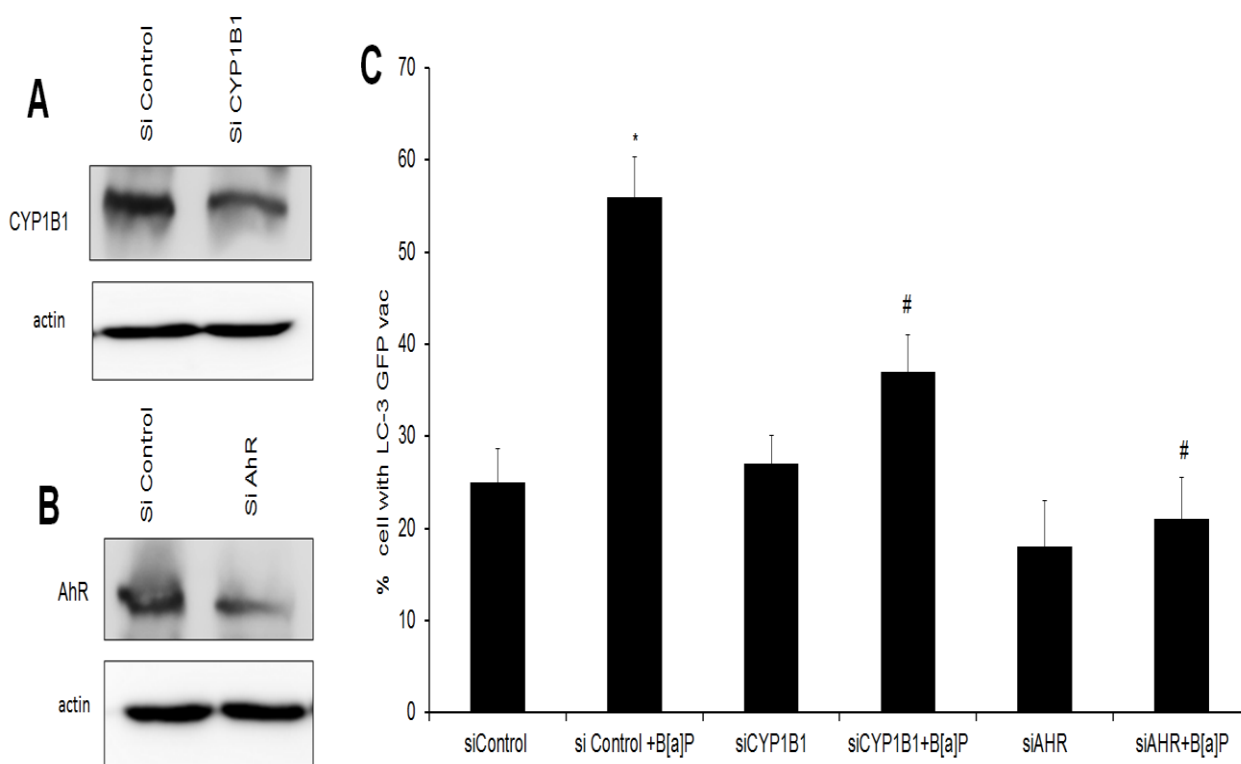


Fig.5.3. Benzo[a]pyrene activated by CYP1B1 and AHR induced autophagic cell death. The siRNA transfected to selectively knockdown CYP1B1 and AHR (A) in HaCaT cells and showed a decrease in autophagic puncta in B[a]P-treated (24 h, 5 μ M) cells as compared to siControl (B) .

5.3.3. Relation between benzo[a]pyrene mediated apoptosis and autophagic cell death

Simultaneous approach apoptosis and autophagic cell death may occur simultaneously and inhibition of autophagic activity in cells may switch responses to death signals from autophagic

cell death to apoptotic cell death and vice versa (Chatterjee et al., 2015). We performed the MTT assay in Beclin-1 knockdown (Fig.5.2.B) and Bax^{-/-} HaCaT cells (Fig.5.4.A) and data showed that the cell viability was decreased in dose dependent manner with having difference among the different groups indicating the B[a]P induced autophagic cell death was independent of apoptosis (Fig.5.4.B). To scrutinize the role of B[a]P mediated autophagic death in apoptosis deficient cells, autophagic death was investigated in Bax^{-/-} HaCaT cells. The Bax^{-/-} HaCaT cells were characterized showing that knockdown of these proapoptotic proteins Bax blocks apoptosis induction by B[a]P (Fig.5.4.C). However, B[a]P treated Bax^{-/-} HaCaT cells did not exhibit higher autophagic phenotypes compared with pcDNA as evidenced by GFP-LC3 puncta vacuole formation (Fig.5.4.D). Further we performed caspase-Glo assay in siBeclin-1 transfected HaCaT cells in presence of B[a]P and data clearly showed that caspase 3/7 activity did not show any change in Beclin knocked down with respect to sicontrol group, confirming the hypothesis (Fig.5.4.E).

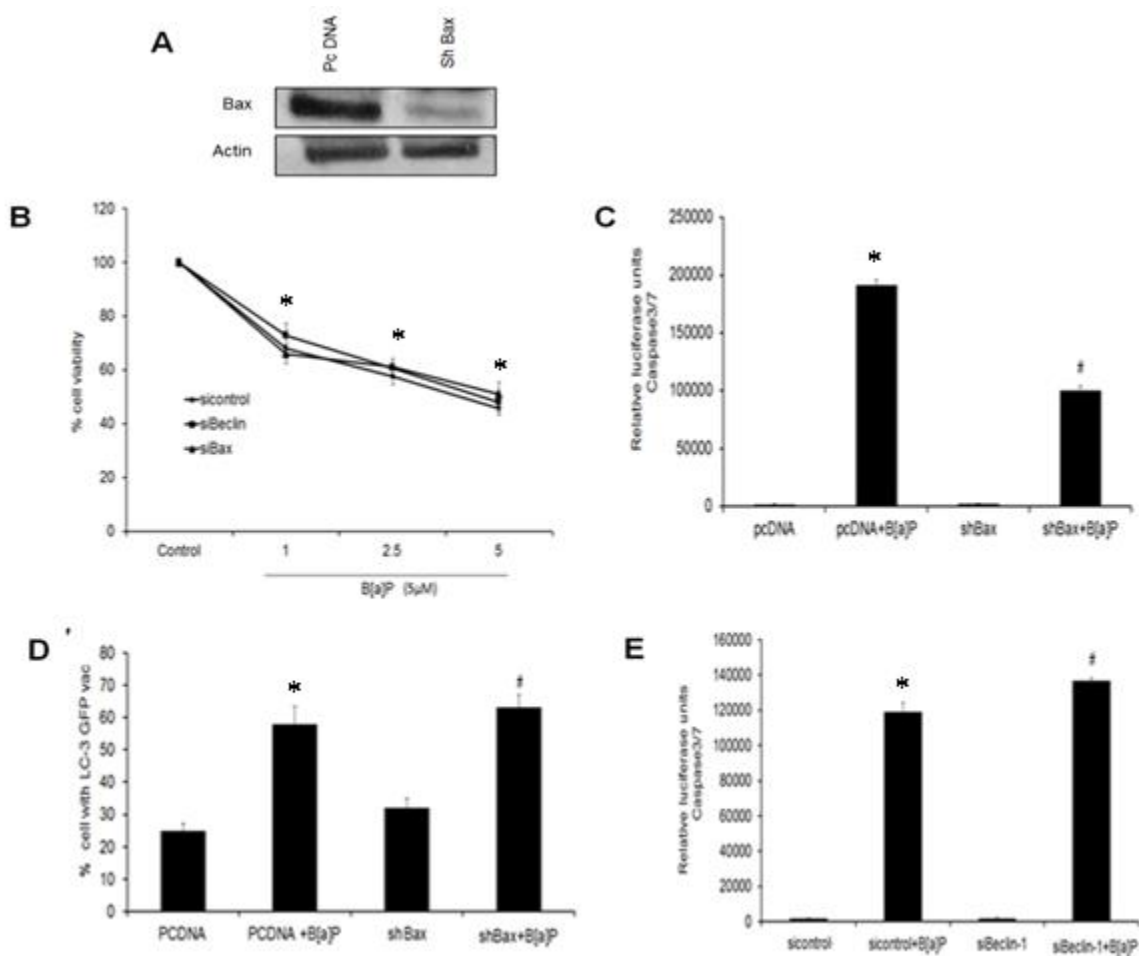


Fig.5.4. Benzo[a]pyrene mediated apoptosis and autophagic cell death occurred simultaneously. (A) The shRNA transfected to selectively knockdown sh Bax (B) MTT assay was performed in HaCaT cells transfected with mentioned targets. (C) Apoptotic progression in Bax^{k/d} HaCaT cells were quantified after B[a]P treatment (24 h, 5 μ M) by Caspase-3/7 expression analysis by Caspase-Glo 3/7 assay. (D) Autophagic progression was analysed by GFP-LC3 puncta enumeration in Bax^{k/d} HaCaT cells in comparison to pcDNA after B[a]P treatment. (E) Again, caspase 3/7 expression was analysed in B[a]P treated siBeclin-1 treated HaCaT cells. * represents a statistically significant change in comparison to sicontrol (*P < 0.05).

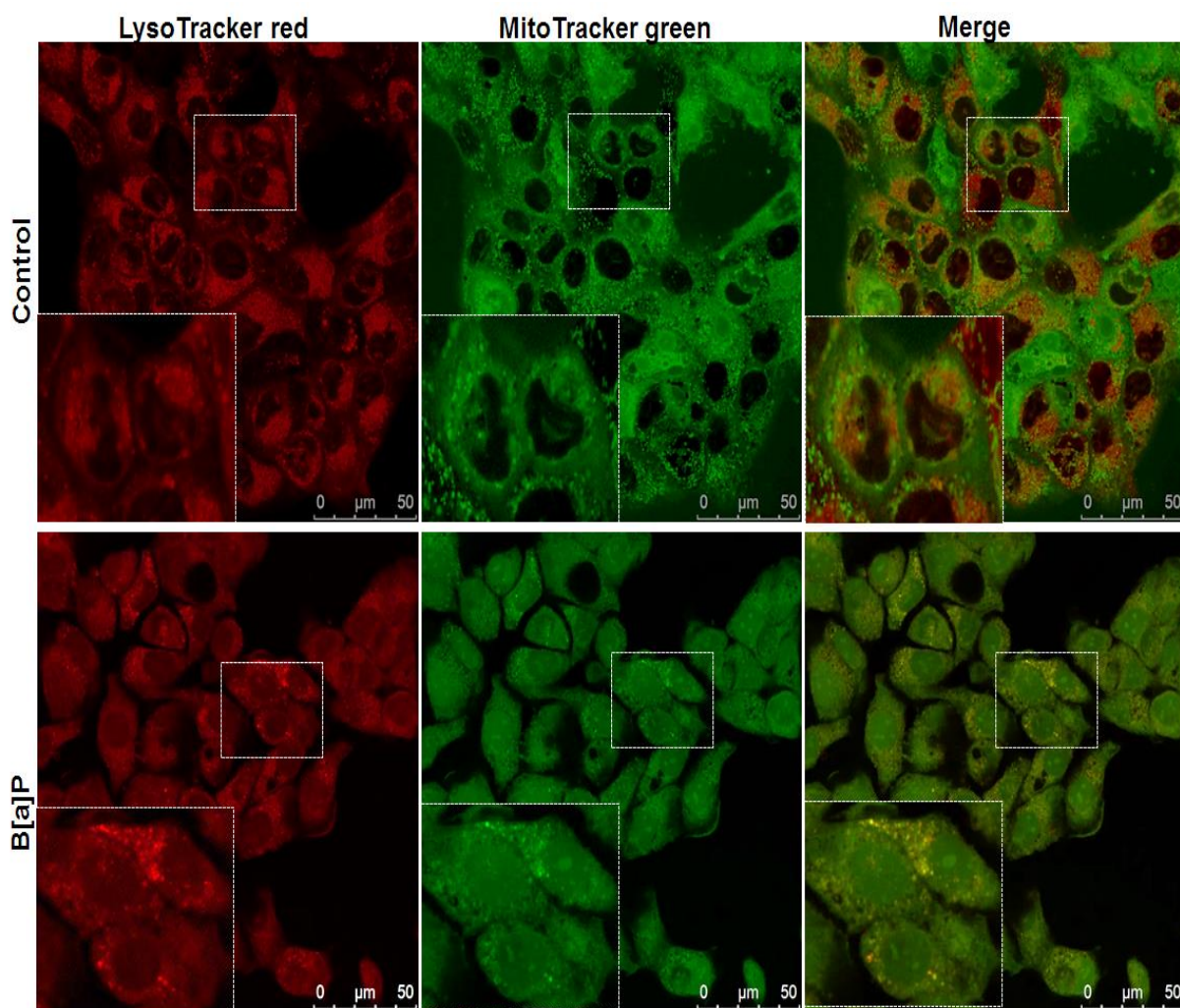


Fig.5.5. Benzo[a]pyrene induced mitophagic cell death. HaCaT cells treated with B[a]P for 12 h and colocalization analysis with Mito Tracker Green (200 nM) and LysoTracker Red (100 nM) was done by confocal microscopy. Merged image represents intense yellow color in comparison to control confirming occurrence of mitophagy after B[a]P treated HaCaT cells. The inset shows higher magnification of boxed area. Scale bar represents (50 μ m).

5.3.4. Benzo[a]pyrene induced mitophagy

However, mitochondria can swiftly change into death-promoting organelles. In response to environmental stress, mitochondria become producers of excessive reactive oxygen species and release pro-death proteins, resulting in disrupted ATP synthesis and activation of cell death pathways (Kubli et al., 2012). Interestingly, cells have developed a defense mechanism against aberrant mitochondria that can cause harm to the cell. This mechanism involves selective sequestration and ensuing degradation of the dysfunctional mitochondrion before it causes activation of cell death. Induction of mitochondrial autophagy, or mitophagy, results in selective clearance of damaged mitochondria in cells. After 24 h treated with B[a]P, HaCaT cells were stained with mitotracker green and lysotracker red and our, data revealed both mitochondria and lysosomes were co-localized (Fig.5.5.) suggesting reactive mitochondria were degraded with autophagolysosome and inducing autophagic cell death by initiating mitochondrial injury. With overwhelming mitochondrial damage, apoptosis becomes dominant, and inactivation of critical proteins of the autophagy pathway allows for cell death.

5.3.5. Benzo[a]pyrene induced cellular energy deficiency leading to AMPK/mTor Pathway- dependent Autophagy

We investigated whether a decrease in ATP/AMP ratio might induce autophagy by affecting cellular bioenergetics (Bhutia et al., 2010). To test this possibility, we monitored changes in cellular ATP levels in response to B[a]P. HaCaT cells infected with B[a]P displayed a dose-dependent decrease in the levels of ATP, suggesting that cellular energy depletion might be responsible for B[a]P induced autophagy (Fig.5.6.A). AMPK is activated as intracellular AMP/ATP ratios rise. B[a]P caused a significant increase of AMPK phosphorylation at Thr-172. Phospho-AMPKThr-172 phosphorylates and activates TSC2, further inhibiting the activation of downstream targets, such as mTOR and S6. Phosphorylation of mTOR and S6 proteins was substantially decreased in B[a]P treated cells (Fig.5.6.B). We next determined whether the depletion of ATP production in HaCaT cells could be reversed by pretreating cells with a cell-permeable form of pyruvate, methylpyruvate (MP), which can be oxidized in the tricarboxylic acid cycle to produce NADH, which fuels the electron transport system and ATP production (Verrax et al.,2011). MP restored ATP production in B[a]P treated cells to levels that paralleled those observed in untreated cells (Fig.5.6.C). Moreover, GFP-LC3 puncta



formation was reduced after addition of MP in HaCaT cells (Fig.5.6.D). Collectively, our data demonstrate that B[a]P induced disruption of cellular bioenergetics contributes to autophagy formation.

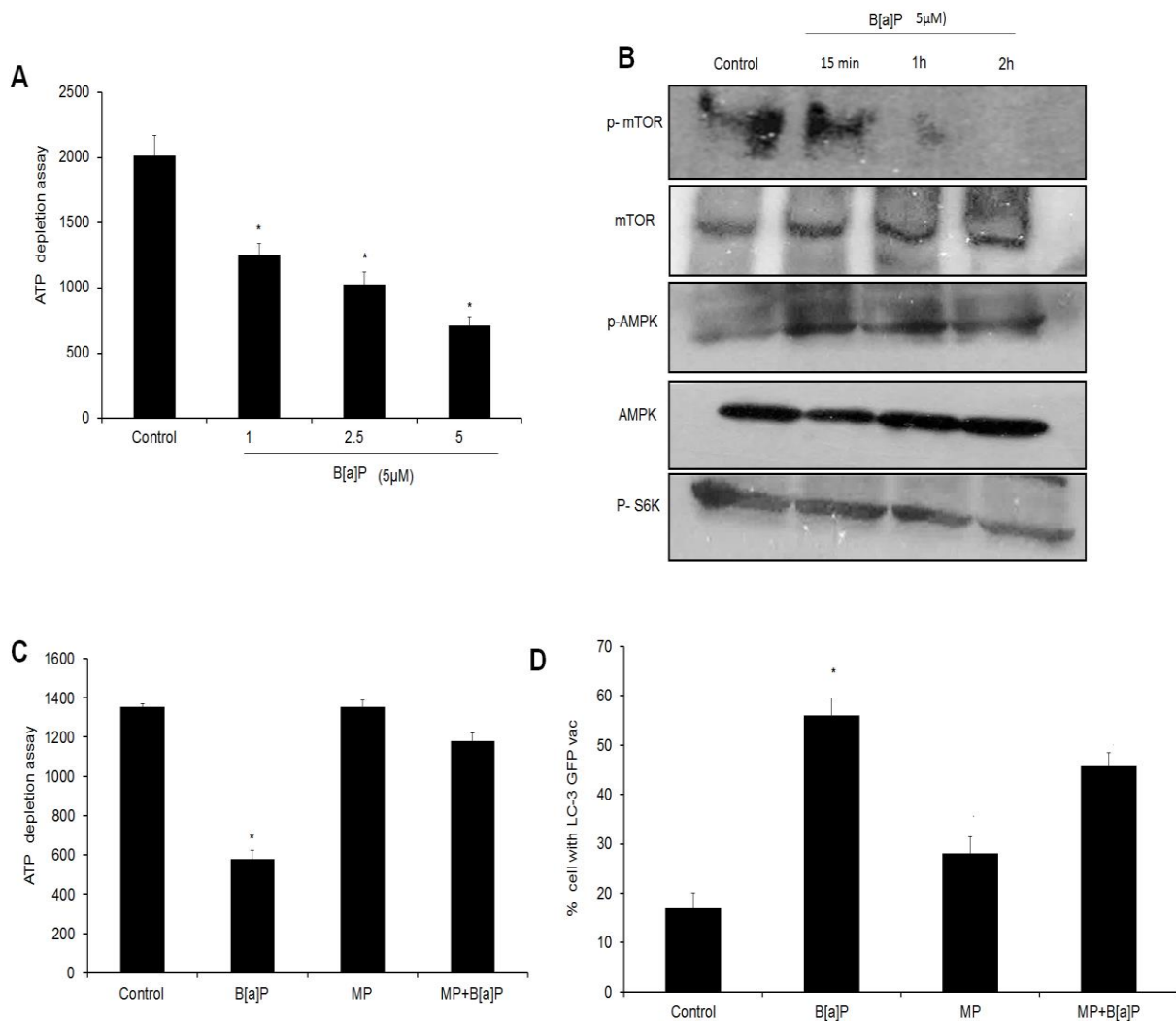


Fig.5.6. Benzo[a]pyrene activated AMPK/mTOR-axis found to lead autophagy dependent cell death in response to cellular energy deficiency in HaCaT cells. (A) HaCaT cells were treated with B[a]P with different doses (1, 2.5 and 5 μM) of B[a]P for 2h followed by measurement of ATP levels as mentioned in material section. (B) Western blot analysis of key AMPK/mTOR-axis activating proteins were analyzed after B[a]P (5 μM) treatment in HaCaT cells at mentioned time points. (C) Methylpyruvate (MP) (1 mM, 2 h) showed recovery in ATP level in comparison to B[a]P treated group. (D) Similarly percentage of GFP-LC3 puncta formation was quantified in (MP) treated group along with B[a]P treated group. *represents a statistically significant change in comparison to control (*P < 0.05).

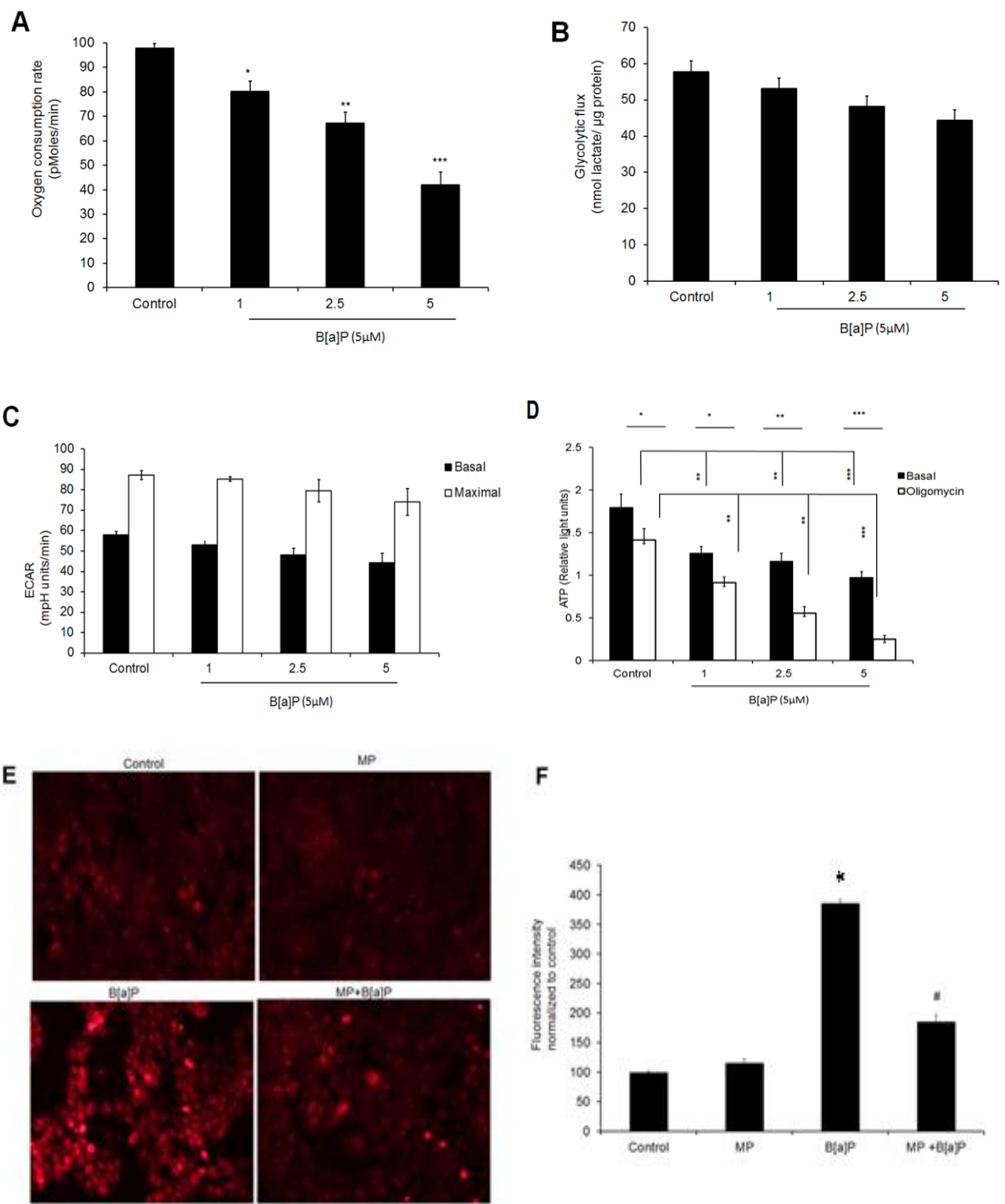


Fig.5.7. Activation of mitochondrial oxidative stress associated with B[a]P mediated autophagy.(A) Bioenergetics analysis was performed by measuring oxygen consumption rate (OCR) in HaCaT cells after B[a]P treatment (1, 2.5 and 5 μM, for 2h) . (B) Glycolytic flux in the presence of mentioned doses of B[a]P was analysed along with basal ECAR and maximal glycolytic capacity (C). (D) The relative level of ATP was determined in

HaCaT cells after 2h of B[a]P treatment under basal and oligomycin treated situation. (E) Measurement of B[a]P induced ROS in the presence of MP was analysed and quantified (F). *Represents a statistically significant change in comparison to control (*P < 0.05).

5.3.6. Mitochondrial oxidative stress was associated with B[a]P mediated autophagy

Our findings showed bioenergetics analysis of mitochondrial oxygen consumption rate (Fig5.7.A), where we found that B[a]P treatment resulted in a dose dependent decrease in OCR in a statistically significant manner. Furthermore, this fall in ATP was not compensated by any increase in the glycolytic activity (Fig.5.7.B). Oligomycin treatment resulted in modest change in glycolysis which was insufficient to maintain the ATP titre (Fig.5.7.C and D). This finding suggests that, B[a]P provides a strong energy imbalance due to mitochondrial damage, that supports the importance of mitochondria in normal keratinocytes as previously reported (Tamiji et al., 2005, Česen et al., 2013). Autophagy is activated in response to cellular oxidative stress from reactive oxygen species (ROS) and we studied that B[a]P induced ROS generation might activate autophagy. Our data showed that B[a]P induced ROS in HaCaT cells as quantified using MitoSox in a fluorescence microscope (Fig.5.7.E and F) and we interrogated whether the MP supplementation was able to downregulate mitochondrial ROS generation (Fig.5.7.E and F). It was clearly demonstrated that external supplementation of MP also reduced the ROS level in B[a]P treated cells, signifying that B[a]P is a definite inducer of mitochondrial damage inflicting to loss of ATP production, which compels the undamaged mitochondria to overwork and subsequently escalate ROS level.

5.4. Discussion

Autophagy, in mammalian cells, is a expansively unknown process and only recently mammalian homologues of yeast genes have been discovered and used as molecular markers for autophagy (Wang et al., 2003). The role of autophagy covers beyond the general homeostatic removal, degradation and recycling of damaged proteins and organelles to various specific physiological and pathological processes such as development, immunity, energy homeostasis, cell death or tumourigenesis (Dhalla et al., 2000; Sayre et al., 2001; Jenner, 2003; Dalle-Donne et al., 2006; Uttara et al., 2009).

Benzo[a]pyrene (B[a]P) are the utmost persuasive according to the Environmental Protection Agency. PAHs can damage human health by causing affects to the immune system,



reduced fertility, developmental abnormalities, and respiratory damage; additionally, they promote the development of various types of cancer. Besides, previous study showed that the inert and inactive B[a]P initially oxidized by CYP1A1 or CYP1B1 to phenols, such as 3-hydroxy-B[a]P and 9-hydroxy-B[a]P, and epoxides B[a]P-7,8-epoxide, which act as a substrate for a second CYP-dependent oxidation, generating toxic BPDE-2. B[a]P-r-7,t-8-dihydrodiol-t-9,10-epoxide (BPDE-2) (Jiang et al., 2005; Das et al., 2014).

Our finding also support that inhibition of CYP1B1 and AHR by siRNA approach suppressed the B[a]P induced Autophagic cell death. We confirmed by GFP-LC3 and acridine orange staining.

The B[a]P induces stress condition by producing ROS. These ROS produce toxic effects by initiating lipid peroxidation directly or by acting as second messengers for the primary free radicals that initiate lipid peroxidation. Thus, the enhanced mitochondrial lung Lipid peroxidation (LPO) in B[a]P-treated animals may be due to the generation of ROS exacerbated by decreased efficiency of host antioxidant defense mechanisms. ROS generation is implicit associated with the malfunction of the mitochondrial respiratory chain and disengagement as well as variation in mitochondrial trans-membrane potential and membrane permeability (Bhat et al., 2015). B[a]P toxicity increased the levels of damage to mitochondria membrane. This study further supports the activity of ATPases perceived in B[a]P induced animals. Mitochondria, particularly when dysfunctional, produce excessive reactive oxygen species and must be removed by quality control pathways. Fascinatingly, the specificity of the B[a]P induces stress pathway for selective autophagy of damaged mitochondria, also known as mitophagy. However, the effect of B[a]P on mitochondria function, and their possible roles in inducing cell death have not been well studied. Our outcomes revealed that the cells with mitochondria dysfunction and ATP depletion underwent necrosis at early time point and apoptosis and autophagy cell death. Evidence is provided that decreased ATP levels in cells play a central role in B[a]P induced autophagy cell death (Ronnett et al., 2009). AMPK is sensitive to the cytosolic AMP to ATP ratio and metabolic stress stimulates autophagy by suppression of mTOR signaling. AMPK plays a major role in energy homeostasis by coordinating a number of adaptive responses under ATP-depleting metabolic stresses.

Our previous study has shown a new approach to perceive apoptotic activity of a known PAH called benzo[a]pyrene (B[a]P), using protein–ligand and protein–protein interaction



through *in silico* approach, followed by *in vitro* validation. This study focused on deciphering the underlying molecular mechanisms of toxic effects caused by B[a]P in a human keratinocyte cell lines. In the present work, we demonstrated that B[a]P could lead to undesirable toxicological effects in human keratinocyte cells, including severe morphological changes and reduction in cell viability, combined with robust activation of Autophagic cell death. It has been demonstrated that TCDD and cationic PAMAM dendrimers, could promote acute lung injury by inducing autophagy and autophagic cell death, indicating that autophagy and toxicity elicited by TCDD and PAMAM dendrimers were probably dependent on surface groups. Recently, an emerging form of literature suggests that dysregulation of autophagy induced by nanomaterials may lead to accumulation of abnormal proteins or damaged organelles, thereby resulting in neurodegenerative diseases. Autophagy and apoptosis have been shown to be coincident or antagonistic, depending on experimental context, and share cross-talk between signal transduction elements (Holczer et al., 2015). Autophagy may modulate the outcome of other regulated forms of cell death such as necroptosis. The changes are signals transmitted through molecular interactions, ultimately leading to two cellular fates, apoptosis and autophagy. Due to genetic variations, the signals may not be efficiently transmitted to modulate apoptotic and autophagic responses.

Our investigation confirms that the decrease in ATP causes a type of metabolic stress, resulting in activation of AMPK followed by alterations in downstream molecules and induction of autophagy. Beclin1 (Atg6) is a well-known strategic regulator of autophagy. Although Beclin1 is enzymatically inert, it governs the autophagic process by regulating PtdIns3KC3-dependent generation of phosphatidylinositol3-phosphate (PtdIns (3)P) and the subsequent recruitment of additional Atg proteins that orchestrate autophagosome formation. Additionally, as manifest from co-localized study of mitochondria (MitoTracker) and lysosome (Lyso Tracker) we showed that treatment with different concentration of B[a]P induced damaged mitochondria and illustration antagonistic effect. Our finding also support that inhibition of Beclin by siRNA approach repressed the B[a]P induced Autophagic cell death. Apoptosis and autophagic cell death may occur simultaneously and inhibition of autophagic activity in cells may switch responses to death signals from autophagic cell death to apoptotic cell death and vice versa. From our study by we examine the role of B[a]P mediated autophagic death in apoptosis deficient and resistant cells, autophagic death was investigated in Bax^{-/-} HaCaT cells.



Although autophagy and apoptosis constitute distinct cellular processes with often opposing outcomes, their signaling pathways are extensively interconnected through various mechanisms of crosstalk. Here our study summarize the importance of autophagy and its role in cellular response to stress, including examples in which consideration of autophagy has contributed to a more complete understanding of toxicant-perturbed systems. The intent of our study focus on advance appreciation of this imperative cellular stress response among toxicologists, a research community focused on stressed biological systems. We found that B[a]P treatment inflicted mitophagy mediated impairment of energy balance disrupting the synchronization of cellular homeostasis. Mitochondria are critically envisaged as an important centre of energy production governing the progression of autophagy and apoptosis (Eguchi et al., 1997). MP supplementation increased the titre of ATP elucidating why MP based strategies to exert anti-oxidative stress and are readily involved in clinical trial (Hurtado et al., 2003, Tagashira et al., 2014).



Chapter 6

Cytoprotective activity of *Bacopa monneiri* against benzo[a]pyrene induced apoptosis through modulation of autophagy



Abstract

In this study, we demonstrated the cytoprotective role of *Bacopa monnieri* (BM) against benzo[a]pyrene induced apoptosis through autophagy induction. Pretreatment with BM rescued the reduction in cell viability in B[a]P treated human keratinocytes (HaCaT) cells indicating the cytoprotective potential of BM against B[a]P. Moreover, BM was found to inhibit B[a]P mediated ROS-induced apoptosis activation in HaCaT cells. Furthermore, BM was found to preserve mitochondrial membrane potential (MMP), and inhibited release of cytochrome c in B[a]P treated HaCaT cells. BM induced protective autophagy; we knocked down beclin-1 and data showed that BM was unable to protect from B[a]P induced mitochondrial ROS mediated apoptosis in Beclin-1 deficient HaCaT cells. Moreover, we established that B[a]P induced damaged mitochondria were found to colocalize and degraded within autolysosomes in order to protect HaCaT cells from mitochondrial injury. In conclusion, B[a]P induced apoptosis was rescued by BM treatment and provided cytoprotection through Beclin-1 dependent autophagy activation.

Key words: *Bacopa monnieri*, benzo[a]pyrene, autophagy, mitochondrial apoptosis, oxidative stress, Beclin-1



6.1. Introduction

Since from the ancient times, Indians and others have been utilizing a diversity of plants and their products as therapeutics against various diseases (Howes et al., 2003; Anand et al., 2011). The World Health Organization (WHO) predicted that for basic health requirements, about 80% of the developing countries population depends on conventional medicines mainly obtained from plants. One of these plants, *Bacopa monnieri* (Brahmi/ BM) is one of the potent ancient medicinal plants used as a traditional ayurvedic medicine (Anand et al., 2011). Besides its role in memory enhancement, BM acts as a natural antioxidant and modulates oxidative stress induced by different toxic, environmental pollutant, and chemical carcinogens. For example, BM was found to prevent mitochondrial oxidative stress and dysfunctions induced by 3-nitropropionic acid through modulation of superoxide dismutase, glutathione peroxidase, glutathione reductase, thioredoxin reductase in mice (Shinomol et al., 2012). Similarly, BM has been shown to prevent the effect of toxic pollutant including nitrobenzene and decabromodiphenyl ether from liver damage in rat and postnatal oxidative stress in the neonate and young female mice respectively (Menon et al., 2010; Verma et al., 2014). The BM extract had also reduced the β - amyloid activity in a transgenic mouse model which examined to induce oxidative stress leading to Alzheimer's disease (Dhanasekaran et al., 2007). The protective actions of BM against the neurotoxic effect of Methyl Mercury (MeHg) have been reported in rats (Sumathi et al., 2012). The protective effect of BM against environmental factors including paraquat/diquat-mediated acute toxicity and rotenone induced cytotoxicity was studied (Singh et al., 2013) suggesting its use as a therapeutic adjuvant for different human disorders involving oxidative stress

Mitochondrial generated ROS had been implicated as an important contributor of PAHs associated diseases. The ROS induces mitochondrial dysfunction and is followed by apoptosis and cytotoxicity (Bansal and Kim.,2015). In this connection, autophagy, a highly conserved evolutionary catabolic process degrades cellular contents including cytoplasmic material, protein aggregates and damaged mitochondria through the formation of double layered autophagosome and provides as the cytoprotective mechanism (Panda et al., 2015; Mukhopadhyay et al., 2014). Autophagy maintains cellular homeostasis by providing a nutrient pool to cope with different types of stress. In an experiment on mice whose Atg5 was genetically removed (Atg5^{-/-}) to stop the action of autophagy were found to be sensitive to



cardiac dysfunction leading to starvation (Kuma et al., 2004). It also showed that inhibition of autophagy by knockdown of Beclin-1 or 3-methyladenine in starved HeLa cell induced activation of caspase-3 and initiation of apoptosis (Boya et al., 2005).

The present study examined the role of BM in the protection of B[a]P induced apoptosis through induction of autophagy. Our data showed that BM treatment rescued the cell viability reduction by B[a]P. Further, we investigated the mechanism of cytoprotection by BM against B[a]P and it clearly indicated that BM was found to inhibit the apoptosis induced by B[a]P. Further, the mitochondrial ROS generated by B[a]P was scavenged by BM. We also deciphered the role of BM in the clearance of reactive mitochondria through mitophagy.

6.2. Material methods

6.2.1. Chemical and reagents

Benzo[a]pyrene B[a]P, dimethyl sulfoxide (DMSO), 3-[4,5-dimethylthiazol-2-yl]-2,5-diphenyltetrazolium bromide (MTT), Propidium iodide from Sigma, USA. The Annexin V from BD Bioscience and Caspase-Glo assay kit for quantification of caspases were purchased from Promega, USA. Beclin-1 siRNA and control siRNA from SantaCruz Biotechnology, USA were procured. *Bacopa monneiri* plant was collected from the wild, Rourkela, Odisha, India and was taxonomically identified and authenticated by to taxonomist, PG department of Botany, Utkal University, Vani Vihar, Bhubaneswar, India and the specimen is preserved in the herbarium (specimen voucher No. UUBD-BM-007). The shade-dried and powdered leaves of *Bacopa monneiri* (10 mg/ml) were weighed and the aqueous extract of BM was prepared under the sterile condition after soaking in PBS for 24 h and used in this study.

6.2.2. Cell culture

The immortalized human keratinocyte cell line (HaCaT) was obtained from National Centre for Cell Science, Pune, India and cultured in Dulbecco's modified Eagle's medium with high glucose (DMEM/high glucose), supplemented with 10% heat-inactivated fetal bovine serum (FBS) containing and 1% penicillin-streptomycin. The cells were maintained at 37 °C in a humidified atmosphere at 5% CO₂. All media, supplements and antibiotics were purchased from Invitrogen.

6.2.3. Cell viability by MTT assay

HaCaT cells were harvested from maintenance cultures in logarithmic phase and were counted by hemocytometer using trypan blue solution. HaCaT (1×10^4 cells/well) were cultured in a 96-



well plate at 37°C, and exposed to various concentrations of B[a]P for 72 h. After 72 h MTT solution (5mg/ml) were added, post 4 h incubation, the resultant formazan crystals were dissolved in dimethyl sulfoxide and the absorbance was measured by a microplate reader (Perkin Elmer) at 595 nm. All experiments were performed in triplicate, and the relative cell viability was expressed as a percentage relative to the untreated control cells (Das et al., 2014).

6.2.4. Beclin-1 knockdown using small interfering RNA

HaCaT Cells were cultured in 60 mm plates and transfected at 80% confluence with Lipofectamine 2000 ® reagent (Invitrogen), in the presence of 100 nM of siRNAs specific for human Beclin-1 and control siRNA. HaCaT cells were used after 48 h transfection for RNA extraction and apoptosis studies (Das et al., 2013).

6.2.5. Annexin V/ Propidium iodine staining

After treatment, HaCaT cells were washed with phosphate buffer saline and then centrifuged at 1200 rpm for 5 min at room temperature. Cell pellets were incubated with annexin V/PI in binding buffer and analyzed by flow cytometer.

6.2.6. Caspase assays

After treatment, caspase activity was measured using Caspase-Glo assay following the manufacturer's protocol (Promega Corp., Madison, WI).

6.2.7. Western blotting analysis

After treatment, HaCaT cell extracts in cell lysis buffer were prepared, and equal amount of proteins were resolved by SDS/PAGE, transferred to PVDF membrane, and protein level was evaluated using antibody against LC3, Beclin-1, ATG5, cytochrome c (Cell Signaling, Boston, MA, USA) as described previously (Mukhopadhyay et al., 2014b).

6.2.8. Measurement of Mitochondrial ROS

Mitochondrial ROS was measured by MitoSox (Invitrogen) in a fluorescence microscope. After specific treatment, HaCaT cell were incubated with MitoSox in incomplete media for 30 min in the CO₂ incubator. Cells were then washed 3 times in PBS and live cell imaging was performed in fluorescence microscope.

6.2.9. Mitochondrial membrane potential measurement

After specific treatment, HaCaT cells were incubated with Rhodamine 123 (Rh123) (5 µg/ml final concentration) for 60 min in dark at 37°C, harvested and suspended in PBS. The mitochondrial membrane potential (MMP) was measured by flow cytometry.



6.2.10. Measurement of autophagy

HaCaT cells were cultured with or without BM for 48 h, washed with PBS and then detection of late autophagic vesicles was done by staining with 0.5 µg/ml of acridine orange for 15 minutes. The media was discarded, and the cells were washed with PBS for three times and observed using an inverted fluorescent microscope (Panda et al., 2014).

HaCaT cells were transfected with pEGFP-LC3 (Addgene plasmid 11546, Jackson et al., 2005) and 48h after transfection, HaCaT cells were incubated in presence of BM for 48 h and the level of autophagy was quantified by counting the mean number cells with puncta fluorescence to autophagosome formation (Mukhopadhyay et al., 2014b).

6.2.11. Visualization of mitochondria and lysosome

After specific treatment, HaCaT cells were incubated with lysoTracker red and MitoTracker green at 37 °C for 30 minutes and followed by three times washing with incomplete media. The cells were observed at 200× magnifications under a confocal microscope (Olympus FV-1000; 630X) (Mukhopadhyay et al., 2015).

6.2.12. Statistical analysis

All data were given as the mean ± SD. Experimental results were analyzed by Student's test. $P < 0.05$ was considered as the level of significance for values obtained for treated compound to control.

6.3. Results

6.3.1. BM found to protect against B[a]P induced cytotoxicity

It is well known that B[a]P induces multiple biological dysfunctional effects including apoptosis and toxicity. To investigate the potential protective role of BM in B[a]P induced cytotoxicity, we treated BM for 2 h prior to B[a]P and assessed the cell viability of B[a]P after 48 h treatment in HaCaT cells. The data showed the B[a]P decreased the cell viability in dose dependent manner in HaCaT cell after 48 h treatment. Interestingly, it demonstrated that BM rescued the decrease of cell viability by B[a]P in HaCaT cell (Fig.6.1.A) indicating the potential involvement of BM in cytoprotection. Further, morphological analysis by phase contrast microscopy confirmed that cell death by B[a]P was suppressed in BM treatment in HaCaT cells (Fig.6.1.B). Moreover, protective role of BM in B[a]P induced apoptosis was examined and data showed that apoptotic activity of B[a]P as the percentage of annexin V positive cell was

very significantly decreased in B[a]P along with BM as compared to alone B[a]P (Fig.6.1.C). Similarly, caspase Glo assay showed that caspase activity was decreased in the presence of BM in B[a]P treated cells as compared only B[a]P treated group (Fig.6.1.D). This study clearly suggested that B[a]P induced apoptosis was rescued by BM treatment in HaCaT cell and provided cytoprotection.

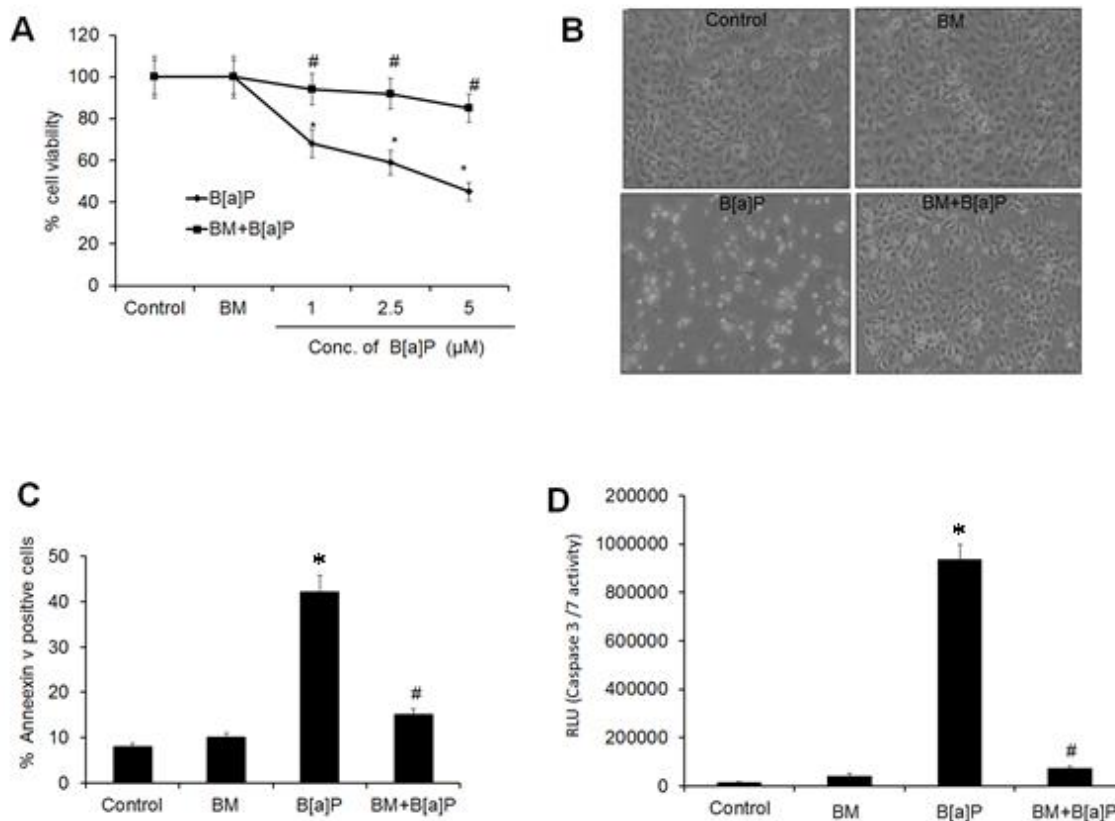


Fig.6.1. *Bacopa monneiri* (BM) found to protect benzo[a]pyrene (B[a]P) induced cytotoxicity in HaCaT cells. HaCaT cells were treated with BM (1 mg/ml) for 2 h prior to B[a]P and followed by treatment with different concentration of B[a]P (1.0, 2.5 and 5.0 μM) for 48 h and cell viability was quantified for MTT assay (A). After treatment with BM and B[a]P, HaCaT were observed in phase contrast microscope (B) and analysed for apoptosis by performing annexin V/PI dual staining through by flow cytometry (C) and caspase activity using caspase-Glo 3/7 assay (D). The values are the means ± SD of three independent experiments. **P* < 0.05 compared with statistically significant change to corresponding control and #*P* < 0.05 compared with corresponding B[a]P treated group.

6.3.2. BM diminished B[a]P-induced mitochondrial dysfunction

To decipher the mechanism of BM mediated cytoprotection, we quantified the generation of mitochondrial ROS by MitoSOX through fluorescence microscopy. The data indicated that ROS generation was increased with the treatment of B[a]P as compared to control. Moreover, B[a]P induced ROS was very significantly inhibited by BM treatment in HaCaT cells (Fig.6.2.A). This study concluded that BM mediated cytoprotection was induced by suppression of B[a]P mediated ROS generation in HaCaT cells. Further, alteration of mitochondrial membrane potential (MMP) was quantified by Rhodamine 123 through flow cytometry. The cell in control and BM group showed accumulation of green fluorescence intensity while cell exposed to B[a]P significantly diminished green intensity indicating that B[a]P induced loss of MMP in HaCaT cells. Interestingly, the cell treated with B[a]P in the presence of BM restored the decreased green intensity (Fig.6.2.B) suggesting BM sustained mitochondrial function following in B[a]P treatment. In addition, we analysed the release of cytochrome c in presence of BM in B[a]P treated group by Western blot and data showed that B[a]P group showed dramatically increased expression of cytochrome c as control and BM group (Fig.6.2.C). But BM decreased the expression of cytochrome c in B[a]P treated cells confirming the role of BM in protection mitochondria from B[a]P toxicity.

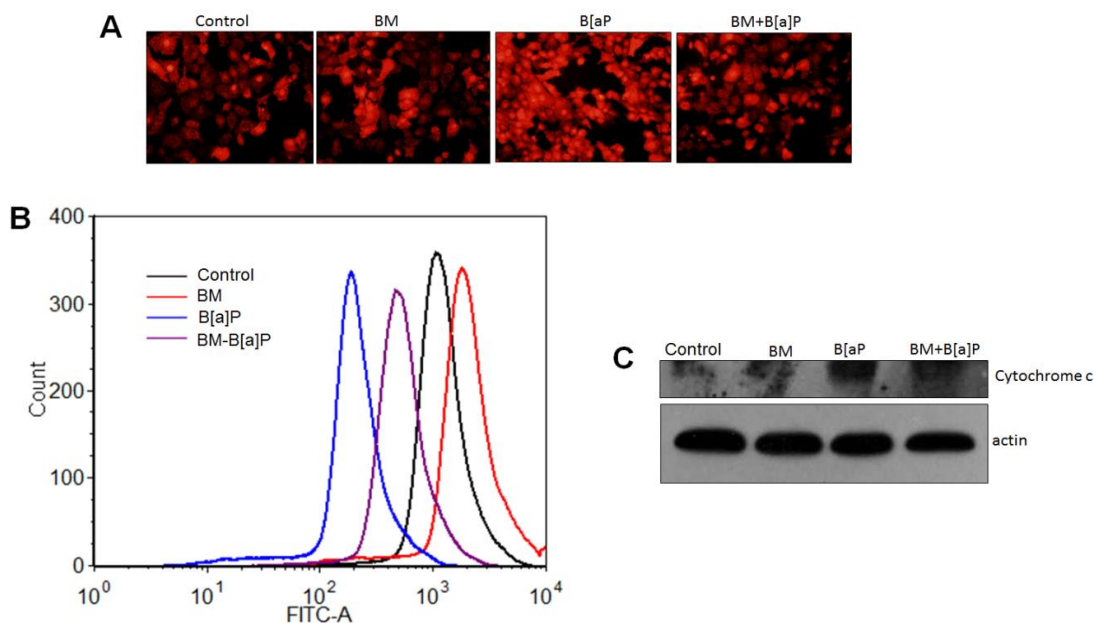


Fig.6.2. BM diminished B[a]P-induced mitochondrial dysfunction. HaCaT cells were treated B[a]P (5.0 μ M) along

with BM (1.0 mg/ml) for 48 h and reactive oxygen species (ROS) generation was measured by MitoSox in an inverted fluorescence microscope (Olympus IX71, 200X) (A), mitochondrial membrane potential (MMP) with Rhodamine 123 by flow cytometry (B) and expression of cytochrome c by Western blot (C).

6.3.3. Autophagy induction by BM in HaCaT cells

To investigate the potential role of BM in prosurvival autophagy induction, HaCaT cells were treated with different doses of BM for 48 h and acridine orange staining was performed to observe acidic contents in the cytoplasm. Acridine orange is a weak base, which traverses freely across biological membranes in an uncharged state characterized by green fluorescence, and its protonated form accumulates as aggregates in acidic compartments specially lysosome characterized by red fluorescence. The red intensity increased in a dose-dependent way in term of greater number of acidic organelles induced in the presence of BM (Fig.6.3.A). Further, we studied the autophagic activity of BM by GFP-LC3 distribution in HaCaT cells. The intracellular localization of LC3 in autophagic vacuoles was analysed by transient transfection of HaCaT cells with GFP-LC3 followed by BM treatment. In the control group, GFP-LC3 was found predominantly as a diffuse green fluorescence in the cytoplasm; however, in the BM-treated cells, characteristic puncta fluorescent patterns were observed, indicating the recruitment of GFP-LC3 during autophagosome formation (Fig.6.3.B). The number of cells with puncta GFP-LC3 staining increased significantly in a dose-dependent manner after 48 h of BM treatment (Fig.6.3.C). To confirm autophagy induction by BM, we monitored changes in expression of endogenous LC3 by Western blot and our data showed that BM induced lipidation of LC3-I and resulted in the accumulation of LC3-II in the treated groups. Further, we analysed the expression of autophagic protein Beclin-1 and ATG5 and Western blot data showed that the expression of these proteins were increased in dose dependent way (Fig.6.3.D). It was noted that the BM extract did not induce any cytotoxicity as demonstrated by cell viability in HaCaT cells (Fig.6.1.A).

6.3.4. BM-induced protective autophagy prevented mitochondrial apoptosis

To figure out the involvement of BM mediated autophagy in the suppression of B[a]P induced apoptosis, Beclin-1 was knockdown in HaCaT cells. The data showed that Beclin-1 expression was decreased in the siBeclin-1 group as compared to sicontrol, demonstrated by Western blot (Fig.6.4.A). The BM induced autophagy was quantified in Beclin-1 knockdown HaCaT cells and showed that number of GFP-LC3 puncta formation was decreased in Beclin-1 deficient



group as compared to sicontrol BM treated group (Fig.6.4.B). Next, the apoptotic potential of B[a]P was quantified in the presence of BM in the siBeclin-1 group by MTT assay and caspase Glo assay. The data showed that cell viability suppressed by B[a]P could not rescue in Beclin-1 deficient HaCaT even in the presence of BM (Fig.6.4.C). In addition, B[a]P activated caspase activity in siBeclin-1 group did not show any difference with sicontrol in presence of BM (Fig.6.4.D) indicating BM-induced autophagy involved in cytoprotection for B[a]P mediated apoptosis.

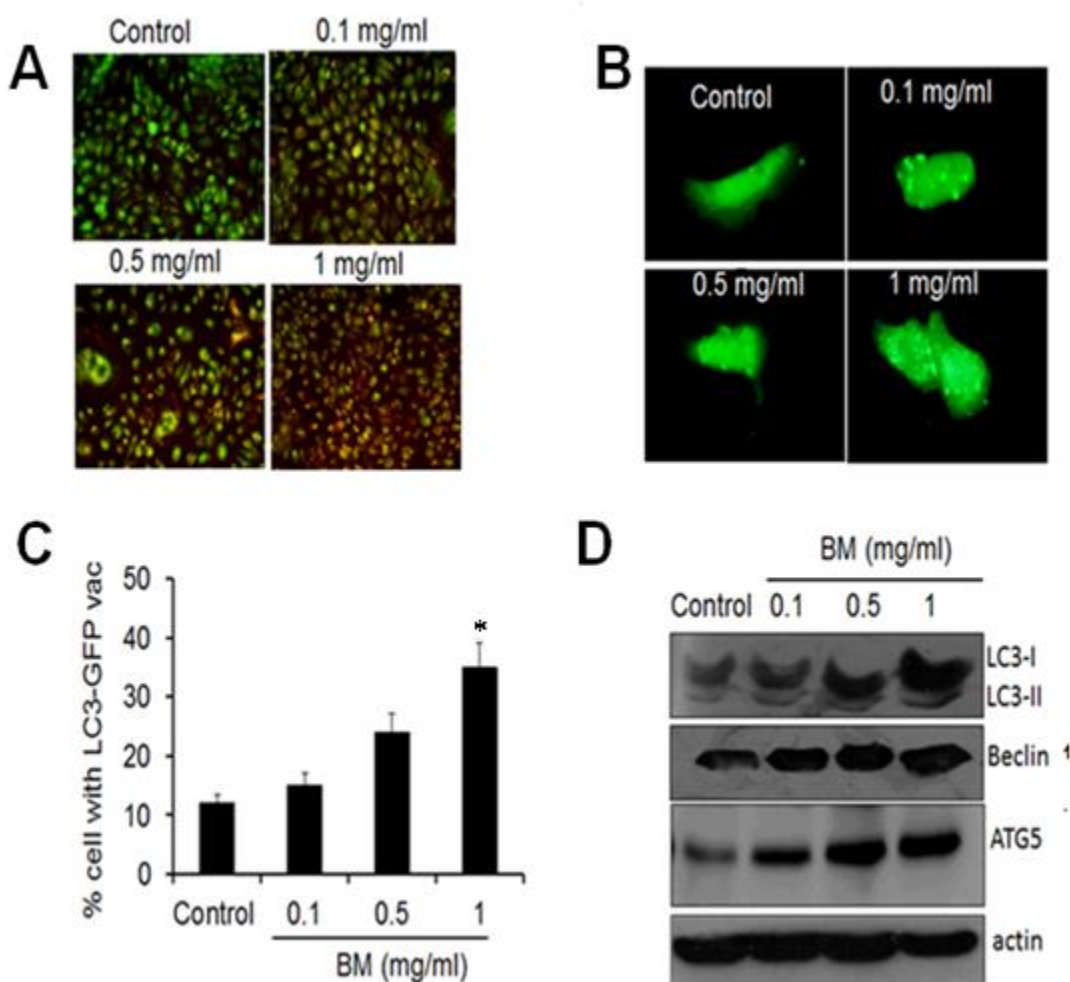


Fig.6.3. Autophagy induction by BM in HaCaT cells. HaCaT cells were treated with different doses of BM (0.1, 0.5, and 1.0 mg/ml) for 48 h, and acridine orange staining was performed for late autophagic vesicles, which were visualized with an inverted fluorescence microscope (Olympus IX71, 200X) (A). HaCaT cells were transfected with pEGFP-LC3 and treated with different doses of BM for 48 h, and the transfected cells were visualized using an inverted fluorescence microscopy (Olympus IX71, 400X). The number of autophagosome puncta were

quantified and compared with the controls (B, C) ($*P < 0.05$, compared with control). HaCaT cells were treated with BM for 48 h and expression of LC3-II, Beclin-1 and ATG5 were analysed by Western blot (D).

Further, the ROS generation by MitoSox was quantified and found that B[a]P induced ROS in siBeclin-1 was comparable to sicontrol even in the presence of BM (Fig.6.5.). This study indicated that BM did not prevent B[a]P activated apoptosis in Beclin-1 deficient HaCaT cells. Finally, HaCaT cells were stained with lysoTracker red and MitoTracker green after 48 h treatment with B[a]P in presence of BM, and data showed that both mitochondria and lysosome were colocalized with Pearson's coefficient (Rr-0.918) as well as total overlap coefficient (R-0.957) (Fig.6.6.) suggesting reactive mitochondria were degraded within autophagolysosome and protected HaCaT cells from mitochondrial injury. Mitophagy is a key mechanism for upholding mitochondrial homeostasis by removing damaged mitochondria, and mitophagy protects against B[a]P-induced injury. Targeting removal of damaged mitochondria by mitophagy or inducing formation of mitochondrial spheroids may be promising therapeutic options for treatment of B[a]P induced toxicity. Mitochondria maintain their homeostasis by various mechanisms. Mitochondria have their own proteolytic system, which degrades misfolded proteins. Mitochondria also utilize the proteasome to degrade damaged outer mitochondrial membrane proteins. In addition, damaged mitochondria can be segregated from healthy mitochondria by mitochondrial fission, and healthy mitochondria can combine their components by mitochondrial fusion. Moreover, mitochondria can degrade oxidized proteins via mitochondria-derived vesicles, which bud off damaged mitochondria and are degraded in the lysosome along with their contents. Furthermore, mitophagy degrades damaged mitochondria in the lysosome, which is a significant mechanism for protection against B[a]P-induced injury and steatosis. Formation of mitochondrial spheroids may serve as an alternate pathway for removal of damaged mitochondria and may also protect against B[a]P-induced skin injury. Removing damaged mitochondria by mitophagy is a protective mechanism against B[a]P-induced skin injury and steatosis because it serves to maintain a healthy population of mitochondria, which prevents cell death by reducing oxidative stress and preserving respiratory chain function and mitochondrial bioenergetics for efficient energy production. Therefore, targeting removal of damaged mitochondria may be an effective therapeutic option for preventing progression of toxicity induced by B[a]P.



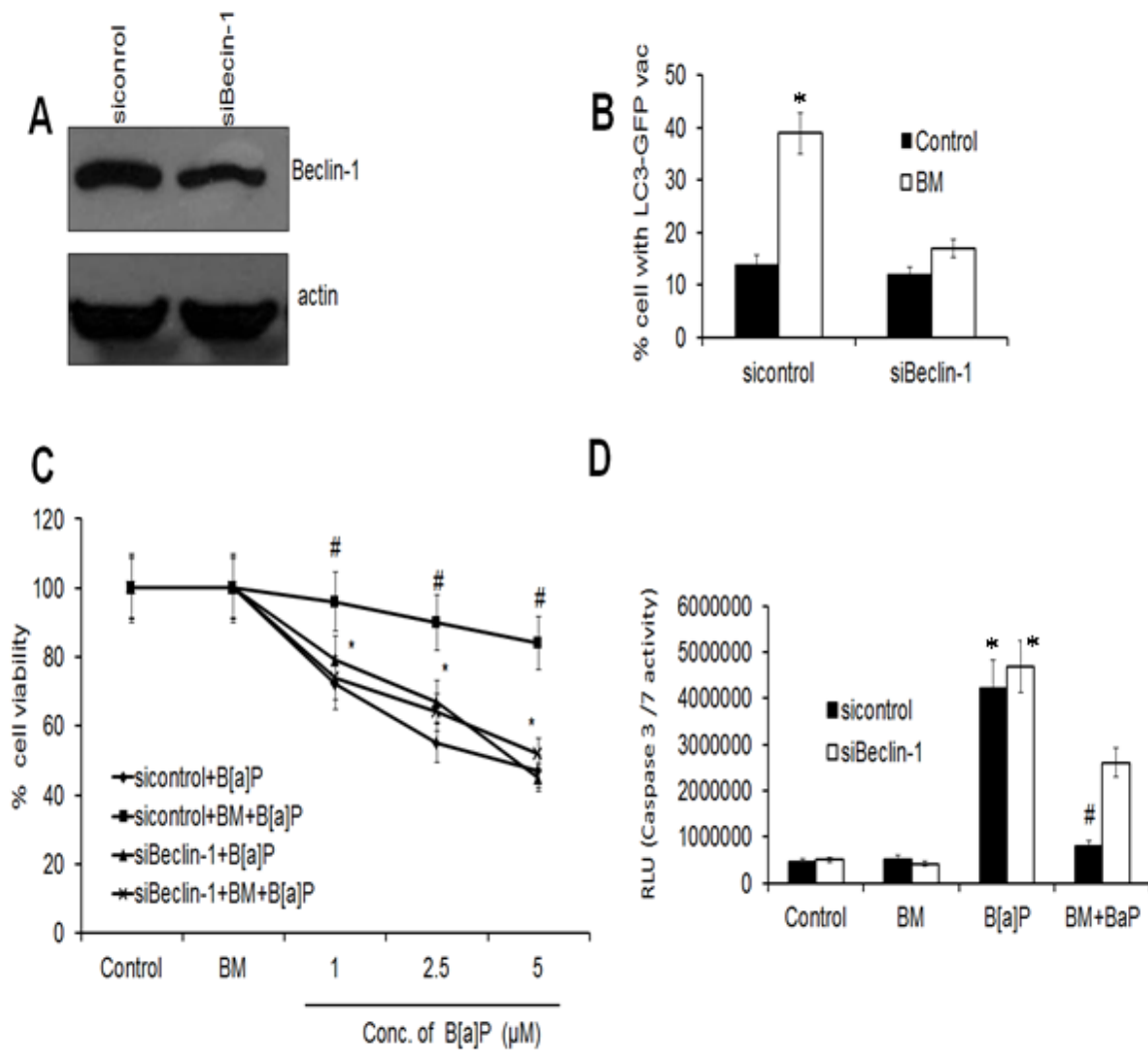


Fig.6.4. Suppression of autophagy block the cytoprotection of BM. HaCaT cells were transfected with the indicated siRNAs, and gene expression was quantified by Western blot (A). The Beclin-1 knockdown HaCaT cells were treated with BM and B[a]P for 48 h and GFP-LC3 puncta was quantified. The number of autophagosome puncta were quantified and compared with the controls (B) (* $P < 0.05$, compared with control). After treatment with BM and B[a]P, the cell viability was measured by MTT assay (C) and apoptosis was quantified by caspase 3/7 Glo assay (D).

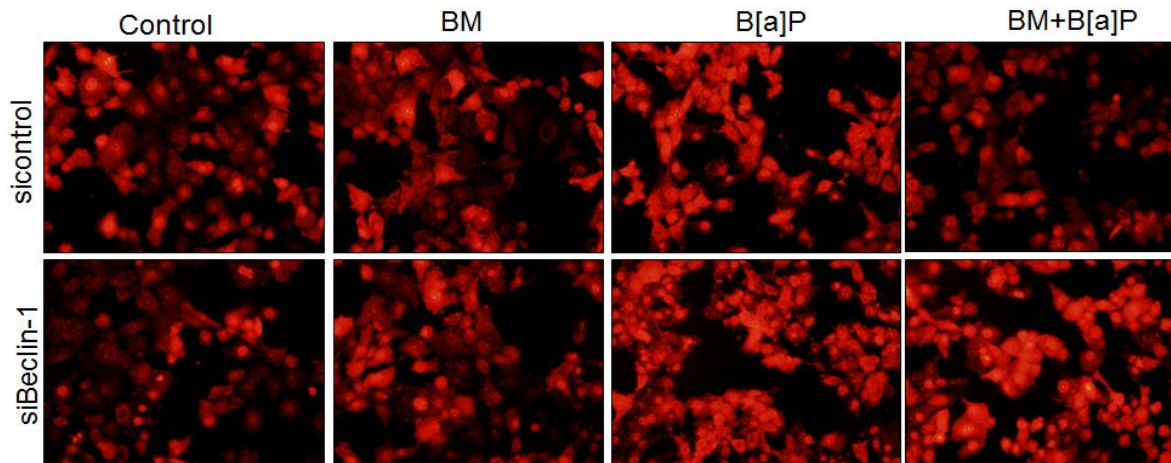


Fig.6.5. Role of BM in mitochondrial ROS generation by B[a]P in beclin-1 deficient HaCaT cells. The beclin-1 knockdown HaCaT cells were treated with BM and B[a]P and generation of ROS was measured by MitoSox in a fluorescence microscope (Olympus IX71, 200X).

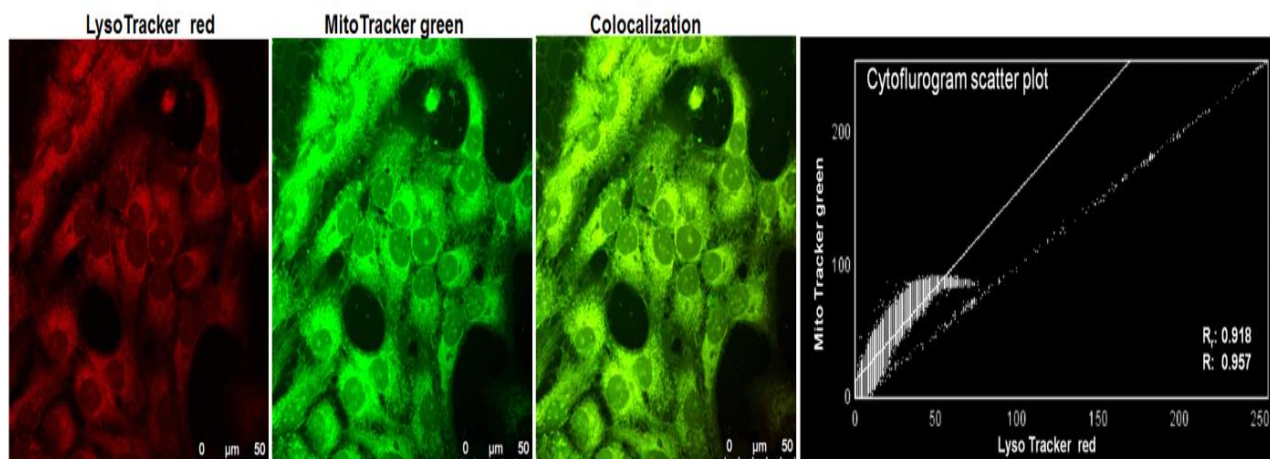


Fig.6.6. HaCaT cells were treated with BM and B[a]P for 48 h and incubated with LysoTracker Red and MitoTracker Green to visualize of lysosome and mitochondria in under a confocalmicroscope (Olympus FV-1000; 630X).

6.4. Discussion

Polycyclic aromatic hydrocarbons, the particulate air pollutants are capable of inducing oxidative stress and cellular injuries leading to cell death and associates with potential toxicity in human (Bansal and Kim, 2015; Miller and Ramos, 2001; Das et al., 2013). The long term exposure of these particulate matters causes inflammation and leads to a significant risk of cancer development. Prevention of B[a]P induced cellular toxicity through regulation of mitochondrial oxidative stress might protect cell death and have therapeutic benefit to human

health. In this study BM was found to protect HaCaT cell from B[a]P induced apoptosis partially through autophagy modulation.

Our study showed that B[a]P induced apoptosis was diminished by BM treatment in HaCaT cells which was supported by previous study. It showed that BM found to protect rotenone induced cytotoxicity in dopaminergic cells and pretreatment of N27 cell with BM provided cytoprotective response by modulation of oxidative stress and apoptosis (Shinomol et al., 2012). Similarly, the beneficial outcomes of BM against apoptosis mediated toxicity due to paraquat/diquat have been studied (Singh et al., 2013). Here, we showed that the protective effect of BM against B[a]P was mediated through antioxidant activity of BM in HaCaT cells. Moreover, it showed that BM treatment decreases the ROS generation as well as preventing mitochondrial depolarization in B[a]P treated HaCaT cells. The antioxidant attribute of BM was reported in different experimental models and the previous study showed that BM showed protective effects against different toxic chemicals including heavy metal, rotenone, Methyl Mercury (Shinomol et al., 2012; Menon et al., 2010; Verma et al., 2014; Dhanasekaran et al., 2007; Sumathi et al., 2012; Shinomol et al., 2012).

Autophagy implicates degradation of cytoplasmic materials, protein aggregates, recycled organelles and is associated to sustain cellular homeostasis under different stress conditions. The autophagy is regulated by autophagy related gene and is initiated through formation of phagophore by Beclin-1 and its associated complex. Another autophagic protein LC3-I is lipidated to form LC3-II on autophagosomal membranes upon autophagy induction (Panda et al., 2015; Mukhopadhyay et al., 2014; Mukhopadhyay et al., 2015). The cell death through autophagy is known as autophagic death, another form of cell death may occur to mitigate excess stress. Autophagy is context dependent and may be protective or toxic (Panda et al., 2015). Autophagy sometimes protects the cells from apoptosis and regard as protective whereas autophagy on other hand switches to autophagic cell death and is independent of apoptosis. Our study showed that BM induced cytoprotective autophagy in HaCaTs cells and the autophagy was increased in dose dependent manner as shown by acridine orange staining, GFP-LC3 puncta cells and LC3-II accumulation (Panda et al., 2014; Mukhopadhyay et al., 2014a) suggesting a natural product with autophagy potential could have great benefit against toxic mediated apoptosis. For example, resveratrol induced protective autophagy has clinical importance and it showed that resveratrol along with calorie restriction have shown to induce



autophagy in heart of rat and protected from cardiac apoptosis against doxorubicin-mediated toxicity. To further explore the importance of BM mediated autophagy in B[a]P-induced apoptosis in HaCaT cells, Beclin-1 was knockdown in HaCaT cells by RNA-interference to inhibit autophagy. The suppression of autophagy by Beclin-1 knockdown dramatically enhanced B[a]P mediated cytotoxicity, suggested that B[a]P-induced cytotoxicity could be altered by autophagy.

The mitochondrial ROS damages the mitochondria leading to impairment of cellular homeostasis and apoptosis. The elimination of reactive mitochondria through mitophagy, a specific type of autophagy involves to protect cells from apoptotic effector generated by dysfunctional mitochondria (Kuma et al., 2014; Moreau et al., 2010; Wang et al., 2015). Our study showed that BM-induced autophagy degraded ROS producing mitochondria and protect the HaCaT cells from B[a]P induced apoptosis. Interestingly, our data showed that BM could not protect the Beclin-1 deficient HaCaT cells from B[a]P induced apoptosis and ROS generation, confirming protective role of BM in B[a]P induced toxicity. Moreover, as demonstrated from colocalized study of mitochondria and lysosome we showed that pretreatment of BM induced degradation of damaged mitochondria and maintain health mitochondria in B[a]P treated cells. Our finding was supported by previous study. For example, autophagy inducer rapamycin found to protect rotenone induced apoptosis in human neuronal SH-SY5Y cells (Pan et al., 2009). In another study, autophagy by rapamycin attenuated triptolide-induced apoptosis in cardiomyocytes and heart tissue by facilitating removal of dysfunctional mitochondria (Zhou et al., 2015). Similarly, sestrin2, a stress-response protein demonstrated to promote autophagy through AMPK dependent pathway and augmented α -synuclein accumulation and suppressed caspase 3 activation of rotenone in dopaminergic cells (Hou et al., 2015). Interestingly, knockdown of sestrin2 or AMPK inhibition diminished autophagy activity and associated with α -synuclein accumulation and apoptosis. In conclusion, the present study revealed distinctive aspects of BM plant extract and identified it as an inducer of protective autophagy, which may directly contribute to the antioxidant promoting potential of BM under different environmental contaminant.



Chapter 7

Summary and conclusion



7.1. Summary

Benzo[a]pyrene, polycyclic aromatic hydrocarbons is capable of inducing oxidative stress and cellular injuries leading to cell death and associated with potential toxicity in human. The long term exposure of these particulate matters causes inflammation and leads to a significant risk of cancer development. B[a]P is oxidised by many cytochrome P450 enzymes to several intermediates which have the ability to bind to the nuclear DNA covalently and this binding result in mutation, replication error and apoptosis mediated cell death. Environmental B[a]P inflict cellular disorders responsible for tissue damage, altering molecular, metabolic, or signaling pathways. With this background information about B[a]P the goals of the present investigation were set up, a) to investigate mutagenic and apoptotic potential of B[a]P identified from industrial city, India, b) mode of apoptotic activity of B[a]P through *in silico* and *in vitro* approaches, c) mitochondria mediated autophagic death, d) protective role of phytotherapeutics in B[a]P mediated toxicity.

The general approaches were undertaken to address the goals

- I. In our investigation, an air quality monitoring program was designed to collect the gaseous and particulate air pollutants from two sites (in front of Indira Gandhi Park and the academic complex of NIT Rourkela) of the industrial city Rourkela. The presence of B[a]P in PM was confirmed by fluorescence spectroscopy and NMR.
- II. Additionally, we examined the mutagenic activity of PM with the Ames test, which determines if substances are capable of inducing mutations and has become an important procedure for safety assessment.
- III. The current study revealed that the generation of ROS after PM exposure could induce cellular oxidative stress and apoptosis.
- IV. Our findings validate that B[a]P and other unidentified PAHs present in the PM are activated by CYP1B1 and induced apoptosis. Accordingly, inhibition of CYP1B1 by siRNA or pharmacologically with the inhibitor CTZ reduced PM-mediated cytotoxicity and apoptosis.



- V. Conversely, our clinical data indicated that PM does not affect the blood cells of people living in Rourkela, as demonstrated by the results of comet tail formation and immunophenotyping analysis.
- VI. The present study has adopted a novel approach to examine the apoptotic activity of B[a]P, using protein–ligand and protein–protein interaction through *in silico* approach, followed by *in vitro* validation. *In silico* study elucidates that the conformational changes and energies involved in the binding of B[a]P to CYP1B1 was crucial with its target proteins. Furthermore, the data confirmed that activated B[a]P had high affinity to bind with aryl hydrocarbon receptor (AHR).
- VII. Interestingly, B[a]P–CYP1B1 complex showed a high binding affinity for caspase-8, -9, -3. To validate our *in silico* work, we confirmed that B[a]P treated HaCaT cells triggered apoptotic cell death with an increase in caspase 8, caspase 9 and caspase 3/7 level.
- VIII. Intriguingly, through *in silico* modeling, we screened clotrimazole as a potent CYP1B1 inhibitor that completely inhibited the cytotoxic effect of B[a]P. This hypothesis was verified by MTT assay, caspase activation measurement, indicating remarkable inhibition of B[a]P mediated apoptotic death; thereby, highlighting a potent therapeutic approach to industrial pollution associated diseases.
- IX. Moreover, we showed that B[a]P stimulated mitochondrial mediated autophagy dependent cell death through the canonical AMPK/mTOR pathway in HaCaT cells.
- X. We showed that B[a]P abrogated ATP generation and activated reactive oxygen production to induce toxic mitophagy in HaCaT cells.
- XI. In addition, we identified *Bacopa monneiri* (BM) plant extract as an inducer of protective autophagy, which may directly contribute to the antioxidant promoting potential of BM on B[a]P induced cell death through Beclin-1 dependent autophagy activation.

To summarise this study, we focused on awareness of the source of the environmental problems in Rourkela and provided an indication on potential environmental issue and elucidated the further scope for the development of phytotherapeutics against environmental air pollutants. This thesis to elucidates the mechanistic aspects of major particulate matter mediated cell death response like apoptosis, autophagic cell death and the natural defense system against its toxicity to propose a pilot study to investigate the potential of *Bacopa monneiri* to overwhelm its adverse



effects. This finding highlights the potential of phytotherapeutics in the form of BM extract for preventive strategy of exposure-related diseases.

7.2. Conclusion

Major research highlights on analysing health deterioration due to air pollutants, but little amount of research is undertaken to examine potential methods of preventing these effects. Benzo[a]pyrene and additional unidentified molecules collected from Rourkela City show a significant mutagenic potential. A new approach has been developed to examine the apoptotic activity B[a]P, using

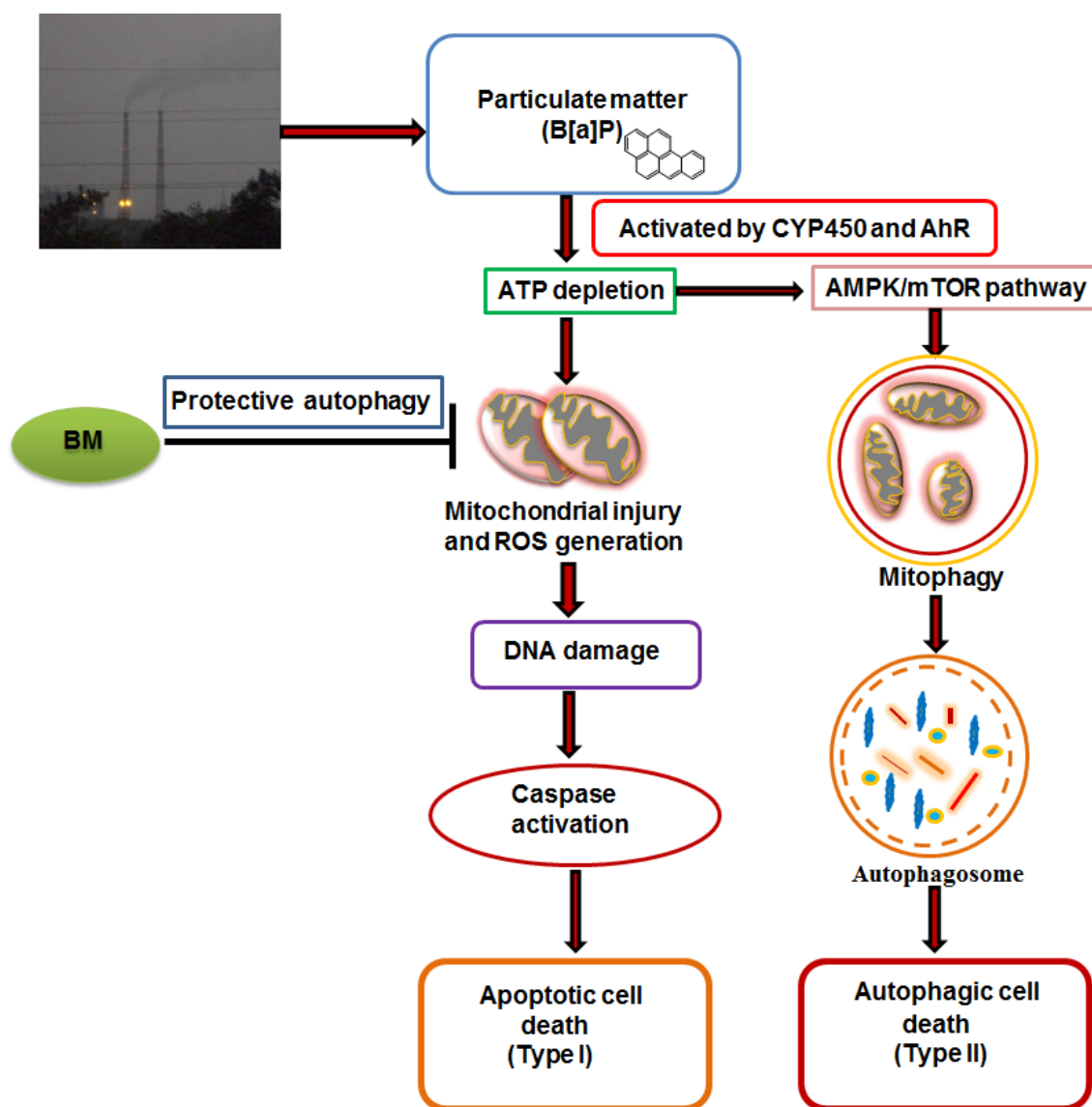


Fig.7.1. Proposed model of molecular mechanism of B[a]P mediated cell death and its prevention by phytochemicals BM.

protein–ligand and protein–protein interaction through *in silico* approach, followed by *in vitro* validation of the same. The prediction revealed that B[a]P was activated by cytochrome P450 (CYP1B1) to induce manifold cellular effects related to activation of the aryl hydrocarbon receptor (AHR) due to formation of toxic metabolites and this in turn activated caspases. For the first time we report that B[a]P induced mitophagy dependent cell death through the canonical pathway mediated through AMPK/mTOR axis. B[a]P abrogated ATP generation and activated reactive oxygen production to induce toxic mitophagy in HaCaT cells. This in turn promotes mitochondria turnover and precludes accumulation of dysfunctional mitochondria that can lead to cellular degeneration. Because of the danger of having damaged mitochondria in the cell, the timely elimination of damaged and aged mitochondria is essential for maintaining the integrity of the cell. In addition, we recognized *Bacopa monneiri* (BM) plant extract as an inducer of protective autophagy, which may directly contribute to the antioxidant promoting potential of BM on B[a]P induced autophagic cell death through Beclin-1 dependent autophagy. The broad field of phytoremediation promises some innovative treatments that are likely to become imperative in preventing allergy prone diseases and cancer. As with any toxic challenge, the obvious solution is to remove, or at least decrease to an acceptable level, the source of trouble.

7.3 Scope of further investigation

Research on mechanisms underlying the adverse health effects of air pollution has suggested potential pharmaceutical or chemopreventive interventions, such as antioxidant agents. In this commentary, we explore the various mechanisms by which autophagy and apoptosis regulate each other and define general paradigms of crosstalk on the basis of mechanistic features. The future study proposes to identify how mitophagy may be linked to the stress response and the related Ras–protein-kinase-A signaling pathway. Furthermore, the study elucidated that mitochondrial dysfunction is a common feature in air pollution adverse effects diseases like neurodegeneration diseases, asthma arthritis, lung and heart and aging. PTEN-induced kinase 1 (PINK1) and Parkin mediated mitophagy study will be used as a model for understanding the further molecular basis of B[a]P mediated mitophagy. Despite extensive investigation, several steps in the mitophagy pathway remain a mystery.



References

- Anand T, Naika M, Swamy, F, Khanum, Antioxidant And DNA Damage Preventive Properties Of Bacopa Monniera (L) Wettst, Free Radicals and Antioxidants. 2011;1: 84-90.
- Anderson JO, Thundiyil JG, Stolbach A. Clearing the air: a review of the effects of particulate matter air pollution on human health. J Med Toxicol. 2012;8: 166-75.
- Andersson H, Piras E, Demma J, Hellman B, Brittebo E. Low levels of the air pollutant 1-nitropyrene induce DNA damage, increased levels of reactive oxygen species and endoplasmic reticulum stress in human endothelial cells. Toxicology. 2009;262:57-64.
- Andreau K, Leroux M, Bouharrou A. Health and cellular impacts of air pollutants: from cytoprotection to cytotoxicity. Biochem Res Int. 2012; 2012:493894.
- Androutsopoulos VP, Tsatsakis AM, Spandidos DA. Cytochrome P450 CYP1A1: wider roles in cancer progression and prevention. BMC Cancer. 2009;9:187.
- Annweiler E, Richnow HH, Antranikian G, Hebenbrock S, Garms C, Franke S, Francke W, Michaelis W. Naphthalene degradation and incorporation of naphthalene-derived carbon into biomass by the thermophile Bacillus thermoleovorans. Appl Environ Microbiol. 2000;66:518-23.
- Arias E, Cuervo AM. Chaperone-mediated autophagy in protein quality control. Curr Opin Cell Biol. 2011;23:184-9.
- Arlt VM, Stiborová M, Henderson CJ, Thiemann M, Frei E, Aimová D, Singh R, Gamboa da Costa G, Schmitz OJ, Farmer PB, Wolf CR, Phillips DH. Metabolic activation of benzo[a]pyrene *in vitro* by hepatic cytochrome P450 contrasts with detoxification *in vivo*: experiments with hepatic cytochrome P450 reductase null mice. Carcinogenesis. 2008;29:656-65.
- Armstrong B, Tremblay C, Baris D, Theriault G. Lung cancer mortality and polynuclear aromatic hydrocarbons: a case-cohort study of aluminium production workers in Arvida, Quebec, Canada. American Journal of Epidemiology. 1994;139: 250-262.
- Atkinson RW, Kang S, Anderson HR, Mills IC, Walton HA. Epidemiological time series studies of PM_{2.5} and daily mortality and hospital admissions: a systematic review and meta-analysis. Thorax. 2014;69:660-5.



Atlanta GA. Polycyclic Aromatic Hydrocarbons. Agency for Toxic Substances and Disease Registry (ATSDR), Public Health Statement. U.S. Public Health Service, U.S. Department of Health and Human Services 1990.

Ba Q, Li J, Huang C, Qiu H, Li J, Chu R, Zhang W, Xie D, Wu Y, Wang H. Effects of benzo[a]pyrene exposure on human hepatocellular carcinoma cell angiogenesis, metastasis, and NF- κ B signaling. *Environ Health Perspect*. 2015;123:246-54.

Bamforth S M, & Singleton, I. Bioremediation of polycyclic aromatic hydrocarbons: current knowledge and future directions. *Journal of Chemical Technology and Biotechnology*. 2005; 80:723-736.

Bansal V, Kim KH. Review of PAH contamination in food products and their health hazards. *Environ Int*. 2015;84:26-38.

Bao L, Jaramillo MC, Zhang Z, Zheng Y, Yao M, Zhang DD, Yi X. Induction of autophagy contributes to cisplatin resistance in human ovarian cancer cells. *Mol Med Rep*. 2015;11:91-8.

Barakat-Haddad C, Elliott SJ, Pengelly D. Health impacts of air pollution: a life course approach for examining predictors of respiratory health in adulthood. *Ann Epidemiol*. 2012; 22:239-49.

Barón E, Eljarrat E, Barceló D. Analytical method for the determination of halogenated norbornene flame retardants in environmental and biota matrices by gas chromatography coupled to tandem mass spectrometry. *J Chromatogr A*. 2012; 1248:154-60

Becker S, Dailey LA, Soukup JM, Grambow SC, Devlin RB, Huang YC. Seasonal variations in air pollution particle-induced inflammatory mediator release and oxidative stress. *Environ Health Perspect*. 2005;113:1032-8.

Begemann P, Srám RJ, Neumann HG. Hemoglobin adducts of epoxybutene in workers occupationally exposed to 1,3-butadiene. *Arch Toxicol*. 2001;74:680-7.

Beischlag TV, Luis Morales J, Hollingshead BD, Perdew GH. The aryl hydrocarbon receptor complex and the control of gene expression. *Crit Rev Eukaryot Gene Expr*. 2008;18:207-50.

Benford D, Bolger PM, Carthew P, Coulet M, DiNovi M, Leblanc JC, Renwick AG, Setzer W, Schlatter J, Smith B, Slob W, Williams G, Wildemann T. Application of the Margin of Exposure (MOE) approach to substances in food that are genotoxic and carcinogenic. *Food Chem Toxicol*. 2010;48:S2-24.



Bhat AH, Dar KB, Anees S, Zargar MA, Masood A, Sofi MA, Ganie SA. Oxidative stress, mitochondrial dysfunction and neurodegenerative diseases; a mechanistic insight. *Biomed Pharmacother.* 2015;74:101-10.

Bhutia SK, Das SK, Azab B, Dash R, Su ZZ, Lee SG, Dent P, Curiel DT, Sarkar D, Fisher PB. Autophagy switches to apoptosis in prostate cancer cells infected with melanoma differentiation associated gene-7/interleukin-24 (mda-7/IL-24). *Autophagy.* 2011;7: 1076-7.

Bhutia SK, Mukhopadhyay S, Sinha N, Das DN, Panda PK, Patra SK, Maiti TK, Mandal M, Dent P, Wang XY, Das SK, Sarkar D, Fisher PB. Autophagy: cancer's friend or foe? *Adv Cancer Res.* 2013;118: 61-95.

Birgisdottir BE, Knutsen HK, Haugen M, Gjølstad IM, Jenssen MT, Ellingsen DG, Thomassen Y, Alexander J, Meltzer HM, Brantsæter AL. Essential and toxic element concentrations in blood and urine and their associations with diet: results from a Norwegian population study including high-consumers of seafood and game. *Sci Total Environ.* 2013; 463-464:836-44.

Boffetta P, Jourenkova N, Gustavsson P. Cancer risk from occupational and environmental exposure to polycyclic aromatic hydrocarbons. *Cancer Causes Control.* 1997;8:444-72.

Bölck B, Ibrahim M, Steinritz D, Morguet C, Dühr S, Suhr F, Lu-Hesselmann J, Bloch W. Detection of key enzymes, free radical reaction products and activated signaling molecules as biomarkers of cell damage induced by benzo[a]pyrene in human keratinocytes. *Toxicol In Vitro.* 2014;28:875-84.

Boya P, González-Polo RA, Casares N, Perfettini JL, Dessen P, Larochette N, Métivier D, Meley D, Souquere S, Yoshimori T, Pierron G, Codogno P, Kroemer G. Inhibition of macroautophagy triggers apoptosis. *Mol Cell Biol.* 2005; 25:1025-40.

Brook RD, Franklin B, Cascio W, Hong Y, Howard G, Lipsett M, Luepker R, Mittleman M, Samet J, Smith SC Jr, Tager I; Expert Panel on Population and Prevention Science of the American Heart Association. Air pollution and cardiovascular disease: a statement for healthcare professionals from the Expert Panel on Population and Prevention Science of the American Heart Association. *Circulation.* 2004;109:2655-71.

Buterin T, Hess MT, Luneva N, Geacintov NE, Amin S, Kroth H, Seidel A, Naegeli H. Unrepaired fjord region polycyclic aromatic hydrocarbon-DNA adducts in ras codon 61 mutational hot spots. *Cancer Res* 2000;60:1849-1856.



Cavalieri E, Rogan E. Catechol quinones of estrogens in the initiation of breast, prostate, and other human cancers: keynote lecture. *Ann N Y Acad Sci.* 2006;1089:286-301.

Česen MH, Repnik U, Turk V, Turk B. Siramesine triggers cell death through destabilisation of mitochondria, but not lysosomes. *Cell Death Dis.* 2013;4:e818.

Chatterjee A, Chattopadhyay D, Chakrabarti G. MiR-16 targets Bcl-2 in paclitaxel-resistant lung cancer cells and overexpression of miR-16 along with miR-17 causes unprecedented sensitivity by simultaneously modulating autophagy and apoptosis. *Cell Signal.* 2015;27:189-203.

Chen Y, Huang C, Bai C, Gao H, Ma R, Liu X, Dong Q. Benzo[α]pyrene repressed DNA mismatch repair in human breast cancer cells. *Toxicology.* 2013; 304:167-72.

Chepelev NL, Moffat ID, Bowers WJ, Yauk CL. Neurotoxicity may be an overlooked consequence of benzo[a]pyrene exposure that is relevant to human health risk assessment. *Mutat Res Rev Mutat Res.* 2015;764:64-89.

Chopra M, Dharmarajan AM, Meiss G, Schrenk D. Inhibition of UV-C light-induced apoptosis in liver cells by 2,3,7,8-tetrachlorodibenzo-p-dioxin. *Toxicol Sci.* 2009;111:49-63.

Chun YJ, Lee SK, Kim MY. Modulation of human cytochrome P450 1B1 expression by 2,4,3',5'-tetramethoxystilbene. *Drug Metab Dispos.* 2005; 33(12):1771-6.

Cordier S, Monfort C, Filippini G, Preston-Martin S, Lubin F, Mueller BA, Holly EA, Peris-Bonet R, McCredie M, Choi W, Little J, Arslan A. Parental exposure to polycyclic aromatic hydrocarbons and the risk of childhood brain tumors: The SEARCH International Childhood Brain Tumor Study. *Am J Epidemiol.* 2004;159:1109-16.

Crasta K, Ganem NJ, Dagher R, Lantermann AB, Ivanova EV, Pan Y, Nezi L, Protopopov A, Chowdhury D, Pellman D. DNA breaks and chromosome pulverization from errors in mitosis. *Nature.* 2012;482:53-8.

Dalle-Donne I, Aldini G, Carini M, Colombo R, Rossi R, Milzani A. Protein carbonylation, cellular dysfunction, and disease progression. *J Cell Mol Med.* 2006;10:389-406.

Dalle-Donne I, Rossi R, Colombo R, Giustarini D, Milzani A. Biomarkers of oxidative damage in human disease. *Clin Chem.* 2006;52:601-23.

Das DN, Panda PK, Mukhopadhyay S, Sinha N, Mallick B, Behera B, Maiti TK, Bhutia SK. Prediction and validation of apoptosis through cytochrome P450 activation by benzo[a]pyrene. *Chem Biol Interact.* 2014; 208:8-17.



Das G, Shrivage BV, Baehrecke EH. Regulation and function of autophagy during cell survival and cell death. *Cold Spring Harb Perspect Biol.* 2012;4.pii: a008813.

Davis JW 2nd, Melendez K, Salas VM, Lauer FT, Burchiel SW. 2,3,7,8-Tetrachlorodibenzo-p-dioxin (TCDD) inhibits growth factor withdrawal-induced apoptosis in the human mammary epithelial cell line, MCF-10A. *Carcinogenesis.* 2000;21:881-6.

Decuypere JP, Paudel RC, Parys J, Bultynck G. Intracellular Ca(2+) signaling: A novel player in the canonical mTOR-controlled autophagy pathway. *Commun Integr Biol.* 2013;6:e25429.

Dhanasekaran M, Tharakan B, Holcomb LA, Hitt AR, Young KA, Manyam BV. Neuroprotective mechanisms of ayurvedic antidementia botanical Bacopa monniera. *Phytother Res.* 2007;21:965-9.

Ding WX, Yin XM. Mitophagy: mechanisms, pathophysiological roles, and analysis. *Biol Chem.* 2012;393:547-64.

Dutta D, Xu J, Dirain ML, Leeuwenburgh C. Calorie restriction combined with resveratrol induces autophagy and protects 26-month-old rat hearts from doxorubicin-induced toxicity. *Free Radic Biol Med.* 2014;74:252-62.

Eguchi Y, Shimizu S, Tsujimoto Y. Intracellular ATP levels determine cell death fate by apoptosis or necrosis. *Cancer Res.* 1997;57:1835-40.

Einem Lindeman T, Poirier MC, Divi RL. The resveratrol analogue, 2,3',4,5' tetramethoxystilbene, does not inhibit CYP gene expression, enzyme activity and benzo[a]pyrene-DNA adduct formation in MCF-7 cells exposed to benzo[a]pyrene. *Mutagenesis.* 2011 ;26:629-35.

Ellard S, Mohammed Y, Dogra S, Wölfel C, Doehmer J, Parry JM. The use of genetically engineered V79 Chinese hamster cultures expressing rat liver CYP1A1, 1A2 and 2B1 cDNAs in micronucleus assays. *Mutagenesis.* 1991; 6:461-70.

Fearon KC, Glass DJ, Guttridge DC. Cancer cachexia: mediators, signaling, and metabolic pathways. *Cell Metab.* 2012;16:153-66.

Fenneteau F, Poulin P, Nekka F. Physiologically based predictions of the impact of inhibition of intestinal and hepatic metabolism on human pharmacokinetics of CYP3A substrates. *J Pharm Sci.* 2010;99: 486-514.



Fernández C, Carbonell G, Babín M. Effects of individual and a mixture of pharmaceuticals and personal-care products on cytotoxicity, EROD activity and ROS production in a rainbow trout gonadal cell line (RTG-2). *J Appl Toxicol*. 2013;33:1203-12.

Fiorito F, Ciarcia R, Granato GE, Marfe G, Iovane V, Florio S, De Martino L, Pagnini U. 2,3,7,8-tetrachlorodibenzo-p-dioxin induced autophagy in a bovine kidney cell line. *Toxicology*. 2011;290:258-70.

Fu PP, Xia Q, Sun X, Yu H. Phototoxicity and environmental transformation of polycyclic aromatic hydrocarbons (PAHs)-light-induced reactive oxygen species, lipid peroxidation, and DNA damage. *J Environ Sci Health C Environ Carcinog Ecotoxicol Rev*. 2012;30 :1-41.

Fujita K, Hidaka M, Takamura N, Yamasaki K, Iwakiri T, Okumura M, Kodama H, Yamaguchi M, Ikenoue T, Arimori K. Inhibitory effects of citrus fruits on cytochrome P450 3A (CYP3A) activity in humans. *Biol Pharm Bull*. 2003;26:1371-3.

Fustinoni S, Campo L, Cirila PE, Martinotti I, Buratti M, Longhi O, Foà V, Bertazzi P. Dermal exposure to polycyclic aromatic hydrocarbons in asphalt workers. *Occup Environ Med*. 2010 ;67:456-63.

Funatake CJ, Marshall NB, Kerkvliet NI. 2,3,7,8-Tetrachlorodibenzo-p-dioxin alters the differentiation of alloreactive CD8+ T cells toward a regulatory T cell phenotype by a mechanism that is dependent on aryl hydrocarbon receptor in CD4+ T cells. *J Immunotoxicol*. 2008;5:81-91.

Galván N, Page TJ, Czuprynski CJ, Jefcoate CR. Benzo(a)pyrene and 7,12-dimethylbenz(a)anthracene differentially affect bone marrow cells of the lymphoid and myeloid lineages. *Toxicol Appl Pharmacol*. 2006;213:105-16.

Gangamma S. Airborne particulate matter and acute lung inflammation. *Environ Health Perspect*. 2013;121 :A11.

Gao M, Li Y, Sun Y, Long J, Kong Y, Yang S, Wang Y. A common carcinogen benzo[a]pyrene causes p53 overexpression in mouse cervix via DNA damage. *Mutat Res*. 2011;724:69-75.

Gao M, Li Y, Sun Y, Shah W, Yang S, Wang Y, Long J. Benzo[a]pyrene exposure increases toxic biomarkers and morphological disorders in mouse cervix. *Basic Clin Pharmacol Toxicol*. 2011;109 :398-406.

Garçon G, Dagher Z, Zerimech F, Ledoux F, Courcot D, Aboukais A, Puskaric E, Shirali P. Dunkerque City air pollution particulate matter-induced cytotoxicity, oxidative stress and



inflammation in human epithelial lung cells (L132) in culture. *Toxicol In Vitro*. 2006;20:519-28.

Garrido-Maraver J, Paz MV, Cordero MD, Bautista-Lorite J, Oropesa-Ávila M, de la Mata M, Pavón AD, de Laveria I, Alcocer-Gómez E, Galán F, González PY, Cotán D, Jackson S, Sánchez-Alcázar JA. Critical role of AMP-activated protein kinase in the balance between mitophagy and mitochondrial biogenesis in MELAS disease. *Biochim Biophys Acta*. 2015. In press.

Gentner NJ, Weber LP. Intranasal benzo[a]pyrene alters circadian blood pressure patterns and causes lung inflammation in rats. *Arch Toxicol*. 2011 ;85:337-46.

Giannapas M, Karnis L, Dailianis S. Generation of free radicals in haemocytes of mussels after exposure to low molecular weight PAH components: immune activation, oxidative and genotoxic effects. *Comp Biochem Physiol C Toxicol Pharmacol*. 2012;155:182-9.

Godschalk R, Curfs D, Bartsch H, Van Schooten FJ, Nair J. Benzo[a]pyrene enhances lipid peroxidation induced DNA damage in aorta of apolipoprotein E knockout mice. *Free Radic Res*. 2003;37:1299-305.

Godschalk RW, Van Schooten FJ, Bartsch H. A critical evaluation of DNA adducts as biological markers for human exposure to polycyclic aromatic compounds. *J Biochem Mol Biol*. 2003;36:1-11.

Greene LM, Nolan DP, Regan-Komito D, Campiani G, Williams DC, Zisterer DM. Inhibition of late-stage autophagy synergistically enhances pyrrolo-1,5-benzoxazepine-6-induced apoptotic cell death in human colon cancer cells. *Int J Oncol*. 2013;43:927-35.

Greene LM, O'Boyle NM, Nolan DP, Meegan MJ, Zisterer DM. The vascular targeting agent Combretastatin-A4 directly induces autophagy in adenocarcinoma-derived colon cancer cells. *Biochem Pharmacol*. 2012;84:612-24.

Guo J, Xu Y, Ji W, Song L, Dai C, Zhan L. Effects of exposure to benzo[a]pyrene on metastasis of breast cancer are mediated through ROS-ERK-MMP9 axis signaling. *Toxicol Lett*. 2015 ;234:201-10.

Hakami R, Mohtadinia J, Etemadi A, Kamangar F, Nemati M, Pourshams A, Islami F, Nasrollahzadeh D, Saberi-Firoozi M, Birkett N, Boffetta P, Malekzadeh R. Dietary intake of benzo(a)pyrene and risk of esophageal cancer in north of Iran. *Nutr Cancer*. 2008;60:216-21.



Han EH, Hwang YP, Kim HG, Choi JH, Park BH, Song GY, Lee GW, Jeong TC, Jeong HG. CCAAT/ enhancer-binding protein β activation by capsaicin contributes to the regulation of CYP1A1 expression, mediated by the aryl hydrocarbon receptor. *Br J Pharmacol*.2011 ;164:1600-13.

Hankinson O. The aryl hydrocarbon receptor complex. *Ann Rev Pharmacol Toxicol*. 1995 ;35:307-340.

Haouzi D, Cohen I, Vieira HL, Poncet D, Boya P, Castedo M, Vadrot N, Belzacq AS, Fau D, Brenner C, Feldmann G, Kroemer G. Mitochondrial permeability transition as a novel principle of hepatorenal toxicity *in vivo*.*Apoptosis*.2002;7:395-405.

Hidaka M, Fujita K, Ogikubo T, Yamasaki K, Iwakiri T, Okumura M, Kodama H, Arimori K. Potent inhibition by star fruit of human cytochrome P450 3A (CYP3A)activity. *Drug Metab Dispos*. 2004;32:581-3.

Hidaka M, Okumura M, Ogikubo T, Kai H, Fujita K, Iwakiri T, Yamasaki K, Setoguchi N, Matsunaga N, Arimori K. Transient inhibition of cyp3a in rats by star fruit juice. *Drug Metab Dispos*. 2006;34:343-5.

Hoesel B, Schmid JA. The complexity of NF- κ B signaling in inflammation and cancer.*Mol Cancer*.2013;12:86.

Hou YS, Guan JJ, Xu HD, Wu F, Sheng R, Qin ZH. Sestrin2 Protects Dopaminergic Cells against Rotenone Toxicity through AMPK-Dependent Autophagy Activation. *Mol Cell Biol*. 2015;35:2740-51.

Howes MJ, Houghton PJ. Plants used in Chinese and Indian traditional medicine for improvement of memory and cognitive function. *Pharmacol Biochem Behav*. 2003 ;75:513-27.

Hsu IC, Metcalf RA, Sun T, Welsh JA, Wang NJ, Harris CC. Mutational hotspot in the p53 gene in human hepatocellular carcinomas. *Nature*. 1991;350:427-8.

Huang S, Eichler G, Bar-Yam Y, Ingber DE. Cell fates as high-dimensional attractor states of a complex gene regulatory network.*Phys Rev Lett*. 2005;94 :128701.

Huc L, Tekpli X, Holme JA, Rissel M, Solhaug A, Gardyn C, Le Moigne G, Gorria M, Dimanche-Boitrel MT, Lagadic-Gossmann D. c-Jun NH2-terminal kinase-related Na⁺/H⁺ exchanger isoform 1 activation controls hexokinase II expression in benzo(a)pyrene-induced apoptosis. *Cancer Res*. 2007;67:1696-705.



Hurtado O, De Cristóbal J, Sánchez V, Lizasoain I, Cárdenas A, Pereira MP, Colado MI, Leza JC, Lorenzo P, Moro MA. Inhibition of glutamate release by delaying ATP fall accounts for neuroprotective effects of antioxidants in experimental stroke. *FASEB J*. 2003;17:2082-4.

Jedrychowski WA, Perera FP, Tang D, Rauh V, Majewska R, Mroz E, Flak E, Stigter L, Spengler J, Camann D, Jacek R. The relationship between prenatal exposure to airborne polycyclic aromatic hydrocarbons (PAHs) and PAH-DNA adducts in cord blood. *J Expo Sci Environ Epidemiol*. 2013;23 :371-7.

Jeyabalan J, Vadhanam MV, Ravoori S, Gupta RC. Sustained overexpression of CYP1A1 and 1B1 and steady accumulation of DNA adducts by low-dose, continuous exposure to benzo[a]pyrene by polymeric implants. *Chem Res Toxicol*. 2011;24:1937-43.

Jiang H, Shen YM, Quinn AM, Penning TM. Competing roles of cytochrome P450 1A1/1B1 and aldo-keto reductase 1A1 in the metabolic activation of (+/-)-7,8-dihydroxy-7,8-dihydrobenzo[a]pyrene in human bronchoalveolar cell extracts. *Chem Res Toxicol*. 2005 ;18:365-74.

Jin C, Guo J, Qiu X, Ma K, Xiang M, Zhu X, Guo J. IGF-1 induces iNOS expression via the p38 MAPK signal pathway in the anti-apoptotic process in pulmonary artery smooth muscle cells during PAH. *J Recept Signal Transduct Res*. 2014;34:325-31.

Jinzhu Y, Qinli Z, Jin Y, Pan K, Jianjun H, Qiao N. Aluminum and benzo[a]pyrene co-operate to induce neuronal apoptosis *in vitro*. *J Toxicol Sci*. 2015;40 :365-73.

Johnson TE, Kassie F, O'Sullivan MG, Negia M, Hanson TE, Upadhyaya P, Ruvolo PP, Hecht SS, Xing C. Chemopreventive effect of kava on 4-(methylnitrosamino)-1-(3-pyridyl)-1-butanone plus benzo[a]pyrene-induced lung tumorigenesis in A/J mice. *Cancer Prev Res (Phila)*. 2008;1:430-8.

Jung KH, Perzanowski M, Rundle A, Moors K, Yan B, Chillrud SN, Whyatt R, Camann D, Perera FP, Miller RL. Polycyclic aromatic hydrocarbon exposure, obesity and childhood asthma in an urban cohort. *Environ Res*. 2014;128:35-41.

Kamdar O, Le W, Zhang J, Ghio AJ, Rosen GD, Upadhyay D. Air pollution induces enhanced mitochondrial oxidative stress in cystic fibrosis airway epithelium. *FEBS Lett*. 2008;582 :3601-6.

Kampa M, Castanas E. Human health effects of air pollution. *Environ Pollut*. 2008;151:362-7.



Kang HJ, Hong YB, Kim HJ, Wang A, Bae I. Bioactive food components prevent carcinogenic stress via Nrf2 activation in BRCA1 deficient breast epithelial cells. *Toxicol Lett.* 2012;209:154-60.

Kasai N, Sakaki T, Shinkyo R, Ikushiro S, Iyanagi T, Kamao M, Okano T, Ohta M, Inouye K. Sequential metabolism of 2,3,7-trichlorodibenzo-p-dioxin (2,3,7-triCDD) by cytochrome P450 and UDP-glucuronosyltransferase in human liver microsomes. *Drug Metab Dispos.* 2004 ;32:870-5.

Kawabata TT, White KL Jr. Suppression of the vitro humoral immune response of mouse splenocytes by benzo(a)pyrene metabolites and inhibition of benzo(a)pyrene-induced immunosuppression by alpha-naphthoflavone. *Cancer Res.* 1987;47:2317-22.

Khaitan D, Dwarakanath BS. Endogenous and induced oxidative stress in multi-cellular tumour spheroids: implications for improving tumour therapy. *Indian J Biochem Biophys.* 2009;46:16-24.

Kim HS, Cho EA, Bae JM, Yu DS, Oh ST, Kang H, Park CJ, Lee JD, Lee JY, Kim SY, Kim HO, Park YM. Recent trend in the incidence of premalignant and malignant skin lesions in Korea between 1991 and 2006. *J Korean Med Sci.* 2010 Jun;25:924-9.

Kim H, Yoon YJ, Shon JH, Cha IJ, Shin JG, Liu KH. Inhibitory effects of fruit juices on CYP3A activity. *Drug Metab Dispos.* 2006;34:521-3.

Kim I, Rodriguez-Enriquez S, Lemasters JJ. Selective degradation of mitochondria by mitophagy. *Arch Biochem Biophys.* 2007;462:245-53.

Kobayashi D, Ahmed S, Ishida M, Kasai S, Kikuchi H. Calcium/calmodulin signaling elicits release of cytochrome c during 2,3,7,8-tetrachlorodibenzo-p-dioxin-induced apoptosis in the human lymphoblastic T-cell line, L-MAT. *Toxicology.* 2009;258:25-32.

Kuma A, Hatano M, Matsui M, Yamamoto A, Nakaya H, Yoshimori T, Ohsumi Y, Tokuhiya T, Mizushima N. The role of autophagy during the early neonatal starvation period. *Nature.* 2004; 432:1032-6.

Labib S, Yauk C, Williams A, Arlt VM, Phillips DH, White PA, Halappanavar S. Subchronic oral exposure to benzo(a)pyrene leads to distinct transcriptomic changes in the lungs that are related to carcinogenesis. *Toxicol Sci.* 2012;129:213-24.



Li D, Day RS, Bondy ML, Sinha R, Nguyen NT, Evans DB, Abbruzzese JL, Hassan MM. Dietary mutagen exposure and risk of pancreatic cancer. *Cancer Epidemiol Biomarkers Prev.* 2007;16:655-61.

Li N, Sioutas C, Cho A, Schmitz D, Misra C, Sempf J, Wang M, Oberley T, Froines J, Nel A. Ultrafine particulate pollutants induce oxidative stress and mitochondrial damage. *Environ Health Perspect.* 2003;111:455-60.

Loxham M, Morgan-Walsh RJ, Cooper MJ, Blume C, Swindle EJ, Dennison PW, Howarth PH, Cassee FR, Teagle DA, Palmer MR, Davies DE. The effects on bronchial epithelial mucociliary cultures of coarse, fine, and ultrafine particulate matter from an underground railway station. *Toxicol Sci.* 2015;145:98-107.

Marangolo M, McGee MM, Tipton KF, Williams DC, Zisterer DM. Oxidative stress induces apoptosis in C6 glioma cells: involvement of mitogen-activated protein kinases and nuclear factor kappa B. *Neurotox Res.* 2001;3:397-409.

Marchi S, Giorgi C, Suski JM, Agnoletto C, Bononi A, Bonora M, De Marchi E, Missiroli S, Patergnani S, Poletti F, Rimessi A, Duszynski J, Wieckowski MR, Pinton P. Mitochondria-ros crosstalk in the control of cell death and aging. *J Signal Transduct.* 2012;2012:329635.

Mc Clean MD, Rinehart RD, Ngo L, Eisen EA, Kelsey KT, Herrick RF. Inhalation and dermal exposure among asphalt paving workers. *Ann Occup Hyg.* 2004;48:663-71.

Menon BR, Rathi MA, Thirumoorthi L, Gopalakrishnan VK. Potential Effect of Bacopa monnieri on Nitrobenzene Induced Liver Damage in Rats. *Indian J Clin Biochem.* 2010;25:401-4.

Miller KP, Ramos KS. Impact of cellular metabolism on the biological effects of benzo[a]pyrene and related hydrocarbons. *Drug Metab Rev.* 2001;33:1-35.

Mizushima N, Tsukamoto S, Kuma A. [Autophagy in embryogenesis and cell differentiation]. *Tanpakushitsu Kakusan Koso.* 2008; 53(16 Suppl):2170-4.

Moffat ID, Boutros PC, Chen H, Okey AB, Pohjanvirta R. Aryl hydrocarbon receptor (AHR)-regulated transcriptomic changes in rats sensitive or resistant to major dioxin toxicities. *BMC Genomics.* 2010;11:263.

Moreau K, Luo S, Rubinsztein DC. Cytoprotective roles for autophagy. *Curr Opin Cell Biol.* 2010;22:206-11.



Mukhopadhyay S, Panda PK, Behera B, Das CK, Hassan MK, Das DN, Sinha N, Bissoyi A, Pramanik K, Maiti TK, Bhutia SK. *In vitro* and *in vivo* antitumor effects of Peanut agglutinin through induction of apoptotic and autophagic cell death. *Food Chem Toxicol.* 2014 ;64:369-77.

Mukhopadhyay S, Panda PK, Das DN, Sinha N, Behera B, Maiti TK, Bhutia SK. Abrus agglutinin suppresses human hepatocellular carcinoma *in vitro* and *in vivo* by inducing caspase-mediated cell death. *Acta Pharmacol Sin.* 2014;35:814-24.

Nabeshi H, Yoshikawa T, Matsuyama K, Nakazato Y, Tochigi S, Kondoh S, Hirai T, Akase T, Nagano K, Abe Y, Yoshioka Y, Kamada H, Itoh N, Tsunoda S, Tsutsumi Y. Amorphous nanosilica induce endocytosis-dependent ROS generation and DNA damage in human keratinocytes. *Part Fibre Toxicol.* 2011;15:8:1.

Nathwani SM, Cloonan SM, Stronach M, Campiani G, Lawler M, Williams DC, Zisterer DM. Novel microtubule-targeting agents, pyrrolo-1,5-benzoxazepines, induce cell cycle arrest and apoptosis in prostate cancer cells. *Oncol Rep.* 2010;24:1499-507.

Nebert DW. The Ah locus: genetic differences in toxicity, cancer, mutation and birth defects. *Crit Rev Toxicol.* 1989; 20: 153–174.

Neff-LaFord H, Teske S, Bushnell TP, Lawrence BP. Aryl hydrocarbon receptor activation during influenza virus infection unveils a novel pathway of IFN-gamma production by phagocytic cells. *J Immunol.* 2007 ;179:247-55.

Nelson DR, Zeldin DC, Hoffman SM, Maltais LJ, Wain HM, Nebert DW. Comparison of cytochrome P450 (CYP) genes from the mouse and human genomes, including nomenclature recommendations for genes, pseudogenes and alternative-splice variants. *Pharmacogenetics.* 2004;14:1-18.

Nikoletopoulou V, Markaki M, Palikaras K, Tavernarakis N. Crosstalk between apoptosis, necrosis and autophagy. *Biochim Biophys Acta.* 2013;1833:3448-59.

Nohara K, Fujimaki H, Tsukumo S, Ushio H, Miyabara Y, Kijima M, Tohyama C, Yonemoto J. The effects of perinatal exposure to low doses of 2,3,7,8-tetrachlorodibenzo-p-dioxin on immune organs in rats. *Toxicology.* 2000;154:123-33.

Ohura T, Amagai T, Fusaya M, Matsushita H. Polycyclic aromatic hydrocarbons in indoor and outdoor environments and factors affecting their concentrations. *Environ Sci Technol.* 2004 ;38:77-83.



Pääjärvi G, Viluksela M, Pohjanvirta R, Stenius U, Högberg J. TCDD activates Mdm2 and attenuates the p53 response to DNA damaging agents. *Carcinogenesis*. 2005 ;26:201-8.

Pallardy M, Biola A, Lebrec H, Bréard J. Assessment of apoptosis in xenobiotic-induced immunotoxicity. *Methods*. 1999;19:36-47.

Pan T, Rawal P, Wu Y, Xie W, Jankovic J, Le W. Rapamycin protects against rotenone-induced apoptosis through autophagy induction. *Neuroscience*. 2009;164:541-51.

Panda PK, Mukhopadhyay S, Behera B, Bhol CS, Dey S, Das DN, Sinha N, Bissoyi A, Pramanik K, Maiti TK, Bhutia SK. Antitumor effect of soybean lectin mediated through reactive oxygen species-dependent pathway. *Life Sci*. 2014;111:27-35.

Panda PK, Mukhopadhyay S, Das DN, Sinha N, Naik PP, Bhutia SK. Mechanism of autophagic regulation in carcinogenesis and cancer therapeutics. *Semin Cell Dev Biol*. 2015;39:43-55.

Patra D. Simple luminescence method for estimation of benzo[a]pyrene in a complex mixture of polycyclic aromatic hydrocarbons without a pre-separation procedure. *Luminescence*. 2003 ;18:97-102.

Pavanello S, Pesatori AC, Dioni L, Hoxha M, Bollati V, Siwinska E, Mielzyńska D, Bolognesi C, Bertazzi PA, Baccarelli A. Shorter telomere length in peripheral blood lymphocytes of workers exposed to polycyclic aromatic hydrocarbons. *Carcinogenesis*. 2010;31:216-21.

Peluso M, Srivatanakul P, Munnia A, Jedpiyawongse A, Meunier A, Sangrajrang S, Piro S, Ceppi M, Boffetta P. DNA adduct formation among workers in a Thai industrial estate and nearby residents. *Sci Total Environ*. 2008; 389:283-8.

Peña-Vilabelda MM, García-Casado Z, Requena C, Traves V, López-Guerrero JA, Guillén C, Kumar R, Nagore E. Clinical characteristics of patients with cutaneous melanoma according to variants in the melanocortin 1 receptor gene. *Actas Dermosifiliogr*. 2014;105:159-71.

Peng RH, Xiong AS, Xue Y, Fu XY, Gao F, Zhao W, Tian YS, Yao QH. Microbial biodegradation of polyaromatic hydrocarbons. *FEMS Microbiol Rev*. 2008;32:927-55.

Perera RT, Fleming AM, Johnson RP, Burrows CJ, White HS. Detection of benzo[a]pyrene-guanine adducts in single-stranded DNA using the α -hemolysin nanopore. *Nanotechnology*. 2015;26: 074002.

Phillips DH. Smoking-related DNA and protein adducts in human tissues. *Carcinogenesis*. 2002 ;23:1979-2004.



Poirier MC, Beland FA. DNA adduct measurements and tumor incidence during chronic carcinogen exposure in animal models: implications for DNA adduct-based human cancer risk assessment. *Chem Res Toxicol*. 1992;5:749-55.

Poirier MC, Santella RM, Weston A. Carcinogen macromolecular adducts and their measurement. *Carcinogenesis*. 2000;21:353-9.

Poon CH, Wong TY, Wang Y, Tsuchiya Y, Nakajima M, Yokoi T, Leung LK. The citrus flavanone naringenin suppresses CYP1B1 transactivation through antagonising xenobiotic-responsive element binding. *Br J Nutr*. 2013;109:1598-605.

Pope CA 3rd, Dockery DW. Health effects of fine particulate air pollution: lines that connect. *J Air Waste Manag Assoc*. 2006;56:709-42.

Preissner SC, Hoffmann MF, Preissner R, Dunkel M, Gewiess A, Preissner S. Polymorphic cytochrome P450 enzymes (CYPs) and their role in personalized therapy. *PLoS One*. 2013 ;8:e82562.

Rao PS, Kumar S. Polycyclic aromatic hydrocarbons and cytochrome P450 in HIV pathogenesis. *Front Microbiol*. 2015;6:550.

Ray SS, Swanson HI. Dioxin-induced immortalization of normal human keratinocytes and silencing of p53 and p16INK4a. *J Biol Chem*. 2004 ;279 :27187-93.

Rodriguez-Antona C, Ingelman-Sundberg M. Cytochrome P450 pharmacogenetics and cancer. *Oncogene*. 2006;25:1679-91.

Roh T, Kwak MY, Kwak EH, Kim DH, Han EY, Bae JY, Bang du Y, Lim DS, Ahn IY, Jang DE, Lim SK, Yoo SD, Kwack SJ, Park KL, Lee YJ, Kim KB, Lee J, Kim HS, Lee BM. Chemopreventive mechanisms of methionine on inhibition of benzo(a)pyrene-DNA adducts formation in human hepatocellular carcinoma HepG2 cells. *Toxicol Lett*. 2012;208:232-8.

Rojas M, Cascorbi I, Alexandrov K, Kriek E, Auburtin G, Mayer L, Kopp-Schneider A, Roots I, Bartsch H. Modulation of benzo[a]pyrene diol epoxide-DNA adduct levels in human white blood cells by CYP1A1, GSTM1 and GSTT1 polymorphism. *Carcinogenesis*. 2000;21:35-41.

Rubinstein AD, Kimchi A. Life in the balance - a mechanistic view of the crosstalk between autophagy and apoptosis. *J Cell Sci*. 2012;125:5259-68.

Rubio V, Valverde M, Rojas E. Effects of atmospheric pollutants on the Nrf2 survival pathway. *Environ Sci Pollut Res Int*. 2010;17:369-82.



Rybicki BA, Nock NL, Savera AT, Tang D, Rundle A. Polycyclic aromatic hydrocarbon-DNA adduct formation in prostate carcinogenesis. *Cancer Lett.* 2006;239:157-67.

Saberi Hosnijeh F, Boers D, Portengen L, Bueno-de-Mesquita HB, Heederik D, Vermeulen R. Plasma Cytokine Concentrations in Workers Exposed to 2,3,7,8-tetrachlorodibenzo-p-dioxin (TCDD). *Front Oncol.* 2012;2:37.

Sánchez-Martín FJ, Fan Y, Carreira V, Ovesen JL, Vonhandorf A, Xia Y, Puga A. Long-term Coexposure to Hexavalent Chromium and B[a]P Causes Tissue-Specific Differential Biological Effects in Liver and Gastrointestinal Tract of Mice. *Toxicol Sci.* 2015;146:52-64.

Sánchez-Pérez Y, Chirino YI, Osornio-Vargas AR, Morales-Bárcenas R, Gutiérrez-Ruíz C, Vázquez-López I, García-Cuellar CM. DNA damage response of A549 cells treated with particulate matter (PM10) of urban air pollutants. *Cancer Lett.* 2009;278:192-200.

Sandberg M, Patil J, D'Angelo B, Weber SG, Mallard C. NRF2-regulation in brain health and disease: implication of cerebral inflammation. *Neuropharmacology.* 2014;79:298-306.

Schüller VJ, Heidegger S, Sandholzer N, Nickels PC, Suhartha NA, Endres S, Bourquin C, Liedl T. Cellular immunostimulation by CpG-sequence-coated DNA origami structures. *ACS Nano.* 2011;5:9696-702.

Shinkyo R, Sakaki T, Ohta M, Inouye K. Metabolic pathways of dioxin by CYP1A1: species difference between rat and human CYP1A subfamily in the metabolism of dioxins. *Arch Biochem Biophys.* 2003;409:180-7.

Shinomol GK, Bharath MM, Muralidhara. Pretreatment with *Bacopa monnieri* extract offsets 3-nitropropionic acid induced mitochondrial oxidative stress and dysfunctions in the striatum of prepubertal mouse brain. *Can J Physiol Pharmacol.* 2012;90:595-606.

Shinomol GK, Mythri RB, Srinivas Bharath MM, Muralidhara. *Bacopa monnieri* extract offsets rotenone-induced cytotoxicity in dopaminergic cells and oxidative impairments in mice brain. *Cell Mol Neurobiol.* 2012;32:455-65.

Singh M, Murthy V, Ramassamy C. Neuroprotective mechanisms of the standardized extract of *Bacopa monnieri* in a paraquat/diquat-mediated acute toxicity. *Neurochem Int.* 2013;62 :530-9.

Singh NP, Nagarkatti M, Nagarkatti P. Primary peripheral T cells become susceptible to 2,3,7,8-tetrachlorodibenzo-p-dioxin-mediated apoptosis *in vitro* upon activation and in the presence of dendritic cells. *Mol Pharmacol.* 2008;73:1722-35.



Smith LE, Denissenko MF, Bennett WP, Li H, Amin S, Tang M, Pfeifer GP. Targeting of lung cancer mutational hotspots by polycyclic aromatic hydrocarbons. *J Natl Cancer Inst.* 2000 ;92:803-11.

Soberanes S, Panduri V, Mutlu GM, Ghio A, Bundinger GR, Kamp DW. p53 mediates particulate matter-induced alveolar epithelial cell mitochondria-regulated apoptosis. *Am J Respir Crit Care Med.* 2006;174:1229-38.

Song J, Lu Y, Pang S, Chiu R. An internal control for immunoblot analysis using the blotted membrane. *Anal Biochem.* 2004;331:201-3.

Spinelli JJ, Demers PA, Le ND, Friesen MD, Lorenzi MF, Fang R, Gallagher RP. Cancer risk in aluminum reduction plant workers (Canada). *Cancer Causes Control.* 2006;17:939-48.

Stevens EA, Mezrich JD, Bradfield CA. The aryl hydrocarbon receptor: a perspective on potential roles in the immune system. *Immunology.* 2009;127:299-311.

Stolpmann K, Brinkmann J, Salzmann S, Genkinger D, Fritsche E, Hutzler C, Wajant H, Luch A, Henkler F. Activation of the aryl hydrocarbon receptor sensitises human keratinocytes for CD95L- and TRAIL-induced apoptosis. *Cell Death Dis.* 2012;3:e388.

Sulentic CE, Kaminski NE. The long winding road toward understanding the molecular mechanisms for B-cell suppression by 2,3,7,8-tetrachlorodibenzo-p-dioxin. *Toxicol Sci.* 2011 ;120:S171-91.

Swenberg JA, Fryar-Tita E, Jeong YC, Boysen G, Starr T, Walker VE, Albertini RJ. Biomarkers in toxicology and risk assessment: informing critical dose-response relationships. *Chem Res Toxicol.* 2008;21:253-65.

Tagashira H, Shinoda Y, Shioda N, Fukunaga K. Methyl pyruvate rescues mitochondrial damage caused by SIGMAR1 mutation related to amyotrophic lateral sclerosis. *Biochim Biophys Acta.* 2014;1840:3320-34.

Tamiji S, Beauvillain JC, Mortier L, Jouy N, Tual M, Delaporte E, Formstecher P, Marchetti P, Polakowska R. Induction of apoptosis-like mitochondrial impairment triggers antioxidant and Bcl-2-dependent keratinocyte differentiation. *J Invest Dermatol.* 2005;125:647-58.

Tanyanont W, Vichit-Vadakan N. Exposure to volatile organic compounds and health risks among residents in an area affected by a petrochemical complex in Rayong, Thailand. *Southeast Asian J Trop Med Public Health.* 2012 ;43:201-11.



Tarantini L, Bonzini M, Apostoli P, Pegoraro V, Bollati V, Marinelli B, Cantone L, Rizzo G, Hou L, Schwartz J, Bertazzi PA, Baccarelli A. Effects of particulate matter on genomic DNA methylation content and iNOS promoter methylation. *Environ Health Perspect.* 2009;117:217-22.

Tsai MJ, Wang TN, Lin YS, Kuo PL, Hsu YL, Huang MS. Aryl hydrocarbon receptor agonists upregulate VEGF secretion from bronchial epithelial cells. *J Mol Med (Berl).* 2015; in press.

Tsay JJ, Tchou-Wong KM, Greenberg AK, Pass H, Rom WN. Aryl hydrocarbon receptor and lung cancer. *Anticancer Res.* 2013;33:1247-56.

Uttara B, Singh AV, Zamboni P, Mahajan RT. Oxidative stress and neurodegenerative diseases: a review of upstream and downstream antioxidant therapeutic options. *Curr Neuropharmacol.* 2009;7:65-74.

Verma P, Singh P, Gandhi BS. Neuromodulatory role of *Bacopa monnieri* on oxidative stress induced by postnatal exposure to decabromodiphenyl ether (PBDE -209) in neonate and young female mice. *Iran J Basic Med Sci.* 2014;17:307-11.

Watabe Y, Nazuka N, Tezuka M, Shimba S. Aryl hydrocarbon receptor functions as a potent coactivator of E2F1-dependent transcription activity. *Biol Pharm Bull.* 2010 ;33:389-97.

Wang T, Wang Q, Song R, Zhang Y, Zhang K, Yuan Y, Bian J, Liu X, Gu J, Liu Z. Autophagy Plays a Cytoprotective Role During Cadmium-Induced Oxidative Damage in Primary Neuronal Cultures. *Biol Trace Elem Res.* 2015; in press.

Wang Q, Xue Y. Characterization of solid tumors induced by polycyclic aromatic hydrocarbons in mice. *Med Sci Monit Basic Res.* 2015;21:81-5.

Xia T, Korge P, Weiss JN, Li N, Venkatesen MI, Sioutas C, Nel A. Quinones and aromatic chemical compounds in particulate matter induce mitochondrial dysfunction: implications for ultrafine particle toxicity. *Environ Health Perspect.* 2004;112:1347-58.

Yang JK. Death effector domain for the assembly of death-inducing signaling complex. *Apoptosis.* 2015;20:235-9.

Yu Y, Wang X, Yang D, Lei B, Zhang X, Zhang X. Evaluation of human health risks posed by carcinogenic and non-carcinogenic multiple contaminants associated with consumption of fish from Taihu Lake, China. *Food Chem Toxicol.* 2014; 69:86-93.

Zalacain M, Sierrasesúmaga L, Patiño A. [The cytogenetic assay as a measure of genetic instability induced by genotoxic agents]. *An Sist Sanit Navar.* 2005;28:227-36.



CURRICULUM VITAE

DURGESH NANDINI DAS
CSIR, Senior Research Fellow
Department of Life Science
National Institute of Technology
Rourkela Odisha, 769 008
India
Lab Phone No-+91-661-2464683/+91-661-2464701
Mobile Number -+ 91-9777067735
Email:durgeshbiotech@gmail.com, 510ls304@nitrrkl.ac.in

CAREER OBJECTIVE:

To work with commitment and passion in an organization focused in the field of Cancer biology that throws challenges to my knowledge and capabilities.

RESEARCH AREA: Cancer Biology, Apoptosis, Autophagy, Bioinformatics.

ACADEMIC QUALIFICATION:

- Ph.D. (Life Science) continuing at National Institute of Technology, Rourkela, Orissa, India-769008. Score : 9.0/10 (CGPA)
(Elucidating mechanisms of benzo[a]pyrene mediated apoptotic and autophagic cell death and its prevention with phytotherapeutics)
- M.Sc (Biotechnology) - SRM University, Chennai, Tamil nadu, India 600 089.
Score: 8.136 / 10 (CGPA) (2008)
- B.Sc (Botany Honours) –Sambalpur university, Rourkela, Odisha , India.
Score: 72% (2006)

RESEARCH EXPERIENCE:

- 1. Identification and molecular characterization of mrsa & mrse by atomic force microscopy and pcr from clinical specimens.** (MRSA – Methicillin resistant *Staphylococcus aureus*, MRSE – Methicillin resistant *Staphylococcus epidemidis*) 2008(SRM University , Chennai).
- 2. Isolation, amplification and incorporation of aspm (exon 18) into suitable vector (PUC18).** (ASPM – Is an acronym for “Abnormal spindle like, microcephaly – associated”) (2009) (Nthrys biotech lab Hyderabad).
- 3. Designing / modelling various scfv fragment in order to human CD4 (T cells) domain to block the access GP120 (HIV)** (Bioinformatics) (2009) (Nthrys biotech lab Hyderabad).
- 4. Nanotechnology training –preparation of chitosan nanoparticle** (2010) (NIT, Rourkela).
- 5. Elucidating mechanisms of Benzo[a]pyrene mediated apoptotic And autophagic cell death And its prevention with phytotherapeutics** (2011 – 2015) (NIT, Rourkela).



IN VITRO / IN SILICO TECHNIQUES:

Molecular Biology: Nucleic acid Isolation , Purification and Estimation, Protein Isolation, purification and Estimation, Agarose Gel Electrophoresis, SDS PAGE , PCR Technique.

Cell culture technique- Cell Viability, Cell Proliferation and Cytotoxicity, Annexin V (apoptosis analysis), cell cycle analysis, Gene Knockdown (Si RNA and sh RNA), cell study by fluorescence and confocal microscopy.

Bioinformatics tools - Blast, Fasta, Molecular Modeling, Molecular Docking, and Restriction Mapping.

Genetic Engineering: Restriction Digestion, Ligation, Competence cell preparation and Transformation, Southern & Northern Hybridization, DNA sequencing, RT PCR.

Nanotechnology: Atomic force microscopy, sonication, particle size analysis.

Immunotechnique: Immunoelectrophoresis, Raising polyclonal antibodies, Western Blotting, Australian antigen testing, hemagglutination, ELISA, precipitation, Agglutinin.

Biochemistry: Estimation of cholesterol, Estimation of protein, Estimation of glucose, Estimation of phosphorous, Determining specific activity of urease.

• Credit courses qualified during graduate studies

Cancer Biology, Research methodology, Molecular Biology and Immunology.

ACADEMIC AWARDS/HONORS

- Young Scientist Award in National conference on 'Current Trends in Life Sciences Research and Challenges Ahead' organized by Sambalpur University, Burla from 28th February to 2nd March, 2014.
- CSIR SRF Fellowship, 2014 by Council of Scientific & Industrial Research, New Delhi, India.

ATTENDED: SEMINAR & WORKSHOP

1. National seminar- National conference on current trends in life sciences research and challenges ahead 2014 –Paper presentation. Prediction and validation of apoptosis through cytochrome P450 activation by benzo[a]pyrene. By **Durgesh Nandini Das** and Sujit K Bhutia.

2. Poster presented at 34th Annual Convention of Indian Association for Cancer Research (IACR) & International Symposium on "Bench to bed side" DNA damage by 2,3,7,8-tetrachlorodibenzo-p-dioxin-induced p53 mediated apoptosis through activation of cytochrome P450/aryl hydrocarbon receptor. By **Durgesh Nandini Das** and Sujit K Bhutia.

3. 2nd International conference on frontiers in Biological sciences, 2015, In vitro mutagenic and genotoxic effects of native airborne particulate matter and its clinical significance. By **Durgesh Nandini Das** and Sujit K Bhutia

4. Poster presented at 32nd Annual Convention of Indian Association for Cancer Research



(IACR) & International Symposium on "Infection & Cancer", New Delhi, 2013 Autophagic cell death induction with Abrus agglutinin. By: Prashanta Kumar Panda, Subhadip Mukhopadhyay , **Durgesh Nandini Das**, Niharika Sinha, Sujit K Bhutia.

5. Flow cytometry training, BD Bioscience, Gurgaon India.

PUBLICATION TILL DATE:

Research paper

1. **Das, D.N.**, Panda, P.K., Mukhopadhyay, S., Sinha, N., Mallick, B., Behera, B., Maiti, T.K., Bhutia, S.K., 2014. Prediction and validation of apoptosis through cytochrome P450 activation by benzo[a]pyrene. *Chemico-Biological Interactions* 208, 8-17.
2. **Das, D.N.**, Sinha N., Naik P.P., Panda P.K., Mukhopadhyay S., Mallick S.K., Sarangi I., Bhutia, S.K., In vitro mutagenic and genotoxic effects of native airborne particulate matter and its clinical significance. (Communicated, *Chemosphere Manuscript No.CHEM37201*).
3. **Das, D.N.**, Naik, P.P., Panda, P.K., Mukhopadhyay, S., Sinha, N., Naik, A., Bhutia, S.K., 2015. Cytoprotective activity of *Bacopa monneiri* against benzo[a]pyrene induced apoptosis through modulation of autophagy. (Communicated, *Journal of Functional Foods*, Manuscript Number: JFF-D-15-01598)
4. **Das,D.N.**, Panda P.K., Mukhopadhyay S., Sinha, N., Naik P.P., Bhutia, S.K., Benzo[a]pyrene mediated mitochondrial stress induces autophagy-dependent cell death. (Under preparation)
5. **Das,D.N.**, Panda P.K., Sinha, N., Mukhopadhyay S., Naik P.P., Bhutia, S.K., DNA damage by 2,3,7,8-tetrachlorodibenzo-p-dioxin-induced p53 mediated apoptosis through activation of cytochrome P450/aryl hydrocarbon receptor. (Communicated- *Chemico Biological Interactions*. Manuscript No. CHEMBIOINT-D-15-00618).
6. Panda, P.K., Mukhopadhyay, S., Behera, B., Bhol, C.S., Dey, S., **Das, D.N.**, Sinha, N., Bissoyi, A., Pramanik, K., Maiti, T.K., Bhutia, S.K., 2014. Antitumor effect of soybean lectin mediated through reactive oxygen species-dependent pathway. *Life Science* 111, 27-35.
7. Mukhopadhyay, S., Panda, P.K., Behera, B., Das, C.K., Hassan, M.K., **Das, D.N.**, Sinha, N., Bissoyi, A., Pramanik, K., Maiti, T.K., Bhutia, S.K., 2014. In vitro and in vivo antitumor effects of Peanut agglutinin through induction of apoptotic and autophagic cell death. *Food and Chemical Toxicology* 64, 369-377.
8. Mukhopadhyay, S., **Das, D.N.**, Panda, P.K., Sinha, N., Naik, P.P., Bissoyi, A., Pramanik, K., Bhutia, S.K., 2015. Autophagy protein Ulk1 promote mitochondrial apoptosis through reactive oxygen species. *Free Radical Biology and Medicine*, In Press.
9. Mukhopadhyay, S., Panda, P.K., **Das, D.N.**, Sinha, N., Behera, B., Maiti, T.K., Bhutia, S.K., 2014. Abrus agglutinin suppresses human hepatocellular carcinoma in vitro and in vivo by inducing caspase-mediated cell death. *Acta Pharmacologica Sinica* 35, 814-824.

Review paper

1. **Das, D.N.**, Panda P.K., Mukhopadhyay S., Sinha N., Naik P.P., Bhutia, S.K., Effects of polycyclic aromatic hydrocarbons on cellular mechanism: possible cause of human carcinogenesis. *Current drug metabolism*.(Communicated, *Cell Biology and Toxicology Manuscript No CBTO-D-15-00138*).



2. Panda, P.K., Mukhopadhyay, S., **Das, D.N.**, Sinha, N., Naik, P.P., Bhutia, S.K., 2015. Mechanism of autophagic regulation in carcinogenesis and cancer therapeutics. *Seminars in Cell and Developmental Biology* 39, 43-55.
3. Mukhopadhyay, S., Panda, P.K., Sinha, N., **Das, D.N.**, Bhutia, S.K., 2014. Autophagy and apoptosis: where do they meet? *Apoptosis* 19, 555-566.
4. Sinha, N., Mukhopadhyay, S., **Das, D.N.**, Panda, P.K., Bhutia, S.K., 2013. Relevance of cancer initiating/stem cells in carcinogenesis and therapy resistance in oral cancer. *Oral Oncol* 49,854-62.

Book chapter

Bhutia, S.K., Mukhopadhyay, S., Sinha, N., **Das, D.N.**, Panda, P.K., Patra, S.K., Maiti, T.K., Mandal, M., Dent, P., Wang, X.Y., Das, S.K., Sarkar, D., Fisher, P.B., 2013. Autophagy: cancer's friend or foe? *Adv Cancer Res* 118:61-95.

HOBBIES:

Painting, listening music, jewellery designing, making arts & craft work, playing computer games.

PERSONAL DETAILS:

Strength: Cracking complex tasks, hardworking , ability to work in TEAM

Date Of Birth: 29.06 1984

Gender: Female

Father name: Dr Krushna Baraha Das

Languages Known: English, Hindi., Oriya

Permanent Address: C/o Dr Krushna Baraha Das

H 3/3 Panchasakha nagar Dumduma, Bhubhaneswar-751019, Odisha, India

Email id: nandininitrkl@gmail.com , 510ls304@nitrkl.ac.in

Citizenship: India

DECLARATION:

Hereby I declare that all the details furnished above are true to my knowledge and belief.

Durgesh Nandini Das

Durgesh Nandini Das

